Characterizing Human-Exoskeleton Fluency for Co-Adaptive Control of Ankle Exoskeletons

by

Man I Wu

A dissertation submitted in partial fulfillment
of the requirements for the degree of
Doctor of Philosophy
(Robotics)
in the University of Michigan
2024

Doctoral Committee:

Professor Leia A. Stirling, Chair
Dr. Brian S. Baum, MIT Lincoln Laboratory
Professor Elliott J. Rouse
Professor X. Jessie Yang

Man I Wu
maniwu@umich.edu
ORCID iD: 0000-0002-5554-0448

ACKNOWLEDGEMENTS

This thesis is the culmination of years of hard work and the invaluable support from my advisor, friends, and family. I entered graduate school during uncertain times at the height of the pandemic and thus was grateful to join the the wonderful community in the Stirling Research Group and Robotics Department. I would like to thank my amazing advisor, Dr. Leia Stirling, for her steady guidance and mentorship throughout this journey. She taught me countless skills, ranging from experimental methods to embodying confidence in my capabilities and work, and encouraged me through the highs and lows of obtaining my degree. Her support undoubtedly played a vital role during my PhD process. I also thank my committee, Dr. Brian Baum, Professor X. Jessie Yang, and Professor Elliott Rouse, for their insightful research advice and feedback on my dissertation.

My friends and labmates in the Stirling Research Group have been a highlight and a source of inspiration through my PhD journey. The group is an amalgamation of bright minds that have offered constant support (and code debugging advice) which was integral to my success. Special thanks to Jacqueline and Hannah W., who motivated me when I felt defeated and celebrated my accomplishments. I also appreciate my peers in the Robotics community that created an environment where students can thrive through diversity of thought, identities, and backgrounds.

I would not have been able to obtain my PhD without my family. Since I was young, my parents and sisters have taught me tenacity and perseverance, which were essential throughout this process. While they didn't always understand my research or the doctoral process, they were steadfast with the belief that I could accomplish my goals. With grit and their encouragement, I have the privilege of being the first person to obtain a doctoral degree in my family. My success would not have been possible without my family's faith and support.

I cannot express enough appreciation for all who have positively impacted my journey. Thank you!

TABLE OF CONTENTS

LIST OF FIGURES

FIGURE

LIST OF TABLES

TABLE

LIST OF APPENDICES

ABSTRACT

The performance of assistive and augmentative lower-limb exoskeletons has been tested in laboratory settings and can achieve goals of improved walking economy and metabolic cost reduction. However, it has been shown that even in controlled laboratory environments, exoskeletons may experience errors of improper torque assistance due to misalignments between the measured and actual state of the human-exoskeleton system. If the torque assistance repeatedly hinders a user's actions due to errors, the user may begin to anticipate errors and resist the exoskeleton. In order for exoskeletons to be adopted for everyday use, it is important to understand the immediate and long-term effects of exoskeleton errors on user motion and trust in the system, as errors are likely to occur in operational settings with complex, changing environments. It is also necessary to understand the strategies that people utilize when interacting with exoskeletons to design control methods to support collaboration between humans and exoskeletons. This work used the Dephy bilateral, powered ankle exoskeleton, which applied an assistive plantarflexion torque during push-off to minimize energy expenditure during walking. The main aims of this thesis are to characterize the (1) immediate effects and (2) residual effects of exoskeleton errors on human gait strategies, as well as (3) develop a co-adaptive exoskeleton controller to support collaboration between the user and exoskeleton.

In Chapter 2, immediate compensatory hip behavior was identified in response to pseudo-random exoskeleton errors (loss of exoskeleton assistance) as users maintained acceptable task performance on a targeted stepping task. Quantitative measures of human-exoskeleton fluency—the alignment of the user and exoskeleton's goals—were developed using joint kinematics and muscle activity metrics. Emergent gait strategies were identified in Chapter 3 using k-means clustering as users walked with imperfect exoskeleton algorithms with fixed error frequencies (0-10% error in all strides) and were characterized as fluent or non-fluent. In Chapter 4, we designed and modeled a co-adaptive control algorithm that supports human-exoskeleton fluency by adjusting torque assistance in response to measures of muscle activity and joint kinematics along the lower limbs. The proposed co-adaptive algorithm successfully modulated peak torque in response to various fluent and non-fluent behaviors compared to an ankle-only controller that did not account for hip and knee compensatory strategies.

These results inform future exoskeleton controller design and evaluation metrics for human-exoskeleton collaboration. For example, developers may utilize measures of fluency during system development and testing. They also contribute to current literature on adaptation to exoskeletons, co-adaptive algorithms, and human-robot interaction metrics for the field of human-exoskeleton research.

CHAPTER 1

Introduction

1.1 Motivation

Exoskeletons are wearable robotic devices designed to assist, augment, or rehabilitate a human's physical capabilities. For healthy individuals, exoskeletons may improve strength and endurance, as well as mitigate musculoskeletal risk, for those performing repetitive or fatiguing tasks, such as industrial workers, soldiers, and search-and-rescue workers [111, 49, 99]. Exoskeletons can also assist people with disabilities and aging populations with activities of daily living by restoring walking capability [28], improving walking economy [73], and aiding grasping [45]. Rehabilitation programs may also benefit from incorporating exoskeleton-based training following injury or physical disease [71, 97, 78]. The benefits of exoskeletons have been tested in laboratory settings and can achieve goals of improving energy expenditure during walking [70, 86, 64] and restoring motion for people with disabilities [28, 73]. In order for exoskeletons to be adopted for every day use, performance must be tested in operational settings with complex, changing environments that may be difficult to observe. It has been shown that even in controlled laboratory settings, exoskeletons may experience errors [86], which may impact the human user's motions and trust in the system.

Exoskeleton errors may involve misalignments between the measured and actual state of the human-exoskeleton system, which may then change the timing and magnitude of assistance provided by the exoskeleton. Improper assistance may inhibit the user's actions, affect their stability, and drive the user to develop strategies that work against the goals of the exoskeleton. For example, if assistance directly and repeatedly impeded a user's actions, the user may begin to anticipate errors and stiffen their limbs to resist the exoskeleton, thereby increasing energy expenditure and muscle recruitment. Thus, it is important to understand the immediate and residual effects of exoskeleton errors on user motion and trust in the system, which can inform the performance requirements of exoskeletons in operational settings. Trust involves the attitude that the user has toward the system (exoskeleton) in an

uncertain environment [54] and is impacted by the system's reliability. It is also necessary to characterize strategies that people utilize when interacting with exoskeletons to ensure proper use, where the user and exoskeleton's actions and goals are aligned (e.g. metabolic cost reduction, trajectory following for rehabilitation). Then, we can develop exoskeleton control methods to support collaboration between humans and exoskeletons.

This thesis addresses the following questions:

1. What are the immediate effects of exoskeleton errors on human gait strategies?

2. What are the residual effects of exoskeleton errors on gait strategies?

3. How do we support human-exoskeleton collaboration through exoskeleton control?

We will first review a subset of the relevant literature and then formulate the specific aims of this thesis.

1.2 Lower-Limb Exoskeletons

Lower-limb exoskeletons typically apply torques about the hip, knee, or ankle joints to reduce the metabolic cost or muscle recruitment associated with locomotion. These torques may be applied passively, using a series of spring and variable dampers [100, 112, 6], or actively through actuators [113, 64, 70]. Exoskeleton assistance must also be applied at the right time, in the right direction, and at the appropriate intensity to be effective. A key metric used to measure the performance of assistive exoskeletons for able-bodied users is metabolic cost, which is typically obtained using respiratory measurements [83] while performing a task such as walking. In laboratory settings, powered lower-limb exoskeletons have demonstrated the ability to decrease energy expenditure by applying an assistive plantarflexion torque about the ankle during gait [70, 110]. It has been shown that the timing of the exoskeleton actuation significantly impacts the magnitude of metabolic cost reduction [109]. Thus, in order to apply appropriate torque, exoskeleton control algorithms must accurately detect the current state of the human-exoskeleton system and apply actuation at the correct phases of movement while remaining transparent in others.

In this section, we discuss current state estimation techniques and control strategies used with lower-limb exoskeletons, as well as human-in-the-loop optimization methods that may inform exoskeleton torque assistance. We also detail the topic of exoskeleton errors in operational settings to highlight a key component of real-world adoption of exoskeletons.

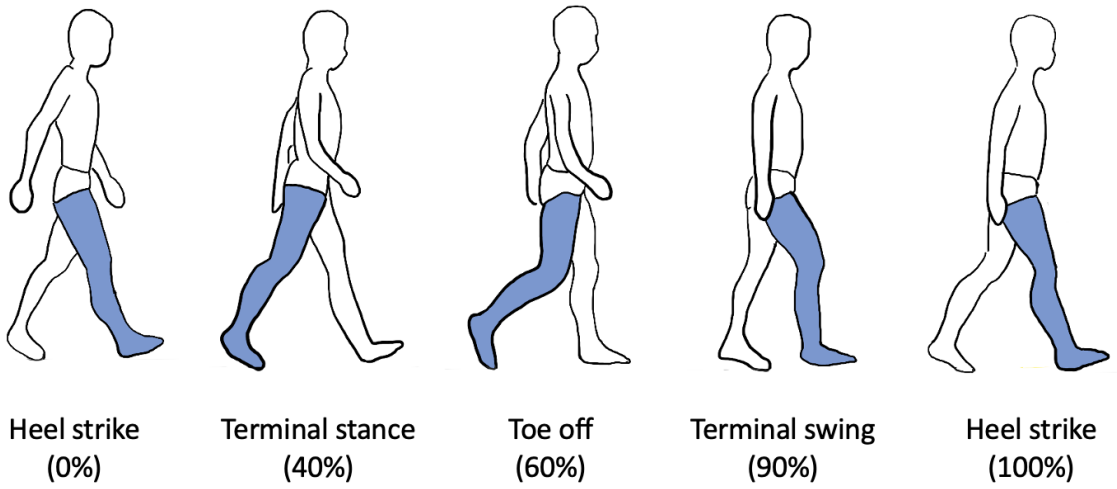

Figure 1.1: A person progressing through a gait cycle that begins and ends with subsequent heel strikes, where stance and swing occur during 0-60% and 61-100% of the gait cycle, respectively.

1.2.1 State Estimation and Control Techniques

State estimation techniques often rely on mechanical sensor input (e.g. encoders, inertial measurement units) to determine the current gait cycle phase to apply the desired level of torque about the joints. One of the key state variables is gait phase, a continuous variable with values between 0 to 100% that represents progression through the gait cycle, where 0 and 100% are successive heel strikes on the same leg during locomotion. The gait cycle is further divided into stance, where the foot is in contact with the ground, and swing, where the foot leaves the ground and moves to the front of the body (Fig. 1.1. Accurate estimation of gait phase is essential for exoskeletons to provide the appropriate assistance to a user for optimal performance, such as maximizing reductions in metabolic cost [109].

A common phase estimation method is a time-based estimator (TBE), which uses previous stride times to predict the current stride time and estimates the gait phase using the time since the last heel strike and the predicted stride time. The previous stride times may be determined using foot contact switches or kinematics derived from inertial measurement units (IMUs) and a pre-specified number of previous stride times may be averaged to predict the next stride time [64, 70]. Another common method is to use a finite state machine (FSM), which may segment the gait cycle into defined states (e.g. stance and swing phases) and apply different assistive torques according to the identified state [58]. Similar to TBE, FSM may also use foot switches and IMUs to detect and transition between states. While

studies have shown significant reductions in metabolic cost using TBE [64, 70] and FSM [58] methods, these studies have been limited to steady-state ambulation, such as constant-speed treadmill walking, as they assume steady, periodic gait. Thus, newer state estimation techniques have integrated advanced techniques to address more complex locomotion modes.

In order for exoskeletons to be adopted to operational settings, they must be robust in changing, uncertain environments. Bayesian filtering has recently been applied for gait estimation in wearable robotics and allows for estimation of the underlying gait state using noisy measurements obtained using sensors such as IMUs [61]. Studies have used Extended Kalman Filters (EKF) to estimate gait phase and other relevant parameters (e.g. ground inclination, phase velocity) with low RMSE for most parameters (< 0.1 degrees) for lower-limb exoskeleton control under varying speeds and slopes [92, 67]. Deep learning approaches have also been used for gait phase estimation with variable-speed walking [86, 48], which have resulted in significant reductions in estimation error compared to TBE methods (> 10 ms reduction in RMSE [86]).

Exoskeletons use information derived via state estimation to control the torque assistance provided to the user. As techniques for state estimation are continuously being developed and validated, it is important to also refine methods of torque profile control and evaluate how human users may react to exoskeleton torque. Many existing studies involving exoskeleton control apply a predefined trajectory dependent on gait state estimates, such as gait phase and stance/swing indicators [70, 86, 67]. There is an implicit assumption that humans are expected to adapt to the exoskeleton and reduce metabolic cost, based on an understanding of the mechanics and energetics of human movement [96] and simulations [95, 21]. However, it has been shown that some users may actively fight against the exoskeleton and stiffen the limb rather than adapting to the exoskeleton during early adaptation [2], preventing reductions in metabolic cost due to muscle co-contraction. Gait strategies developed while walking with an exoskeleton are often user-specific [2, 46, 102] and evolve over time [31, 56, 53]. Thus, it is important to incorporate feedback on the user's state within the control algorithm to allow an exoskeleton to make adjustments to torque assistance to align with the user's intent and encourage fluent strategies. A gait strategy may be considered fluent when the user's actions and underlying goal is aligned with that of the exoskeleton, such as minimizing energy expenditure or muscle recruitment. There exist various ways to determine torque profile parameters, including human-in-the-loop optimization, user preference, and identified heuristics.

1.2.2 Defining Torque Profile Parameters

Human-in-the-loop (HIL) optimization presents a promising approach to modify control laws for individual users and facilitate learning. During optimization, device control is systematically varied via parameter values in order to minimize the cost function, such as human metabolic cost, and maximize performance. However, several challenges are presented during HIL optimization. The objective function involving human performance may be difficult to approximate and are based on measurements that typically involve lengthy evaluation periods and low signal-to-noise ratio. For instance, metabolic cost via respiratory breath analysis is inferred indirectly by averaging noisy respiratory measurements over a number of breaths, usually over a period of 1 to 2 seconds [83]. Additionally, control laws that approximate globally optimal assistance strategies involve multiple parameters per assisted joint, which created high-dimensional optimization problems [35].

Initial optimization methods have been explored to optimize a single gait or device parameters, such as gradient descent [52] and line search [25]. These methods, however, may be sensitive to drift and noise [77], scale poorly, and require many samples and evaluations for each parameter due to high dimensionality. To address these concerns, Zhang et al. [110] developed a sample-based optimization method for identifying exoskeleton control parameters (peak torque, peak torque time, rise and fall times) which minimize the metabolic cost of walking. During optimization, exoskeleton control laws and the subsequent torque profile are continuously updated as metabolic rate is measured. Then, steady-state metabolic cost is estimated using 2 minutes of transient metabolic data, which is then used to update the control laws to represent the best estimate of optimal control parameters. The strategy from Zhang et al. [110] is relatively tolerant to sensor noise and human adaptation and scales well to benchmarking problems.

While this method achieved a mean reduction of 33% in metabolic cost compared to zero torque, optimization requires relatively long measurement times, which may require multi-day protocols to avoid user fatigue that can cause significant changes in muscle energy efficiency [104]. Users are also forced to walk with diverse control laws during optimization, some of which have been uncomfortable and sub-optimal. To address long optimization protocols, Gordon et al. [30] proposed a HIL methodology that optimizes exoskeleton assistance profiles using online simulations of metabolic rate based on musculoskeletal models, thus significantly reducing time investments required for sampling specific torque profiles. However, the experimental protocol was conducted over two days and the difference in relative reduction in metabolic cost between HIL simulation-based control and generic, fixed control was dependent on the participant. Additionally, the optimal control law is used as a static control law after optimization and does not change even though humans may continue to

adapt after the optimization protocol.

Studies have also explored preference-based selection of torque parameters for customized control of exoskeletons [43, 44]. Incorporating user preference into exoskeleton control may support human-exoskeleton collaboration, as it allows the user to guide device behavior based on perceptions of speed, exertion, comfort, and other performance factors. Ingraham et al. [43] demonstrated that users can reliably identify preferred assistance parameters, such as the timing and magnitude of peak torque, through self-exploration. Lee et al. [55] developed a preference-based optimization of control parameters using sample-efficient learning, which enabled users to converge on preferred parameters with 88% accuracy within 43 queries compared to randomly generated parameters. Overall, utilizing user preference is an exciting approach for defining exoskeleton control, but results in a static torque profile, similar to HIL optimization. It has been shown that experienced users preferred higher torque compared to novices [43], motivating the need for algorithms that evolve over time with the human. Thus, control algorithms that promote co-adaptation between the user and exoskeleton may address issues with fixed exoskeleton control and HIL optimization.

1.2.3 Exoskeleton Errors

While exoskeleton control algorithms are continuously being developed and improved, they are unlikely to be perfect and will experience errors. For instance, although Sheperd et al. [86] achieved an root-mean-squared error (RMSE) of 3.9% across all online validation trials, the authors reported that in approximately 10% of all training and testing trials, the exoskeleton had "critical errors", which caused the boot to become unstable. Users' trust may have been affected by these errors, yielding alterations in gait to ensure stability. Additionally, machine learning may not generalize well across set speeds and individuals, as the model outputs are limited by various features represented the training dataset. Speeds and environment states outside of the training set and differences in user characteristics, such as anthropometrics and mobility, may impact model performance and thus the gait phase estimation used for low-level torque control. For example, initial research on transfer learning techniques for torque estimation may reduce model training time through parameter sharing across subjects [90], but used a limited subject pool, which may affect generalizability.

Gait phase estimation errors may also result in errors in exoskeleton torque assistance and performance. If gait phase estimates are inaccurate, assistive torques may be applied earlier or later in the gait cycle than appropriate, which may impact a user's stability and prevent reductions in metabolic cost [109, 64]. The exoskeleton may also fail to actuate during a stride, thus affecting the user's joint kinematics and energetics due to loss of exoskeleton

torque. Thus, it is important to understand how humans respond to exoskeleton errors, which are likely to occur in uncertain, dynamic environments found in operational settings. The formation and modification of human motor strategies can inform our understanding of the impact of exoskeleton errors on gait and use of exoskeleton systems.

1.3 Factors That Influence Human Movement

Human motor strategies have been attributed to internal mental models, which is a theory that there exist state-dependent approximations of external forces that inform motor commands and predictions [94, 105]. In a novel environment with external forces, the central nervous system minimizes movement errors by either stiffening the limb or learning internal models to respond to the force [91]. An internal model comprises of an *inverse model* of body mechanics that calculates the neural commands necessary to produce a specific movement and a *forward model* which uses an copy of the neural commands to predict the sensory feedback when movement occurs (Fig. 1.2). Movement errors due to unforeseen perturbations in novel environments then prompt motor adaptations, which are modifications of movement in response to trial-to-trial error feedback [65] or the changes in strategy and the internal model over time. Internal models also account for high and low-level control, as humans can alter feedforward strategies and reflex responses depending on the given task and environment [37]. Multiple internal models may also be formed or combined to support motor strategies in various environments [18].

Random trials with unexpectedly altered dynamics—catch trials—have been introduced by researchers to understand internal model formation. During gait, catch trials have been used to examine internal models formed when participants experience environments with external forces. Bucklin et al. [11] showed that participants walking towards a target in a uniform force field adapted motor strategies for center-of-mass trajectories. During catch trials, participants' trajectories deviated in the direction opposite of the force, indicating a learned internal model corresponding to the force field. Similarly, Cajigas et al. [12] observed that participants modified their hip and knee kinematics when walking in a constant force field. Similar to these force-field studies, exoskeletons apply external torques that can be learned and anticipated (Fig. 1.3). Catch trials involving the absence of external torques can be used to understand the internal models developed with exoskeletons while completing goal-directed tasks. Catch trials may also be used to examine behavior in uncertain situations with unexpected dynamics. However, catch trials may affect users' trust and thus system usage.

Exoskeleton errors, such as loss of assistive torque for a stride, may induce movement

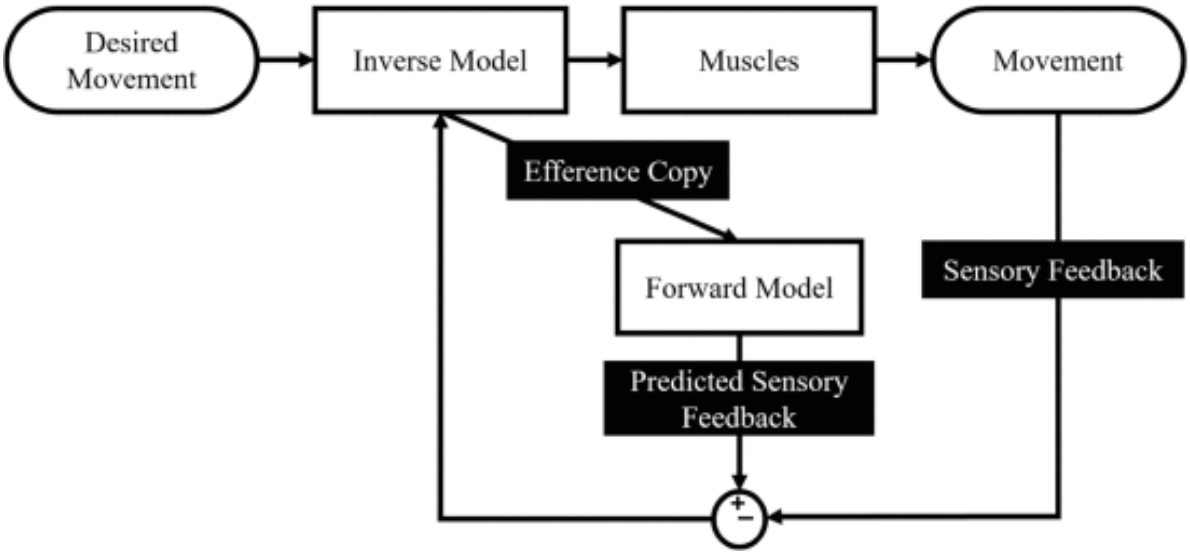

Figure 1.2: (From Hybart et al. [41]) Internal models involve an inverse and forward model of body dynamics for controlling body movements. The nervous system calculates the necessary efferent signals to stimulate muscles for the desired movement. A copy of the signal is sent to the forward model to predict expected sensory feedback, which is then compared to the actual sensor feedback during the movement. This process is how the nervous system learns to improve control of body movements.

errors and may prompt motor adaptations if errors consistently occur. These errors may be viewed as a type of catch trial, as the exoskeleton behavior deviates significantly from nominal torque assistance. It is also currently unclear if there exists a threshold of error frequency where a user would modify their internal model or develop a different internal model when walking with imperfect exoskeleton control, resulting in different or sub-optimal gait strategies even during strides with nominal exoskeleton behavior. Several studies investigating the internal models for reaching movements in force fields have induced catch trials at frequencies of 1/6 to 1/7 (16.7 to 14.3%) [91, 51], but error frequencies may impact gait differently due to stability and other considerations for locomotion. There also exist various factors that may influence gait strategies, such as human-exoskeleton fluency and human trust in exoskeletons, which will be detailed in this section.

1.3.1 Human-Exoskeleton Fluency

Fluency is defined as the coordinated meshing of actions between the human and robot [39] and is a necessary component of human-robot interaction to consider when developing robots that will be adopted in the real world [20]. Human-robot interaction metrics are mainly evaluated in applications involving human supervisory control of robots, teleop-

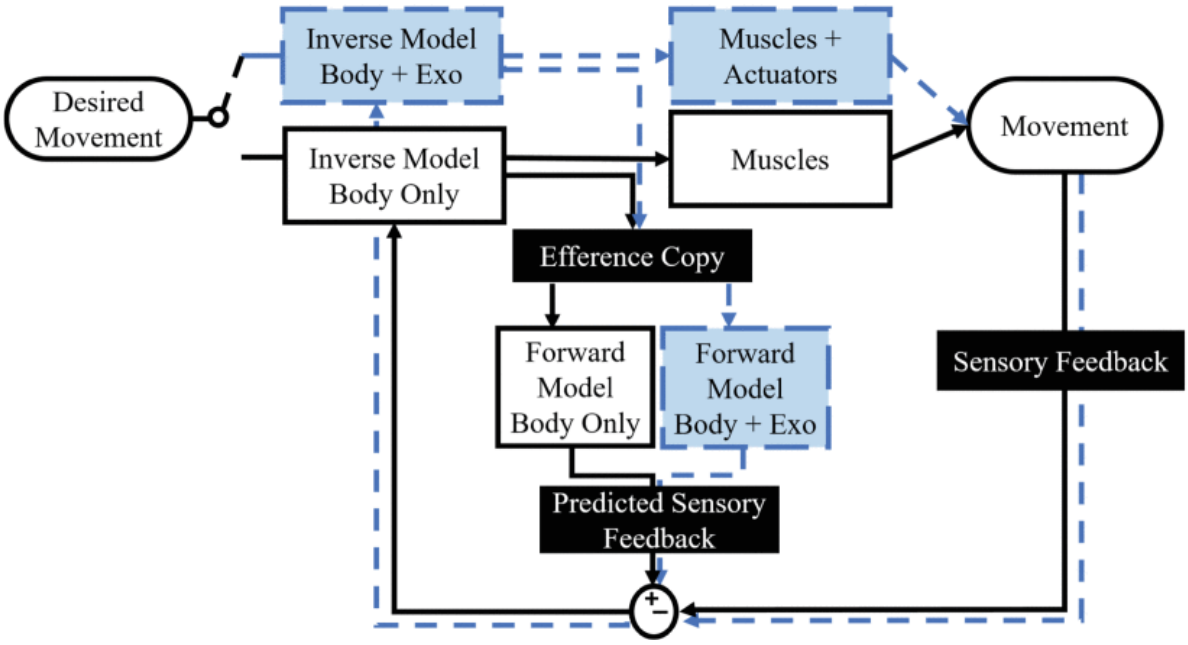

Figure 1.3: (From Hybart et al. [41]) Internal model of the coupled human-exoskeleton system, which accounts for the exoskeleton's actuators and dynamics in addition to the human's muscles and dynamics.

eration, autonomous vehicles, and human-robot social interactions [87]. Unlike these four application areas, exoskeletons are physically coupled with the human and directly apply forces upon their body. Thus additional metrics may be interpreted to align with the interactions that occur between humans and exoskeletons. Using the definition of fluency, we can then consider that human-exoskeleton fluency occurs when the human and exoskeleton's goals align. For example, human users may decrease muscular activity and metabolic cost when using exoskeletons designed to reduce energy expenditure. When exoskeleton errors occur, users may modify their gait strategy and underlying internal model to increase muscle activity in anticipation of repeated errors. This strategy may negatively affect fluency as increased muscle activity opposes the exoskeleton's goal of metabolic cost reduction. For a supervisory tasks that is not physically coupled, errors may be less noticeable and operators may underestimate the frequency and impact of errors [72, 9]. Thus, it is important to understand how exoskeleton errors impact gait strategies and human-exoskeleton fluency in order to inform performance requirements for exoskeleton algorithms.

Human-exoskeleton fluency can also be linked to embodiment of lower-limb exoskeletons. Embodiment describes the acceptance of an external object as part of one's own body and long-term use of the object may modify the body's representation in the sensory motor system [14, 10]. Studies have investigated how humans adopt a prosthesis to their body schema

after limb-loss, where embodiment of the prosthesis may impact the user's stability [42] and greater familiarity with the prosthesis may be connected to feelings of embodiment [24]. Exoskeletons are also objects that directly interface with humans and may be incorporated into the body's representation and internal models. Recently, Hybart et al. [41] determined that embodiment of lower-limb exoskeletons is dependent on whether the human can form an internal model that combines their own biological system dynamics with robotic dynamics (Fig. 1.3). Discrepancies between the exoskeleton's actions and the human's intentions may be registered as errors by the nervous system, affecting the internal model developed [41]. If the representations stored in the internal model and the actions of the exoskeleton are misaligned, this may negatively impact human-exoskeleton fluency, as the human's movements and strategies no longer align with the designed control.

1.3.2 Trust in Human-Robot Systems

Trust in human-automation systems is defined as "the attitude that another entity (e.g., human, machine, system) will help achieve a person's goals in a situation characterized by uncertainty and vulnerability" [54] and may be impacted by the automation's reliability [79]. Calibrated trust exists when the perceived and actual capabilities of the automation are aligned [54]. However, if the automation's perceived capabilities are higher than its actual capabilities, the user may over-trust the system and misuse the automation. Alternatively, if automation capabilities are perceived as lower than they actually are, the human will distrust the system, which may lead to disuse in situations where the exoskeleton could provide benefit. Studies involving simulated search-and-rescue and process-control tasks have shown that as automation reliability decreased from 100% to as low as 60%, the user's perceived trust in the system decreased [79, 15]. Even small degradations in fidelity, as low as 0.1% in near-perfect automation with supervisory control tasks, have been shown to significantly impact trust [27]. While studies have investigated trust and trust calibration with autonomous systems, human trust in exoskeletons during imperfect operation has not been explored as of this time.

Wearable robotic devices are designed to support specific tasks while interacting with humans similar to automation; however, wearable systems also physically interact with the human. The impact of errors on trust and perceived capabilities may be different when considering wearable systems. During supervisory control tasks, it is possible that humans will miss automation errors. However, exoskeletons directly apply torque on the human's body and the human-exoskeleton system is tightly coupled. The threshold to perceive an exoskeleton error in timing has been shown to be as low as 2.8% of a stride period [74].

Thus, exoskeleton errors may be more easily perceived, which impacts the effect of errors on trust. It is important to understand the effect of exoskeleton errors on trust, as it influences the user's behavior when interacting with the exoskeleton and the likelihood of adoption to the real world.

1.4 Adaptation Between the Human and Exoskeleton

Co-adaptation between a human user and exoskeleton involves changes to the exoskeleton torque output in response to real-time human adaptation of gait strategies. A co-adaptive control scheme draws inspiration from human-in-the-loop optimization, which modifies control laws to minimize the cost of walking for individual users [110, 30]. However, while HIL optimization results in a static optimal torque profile, co-adaptive control updates during real-time operation to continuously support various metrics of human performance, such as metabolic cost or muscle recruitment. Co-adaptive control can be viewed as a type of human-in-the-loop control, where the human is involved in the control loop and is actively performing a task (e.g. walking) while the robot provides support and guidance simultaneously. Control algorithms which continuously modify torque assistance in response to human actions and intentions may support human-exoskeleton fluency as the user adapts to the exoskeleton. Additionally, training protocols have been shown to support the formation of gait strategies that minimize metabolic cost [83]. In this section, we discuss current approaches to co-adaptive and human-in-the-loop control, as well as guided training protocols to encourage certain gait strategies.

1.4.1 Co-Adaptive Control

Control schemes to support adaptation between the human and exoskeleton have been an emerging area of interest in the exoskeleton community. Jackson et al. [47] demonstrated heuristic-based control of an ankle exoskeleton to support co-adaptation using EMG signals from muscles involved with ankle movement and ankle kinematics. The algorithm used muscle activity that worked cooperatively with and antagonistically against the desired plantarflexion torque supported by the exoskeleton to increase and decrease the exoskeleton assistance, respectively. Users were able to reduce metabolic cost by 22% and soleus muscle activity by 35% using the co-adaptive controller compared to normal walking and the controller was responsive to changes in each user's coordination strategies. While this study showed significant success, only ankle muscles and kinematics were used as inputs in the algorithm and it has been shown that assistive devices that act upon one joint may affect

the activity of muscles for another joint within the limb [21]. Thus, all joints across the lower-limbs should be evaluated and incorporated into co-adaptive algorithms to ensure that sub-optimal strategies using the hip or knee are not present when walking with an ankle exoskeleton.

A different approach to human-in-the-loop control leveraged variable impedance control to support human-robot collaboration across multiple joints of a lower-limb exoskeleton [60, 59, 40]. Impedance control regulates the interaction forces between the human and robot, which may improve exoskeleton compliance and comfort when walking with the exoskeleton. Li et al. [59] demonstrated two cooperative control frameworks of a 10 DoF exoskeleton that had active joints at the hip and knee and passive joints at the ankle. The control frameworks also incorporated an adaptive method to perceive and follow the human user's intentions and joint trajectories to minimize interaction forces. While this method was able to provide assistance to the user and incorporate multiple lower-limb joints, the control algorithm was developed for individuals with muscle injuries during rehabilitation to accurately track and follow the user's actions. Additionally, while Li et al. [59] were able to minimize interaction forces, they did not include measures of human performance, such as metabolic cost or muscle recruitment, which are commonly used to evaluate the effect of exoskeleton assistance for able-bodied users.

By combining the heuristic-based co-adaptive control developed by Jackson et al. [47] and incorporating all lower-limb joints similar to the impedance control methods, we can extend existing work on co-adaptive control to account for strategies involving joints and muscles higher in the leg kinematic chain. Additionally, utilizing muscle activity in the control framework gives additional insight on human intention from agonist-antagonist muscle activity when walking with ankle exoskeletons that was not included in control methods in [60, 59]. Increases in muscle activity across a joint may cause higher co-contraction, which stiffens the joint and may signify that a user is resisting the motions of the exoskeleton. Muscle activity is also linked to metabolic cost [89], and may be used as a metric that indirectly informs metabolic cost without respiratory measurements.

1.5 Aims of this Thesis

The literature discussed in this chapter has informed the direction of this thesis and has the following three main research questions:

1. What are the immediate effects of exoskeleton errors on human gait strategies?

2. What are the residual effects of exoskeleton errors on gait strategies?

3. How do we support human-exoskeleton collaboration through exoskeleton control?

To address these questions, this project is the following corresponding aims:

1. Characterize the immediate effects of exoskeleton errors on human gait strategies (Chapter 2)
2. Characterize the residual effects of exoskeleton errors on gait strategies in terms of human-exoskeleton fluency (Chapter 3)
3. Develop a co-adaptive exoskeleton controller which incorporates all major lower-limb joints and muscles to support human-exoskeleton fluency

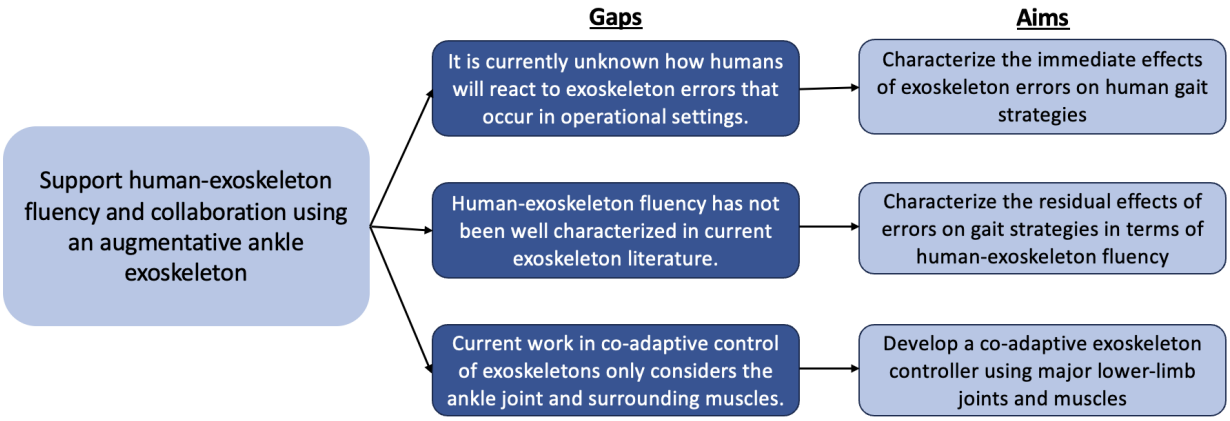

Figure 1.4: The overarching goal of this thesis, the identified gaps in literature, and corresponding aims of this thesis.

We introduced relevant work on exoskeleton control, human movement, and co-adaptive control in the literature that we will incorporate to address each of the gaps and aims identified in the thesis (Fig. 1.4). Chapter 2 of this thesis addresses the immediate effects of catch trials (exoskeleton errors), which informs our understanding of the internal model formed when walking with an exoskeleton. The work presented in Chapter 2 also is one of the first in the literature to investigate and characterize trust in exoskeletons. Chapter 3 investigates the residual effects of different fixed levels of exoskeleton errors on gait strategies, task performance, and the underlying internal models when normal torque assistance is present. Both Chapters 2 and 3 interpret gait strategies in the context of human-exoskeleton fluency, trust, and internal model development. Chapter 4 proposes a co-adaptive controller to support fluent gait strategies by modifying torque assistance in response to changes in joint kinematics and muscle activity across the lower-limbs. Finally, Chapter 5 provides the proposed timeline of the remaining work of this thesis and the proposed contributions to the field.

CHAPTER 2

Immediate Effects of Exoskeleton Errors on Gait Strategies

In addition to human-exoskeleton fluency and trust, there exist several other factors that can impact motor strategies. Task performance time and accuracy are considered when performing a goal-oriented task. Gait strategies are also linked with energy expenditure [103], stability [34], and comfort [101]. These factors may interact, as different motivational prompts have supported interactions between metabolic cost and stability [69]. These interactions are beginning to be examined with exoskeletons [33]. Understanding trust and internal model development in context with human-exoskeleton fluency and task accuracy will broaden our understanding of tightly-coupled human-machine systems and support requirement definition for exoskeletons.

In this study, we introduced catch trials via missed actuations to understand how humans interact with imperfect exoskeleton algorithms found in operational settings. Catch trials also allow us to understand the internal model developed when adapting to a powered exoskeleton and how that model changes with repeated exoskeleton errors. We explored human-exoskeleton fluency and gait characteristics when completing a targeted stepping task. We hypothesized that there would be time-dependent changes in (1) step characteristics (step length and width), (2) task performance (step accuracy), (3) joint kinematics (selected peak hip, knee, and ankle angles within the stride), and (4) muscle activity in response to catch trials.

These measures are interpreted in the context of human-exoskeleton fluency, trust, and internal model development. In this study, human-exoskeleton fluency may manifest as a decrease in muscle activation used to support plantarflexion during normal operation. If fluency is negatively impacted by exoskeleton errors, muscle activation may increase to support plantarflexion and task performance, which opposes this exoskeleton's primary goal. Changes in trust may result in changes in gait strategies over the course of the experiment. For instance, muscle activity may increase over time as users learn to anticipate errors in

exoskeleton performance. Finally, catch trials will allow us to understand the internal models developed while walking with a lower-limb exoskeleton.

2.1 Materials and Methods

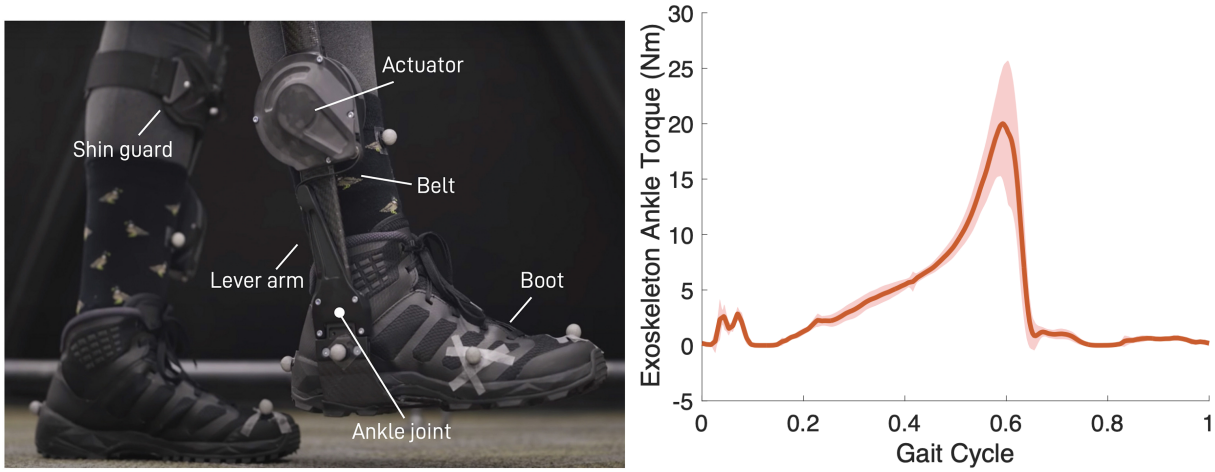

Figure 2.1: (top) Powered ankle exoskeleton, which provides assistance by applying torque via the inelastic belt attached to the lever arm (DpEb45, Dephy Inc) [2]. (bottom) Exoskeleton torque profile applied at all non-catch trial strides for one representative participant. The solid line is the average torque applied throughout the stride and the shaded region includes ±1 standard deviation.

2.1.1 Participants

Participants (N = 15, age = 30.7±9.9 years (mean±SD), height = 1.73±0.10 m, mass = 74.9±13 kg, leg length = 931.6±64.2 mm, 6 female and 9 male) provided written informed consent. The exclusion criteria included lower extremity injuries within the past 6 months and the use of assistive walking devices. The experimental protocol was approved by the Massachusetts Institute of Technology Committee on the Use of Humans as Experimental Subjects.

2.1.2 Experimental Setup

Participants walked on a split-belt, instrumented treadmill in a Computer Assisted Rehabilitation Environment (CAREN) System (Motekforce Link, Amsterdam, the Netherlands), which included an 18-camera optical motion capture system (Vicon Motion Systems Ltd,

Oxford, UK) and a 24-foot diameter virtual reality dome with a 360 degree projection screen. Reflective markers were placed according to the Vicon Plug-in Gait model, adjusted for the exoskeleton by placing the lower limb markers on the lateral side of the exoskeleton when necessary. Markers were also placed on the treadmill on the four corners of the stepping target. Electromyography (EMG) sensors (Delsys, Natick, MA, USA) were placed on following 7 muscles on each leg: tibialis anterior (TA), soleus (SOL), medial gastrocnemius (GAS), biceps femoris (BF), rectus femoris (RF), tensor fasciae latae (TFL), and gluteus maximus (GMax). The treadmill, motion capture, EMG sensors, and exoskeleton were controlled and time-synchronized via D-Flow software. Motion capture and EMG data were collected at 100 and 2000 Hz, respectively. Participants wore the Dephy ExoBoot on both legs (DpEb504, Dephy Inc, Maynard, MA, USA) [63]. Torque was applied at push-off during the stance phase of the gait cycle, learned from 25 strides (Fig. 2.1).

2.1.3 Protocol

Anthropometric measures were collected prior to walking with the exoskeleton. Leg length was measured as the distance from the anterior superior iliac spine to the medial malleolus. Participants were introduced to a targeted stepping task (a 320 mm long projected rectangle that spanned the treadmill width), while walking at 1.25 m/s through a virtual city scene. The length of the stepping target was chosen to be the length of the largest exoskeleton boot size, a Men's size 13. Participants were asked to focus on aiming their heel at the horizontal center-line of the target at the end of every stride. Each participant first underwent a training period, where they walked for 30 minutes with the exoskeleton powered on with torque applied during each stride and completed the stepping task. Then, participants were given a 5-minute break before proceeding to the testing portion, where catch trials were randomly dispersed among normal strides (1900 strides total), with 20-100 strides between each catch trial. 32 catch trials (1.68% of 1900 total strides; 16 per limb) were included by not actuating the exoskeleton for a single stride. The number of catch trials was selected after a power analysis to ensure there were sufficient number of trials to assess significant differences between catch trials and baseline behavior. The exoskeleton algorithm also included a recovery period after each catch trial, where the exoskeleton torque ramps up from 0% to 50% of the normal torque on the first stride after a catch trial, then 80% on the second stride after a catch trial, and finally back to 100% from the third stride onward. These strides were not included in the analysis to avoid confounding factors.

2.1.4 Data Analysis

Gait cycles were segmented with a custom MATLAB script using the treadmill's force plates to identify heel strikes. Normalized step length (NSL), normalized step width (NSW), and task accuracy were calculated using heel marker positions. Step length and step width were the difference in anterior and lateral heel marker position at consecutive heel strikes, respectively, and were normalized by leg length. Task accuracy was calculated as the difference between anterior footfall locations at each heel strike and the center-line of the stepping target. Acceptable task error was within ±160 mm of the center-line, as the target was 320 mm long. Joint kinematics were calculated per stride according to the Plug-in Gait model. Three metrics of interest were identified for each stride (Fig. 2.2) – maximum hip flexion during swing, minimum knee flexion after loading response, and maximum ankle plantarflexion. Joint kinematics and muscle activity were separated to the ipsilateral leg (the leg on which the catch trial occurred) and the contralateral leg (the opposite leg).

EMG data were pre-processed using a high-pass 3rd-order Butterworth filter at 40 Hz, rectification, and a low-pass 3rd-order Butterworth filter at 10 Hz. EMG data for each muscle was normalized to the peak value across the entire protocol. Heel strikes and toe off identified from force plate data were used to segment the EMG data to strides, then stance and swing phases. To quantify changes in muscle activation, the root-mean-square (RMS) value of each muscle was calculated. Muscle activity for BF and RF were segmented into the stance and swing phase, as they are biarticular muscles across the knee and hip and may result in changes at the knee during stance and the hip during swing. The GAS RMS values were calculated across the entire stride period even though it is a biarticular muscle, as the muscle activation occurs in a single burst. The RMS values for the SOL, TA, GMax, and TFL were calculated across the entire stride period, as they primarily act across a single joint.

Steps and strides were segmented into the following Trial Type: the step/stride of the catch trial (CT), 1 step/stride after to the catch trial (CT+1), and baseline (B) as the 6th to 25th step/stride after each CT. NSL, NSW, and task accuracy were evaluated when parsed by step. Joint kinematics and muscle activity metrics were evaluated when parsed by stride.

2.1.5 Statistical Analysis

A custom R (version 4.2.1, R Foundation) script was used to compute all statistical models. All participants showed similar trends for joint kinematics, step characteristics, and task accuracy, so independent linear mixed-effects models were fit for each metric. Joint kinematics models were fit with factors of Trial Type (2 fixed levels, CT and B), Timing (continuous,

[1,32]), and a random factor of Participant. Step characteristics and task accuracy models were fit with an additional Trial Type (3 fixed levels, CT, CT+1, B) to capture the effects of both the ipsilateral and contralateral legs, Timing (continuous, [1,32]), and a random factor of Participant. The Timing factor was determined to be a continuous variable, as time increases linearly throughout the experiment and a slope was fitted to each CT and B condition to investigate the effects of time.

A linear model was fit for each participant for all muscle activity RMS metrics to evaluate the effect of catch trials and timing for each individual, as previous studies have shown individual strategies for muscle adaptation with exoskeletons [1]. Each linear model was fit with a random intercept, Trial Type (2 fixed levels, CT and B), and Timing (continuous, [1,32]) with significance level at $\alpha = 0.05$.

2.2 Results

2.2.1 Task Accuracy and Step Characteristics

There was an effect of Participant on NSL, NSW, and Task Accuracy, but no effect due to Trial Type or Timing (Table 2.1). Participants maintained their step characteristics and task performance with the absence of the actuation during catch trials (Fig. 2.3).

2.2.2 Joint Kinematics

There were main effects of Trial Type and Timing on the ipsilateral and contralateral joint ankle metrics. Catch trials resulted in a significant difference between CT and B on the ipsilateral leg (Fig. 2.4). During ipsilateral CT, hip flexion during swing increased (B vs CT: $p < 0.001$), minimum knee flexion after loading response increased (B vs CT: $p < 0.001$), and peak plantarflexion decreased (B vs CT: $p < 0.001$). The slope fitted to the timing factor of ipsilateral knee flexion at CT over time was significantly greater than at B (Timing: $p < 0.005$). During contralateral CT, peak hip flexion during swing increased (B vs CT: $p < 0.001$) and peak plantarflexion decreased (B vs CT: $p < 0.001$) to a lesser extent compared to the ipsilateral leg, as shown by the fitted estimates. Contralateral minimum knee flexion was not significantly impacted by catch trials.

2.2.3 Muscle Activity

There were main effects of Trial Type and Timing on muscle activity across the hip, knee, and ankle joints. Changes in muscle activity about the ipsilateral and contralateral joints were

observed on the individual level (Fig. 2.5). There were main effects of Trial Type and Timing for select participants. TFL, GMax, RF, and BF on both legs were evaluated in the swing phase of gait (Fig. 2.5a,d). At ipsilateral CT, 11 (73%) participants significantly increased TFL activity ($p < 0.01$, mean=62.7%), 5 (33%) participants increased BF activity during swing ($p < 0.05$, mean=15.1%), 3 (20%) participants increased GMax activity ($p < 0.01$, mean=18.9%), and 4 (27%) participants increased RF activity during swing when compared to B ($p < 0.05$, mean=20.5%). At contralateral CT, 2 (13%) participants significantly increased TFL activity ($p < 0.05$, mean=21.6%), 3 (20%) participant increased BF activity during swing ($p < 0.01$, mean=13.0%), 1 (6%) participant increased GMax activity ($p < 0.005$, 16.3%), and 6 (40%) participants increased RF activity ($p < 0.05$, mean=23.7%) during swing when compared to B.

Knee muscle activity was assessed by changes in GAS, BF, and RF during stance. At ipsilateral CT, 6 (40%) participants decreased GAS activity ($p < 0.05$, mean=-12.0%), 6 (40%) participants increased RF activity ($p < 0.01$, mean=13.5%), and 2 (12%) participant increased BF activity ($p < 0.05$, mean=25.5%) when compared to B. At contralateral CT, 9 (60%) participants increased GAS activity ($p < 0.05$, mean=13.8%), 10 (67%) participants increased RF activity ($p < 0.05$, mean=25.4%), and 13 (87%) participants increased BF activity ($p < 0.05$, mean=71.4%).

Ankle muscle activity assessed by changes in GAS, SOL, and TA, which were affected by CT. At ipsilateral CT, 11 (73%) participants increased SOL activity ($p < 0.05$, mean=13.2%) and 6 (40%) participants increased TA activity ($p < 0.05$, mean=17.1%). At contralateral CT, 12 (80%) participants increased SOL activity ($p < 0.05$, mean=12.8%) and 9 (60%) participants increased TA activity ($p < 0.05$, mean=25.0%).

Table 2.1: Summary of statistics for linear mixed-effects models fitted to step characteristics and task accuracy for 15 participants with a total of 10,480 steps for Normalized Step Length, Normalized Step Width, and Task Error. CT refers to all catch trial steps, CT+1 is the first step after each CT, and B includes the 6th to 25th steps after each CT.

	Normalized Step Length		Normalized Step Width		Task Error	
	Estimate	p	Estimate	p	Estimate	p
Participant	0.934	**<0.001**	0.156	**<0.001**	-92.93	**0.004**
CT+1 vs CT	-0.020	0.373	0.007	0.079	-7.346	0.586
B vs CT	0.004	0.800	0.004	0.115	-1.673	0.856
Timing	<-0.001	0.248	<-0.001	0.116	0.059	0.902
CT+1 * Timing	0.002	0.125	<-0.001	0.991	0.266	0.692
B * Timing	<0.001	0.598	<-0.001	0.165	0.540	0.269

Table 2.2: Summary of statistics for linear mixed-effects models fitted to joint kinematics for 15 participants with a total of 9,881 strides for Ipsilateral and Contralateral Peak Hip Flexion, Minimum Knee Flexion, and Peak Plantarflexion. CT refers to all catch trial strides and B includes the 6th to 25th strides after each CT.

	Ipsilateral						Contralateral					
	Peak Hip Flexion		Min Knee Flexion		Peak Plantarflexion		Peak Hip Flexion		Min Knee Flexion		Peak Plantarflexion	
	Estimate	p	Estimate	p	Estimate	p	Estimate	p	Estimate	p	Estimate	p
Participant	2.289	**<0.001**	3.637	**<0.001**	-10.11	**<0.001**	1.735	**<0.001**	0.320	0.065	-0.575	**0.003**
B vs CT	-2.428	**<0.001**	-3.543	**<0.001**	10.20	**<0.001**	-1.828	**<0.001**	-0.172	0.328	0.745	**<0.001**
Timing	0.002	0.794	0.028	**0.002**	-0.007	0.545	-0.013	0.056	-0.005	0.613	-0.0223	**0.029**
B*Timing	0.003	0.651	-0.038	**<0.001**	0.685	0.548	0.017	**0.017**	-0.005	0.556	0.0226	**0.031**

2.3 Discussion

This study explored the interaction of human-exoskeleton fluency, task accuracy, muscle activity, and gait characteristics in response to pseudo-random exoskeleton errors during walking. Exoskeleton torques can be learned and anticipated by developing internal models to represent their anticipated dynamics. However, human-exoskeleton fluency may shift across the continuum of trust with the exoskeleton. For instance, if a user becomes less trusting of the system, they may prioritize stability over task performance and thus increase muscle activation, which conflicts with the goal of this exoskeleton. These changes in trust may be assessed by differences in performance throughout the study, which were assessed here using task accuracy, joint kinematics, muscle activity, and step characteristics.

2.3.1 Gait Strategies and Task Performance

Our first two hypotheses posited that there would be changes in step characteristics and task accuracy in response to catch trials. In our initial analysis, Wu et al. [106] found there was not evidence that missed actuations at the provided level affect NSL, NSW, or task accuracy. As the exoskeleton torque was removed for the catch trials, the motor actions must be adjusted to maintain task goals.

Our third hypothesis that joint kinematics would have time-dependent changes in response to catch trials was supported by the data and the changes were driven by muscle activation modulation. Peak ipsilateral ankle plantarflexion decreased during catch trials when the exoskeleton's assistive torque was not applied (Fig. 2.2f, 2.4c). A previous study observed participants reduced their muscle-generated plantarflexion after adapting to the same exoskeleton, which was interpreted as fluency between the human and exoskeleton [1]. These reductions were interpreted as the participants coordinating with the exoskeleton. During catch trials in the present study, the exoskeleton did not generate assistive plantarflexion torque; thus, participants relied on their muscle-generated plantarflexion for push-off. The

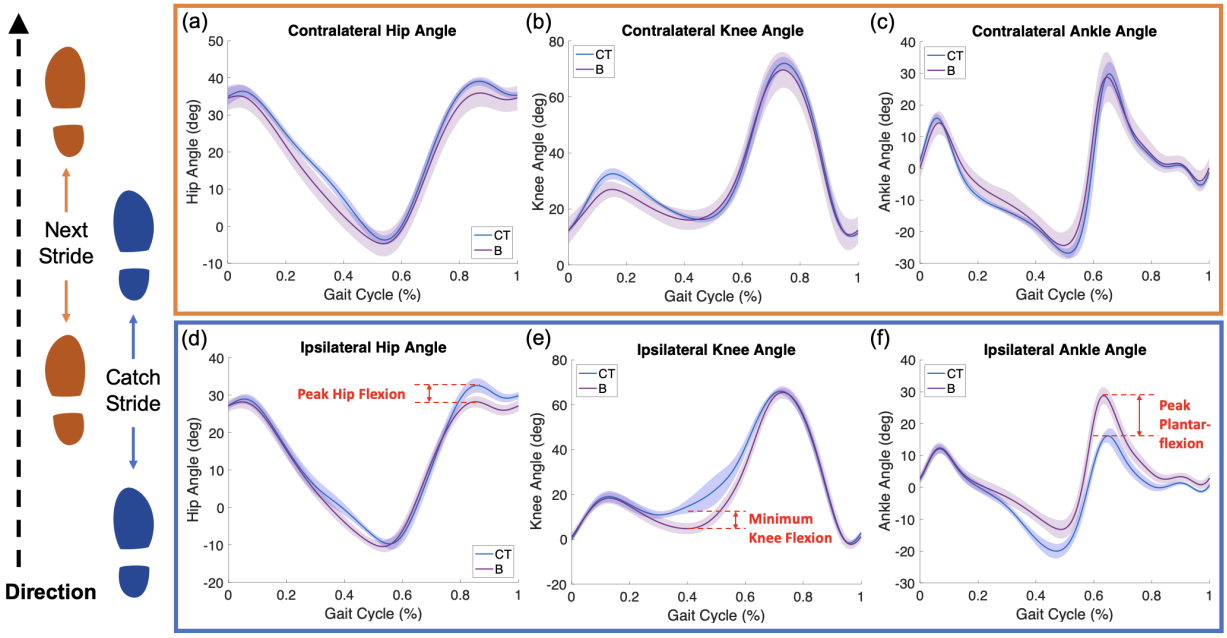

Figure 2.2: Hip, knee, and ankle kinematics for ipsilateral leg (blue, d-f) and contralateral leg (orange, a-c) for a representative participant. Flexion/plantarflexion is positive and extension/dorsiflexion is negative. Regions of interest include peak hip flexion during swing, knee flexion after loading response, and peak ankle plantarflexion, indicated by the red arrows and dotted lines. CT conditions include 16 strides each and B contains the 6th to 25th strides after each catch trial.

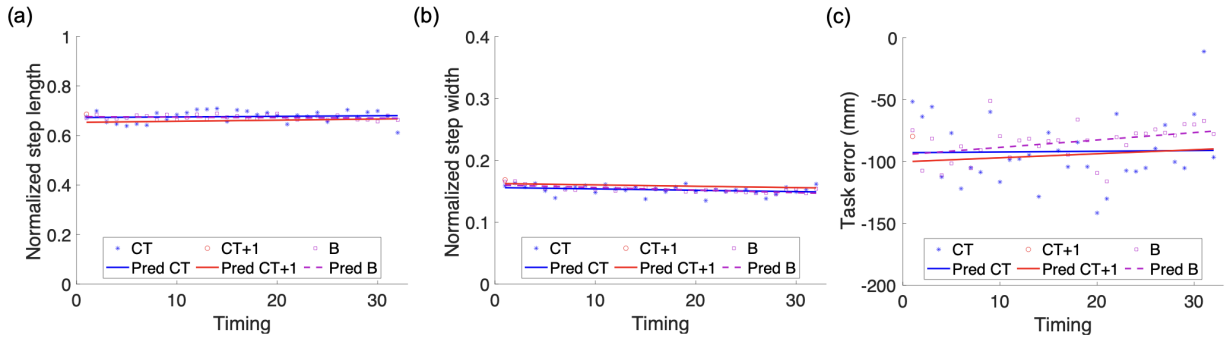

Figure 2.3: (a) NSL, (b) NSW, (c) and task accuracy in response to catch trials (N=15). CT and CT+1 conditions include 32 steps and B contains 6th to 25th stride after each catch trial.

ankle muscles that could compensate for the lost plantarflexion include the ipsilateral SOL and GAS. While 53% of all participants increased ipsilateral SOL activation, 42% of those participants also decreased ipsilateral GAS activation. Reductions in this muscle activity and the resulting plantarflexion moment align with the decreased peak ankle angles observed.

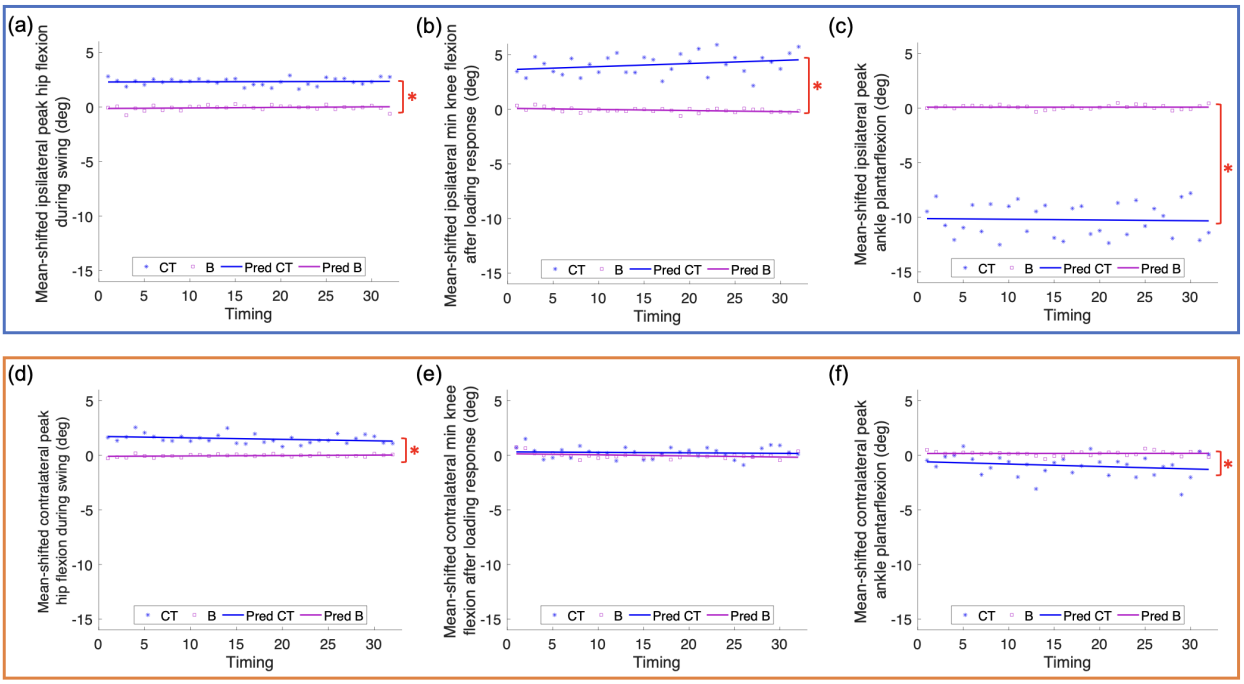

Figure 2.4: Mean-shifted (a-c) ipsilateral and (d-f) contralateral peak hip flexion during swing, minimum knee flexion after loading response, and maximum ankle plantarflexion in response to catch trials (N=15). Joint angles were shifted by subtracting the mean of each participant's baseline. CT conditions include 16 strides each and B contains the 6th to 25th strides after each catch trial. Red brackets marked with bars indicate that CT vs B were significantly different.

The reduced plantarflexion then affected behavior in the proximal joints of the kinematic chain. In our previous study, Wu et al. [106] observed that ipsilateral knee flexion increased after loading response due to a diminished knee extension moment during catch trials (Fig. 2.2e, 2.4b). Ipsilateral GAS activity decreased to mitigate the increase in knee flexion, as the GAS acts bilaterally for ankle plantarflexion and knee flexion. 40% of participants also increased RF activation, which would generate additional knee extension torque in response to increased knee flexion, thus stiffening the knee and preventing the leg from buckling.

The changes in ankle and knee kinematics align with the feedforward mechanisms of an internal model of the exoskeleton. These data support that participants may have learned and applied internal models that support human-exoskeleton fluency by lessening their contribution to total ankle plantarflexion during baseline. Wu et al. [106] postulated that participants used visual feedback and increased ipsilateral hip flexion during swing to correct for potential stepping task errors during catch trials (Fig. 2.2d, 2.4a). The increase in hip flexion compensated for the decreased ankle torque during push-off, resulting in no net change in NSL and task accuracy. The change in ipsilateral hip flexion was driven by the increase in TFL

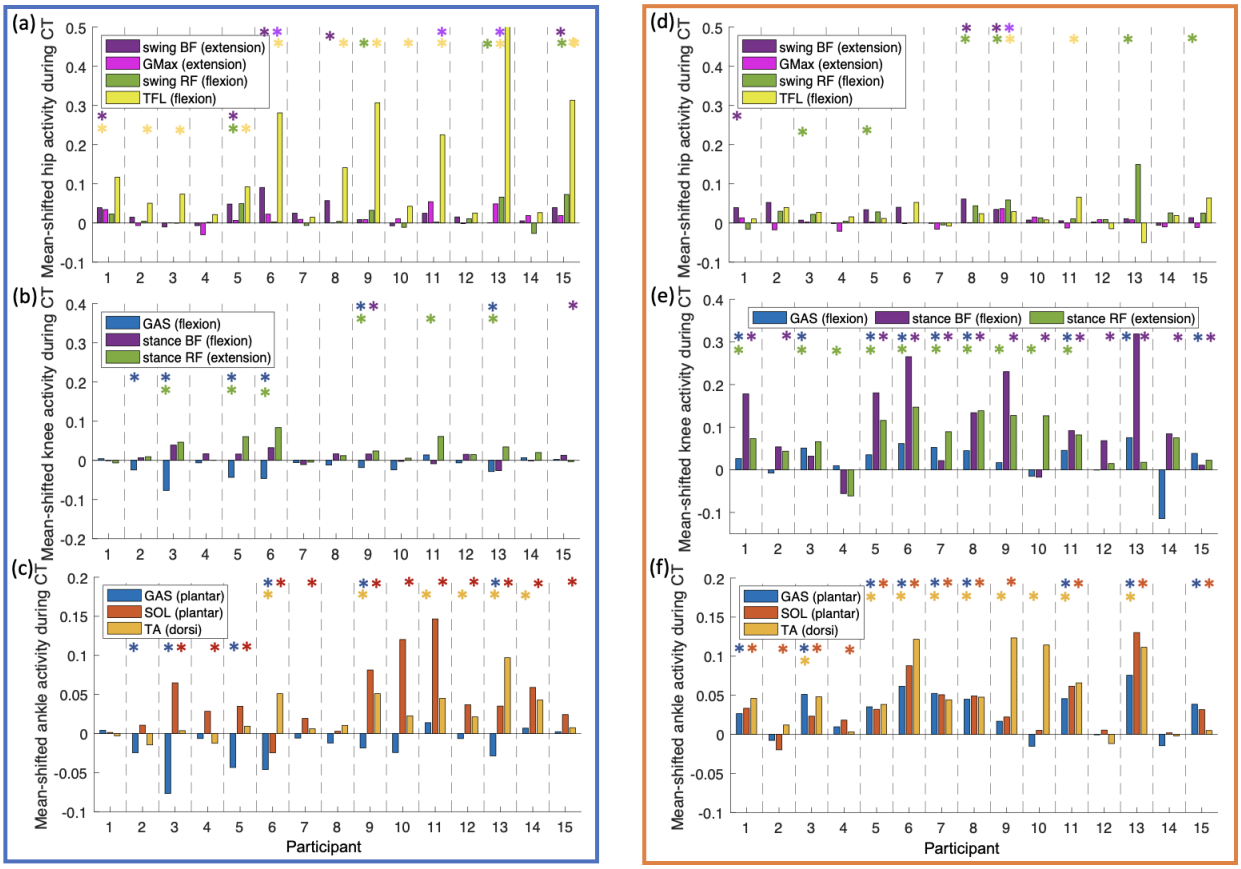

Figure 2.5: Changes in muscle activity about the (a-c) ipsilateral and contralateral (d-f) hip, knee, and ankle during catch trials. Each bar represents the average difference between CT and the mean of B for each participant. Flexion/extension is about the respective joint shown in each plot. Stars indicate significant differences between CT and B. CT includes all catch trials and B includes the 6th to 25th stride after each catch trial.

activity during swing, which is a secondary hip flexor. There was a corresponding increase in BF and GMax activation, which act as antagonistic muscles to the TFL, and increased hip stiffness to stabilize the leg. The modulation of hip flexion was driven by increases in muscle activation about the hip, which opposes the intended design goals of the exoskeleton to reduce energy expenditure and impacts human-exoskeleton fluency.

Following the ipsilateral catch trial, an exoskeleton torque was applied on the contralateral leg. There was a smaller but significant change in the contralateral hip and ankle angles, which is reflected by the changes in contralateral muscle activity. While there was no significant change in contralateral knee kinematics, contralateral muscle activity about the knee and ankle increased for 87% of participants during catch trials. Muscle activation of the SOL and GAS was greater in the step following the catch trial on the contralateral leg for 80% and 60% of participants, respectively. This increase aligns with participants expecting

the contralateral actuation to also be removed. However, this actuation was present for the contralateral leg. 60% of participants increased activation of the TA, which would stiffen the joint to limit, but does not eliminate, excess ankle motion from the unneeded additional torque provided by the user when the exoskeleton is actuating. The additional plantarflexion torque then affected joints more proximal in the leg's kinematic chain, thus passively increasing hip flexion rather than the active change seen on the ipsilateral leg. As the participant proceeded from contralateral stance to swing, the exoskeleton operated without a missed actuation, thus eliminating the need for active compensation at the hip.

While the data support the formation of an internal model corresponding with normal exoskeleton operation, there is no indication of an internal model of the catch trials. The stiffening of the contralateral joints following a catch trial may indicate that an internal model of the catch trials was not formed, as studies have shown that people may stiffen their limbs in response to novel forces rather than adapting motor strategies [91]. If an internal model of the catch trials were formed, gait strategies at CT would change over time, as participants learn and adapt to the missed actuations. However, there was no significant change in most CT joint kinematics over time for both legs. This study had a low level of exoskeleton errors (1.68%), which may have been too infrequent for participants to form an internal model of missed actuations.

2.3.2 Implications for Trust in Exoskeletons

Trust in wearable robotics, such as exoskeletons, has been largely undefined. A recent framework proposed the concept of relational trust, which may be adapted to describe trust in exoskeletons. Relational trust describes the relationship where humans and automation are considered agents engaged in a joint activity by a shared awareness of each other being engaged in the activity [16]. The relational trust framework states that the behavior of each agent depends on the environment, tasks, and interactions with other agents over time. The framework portrays automation as an agent that is capable of adapting to both the human and environment, which differs from earlier frameworks with primarily supervisory control tasks. Thus, the automation described by relational trust is similar to robots that are able to perform tasks while interacting with both the human and environment. The concept of relational trust may be applied to human-exoskeleton systems, as exoskeletons may modulate behavior based on the human, the environment, and estimated task. The framework also highlights scenarios where the human and automation's goals and tasks align, which we can relate to human-exoskeleton fluency.

By adapting the concept of relational trust proposed for human-automation teams [16],

the actions of the exoskeleton then affect the human's trust in the system, which may cause them to modulate their own behavior depending on the environment and their tasks. In this study, we introduced an exoskeleton algorithm that exhibited operational errors of missed actuations throughout the experiment. If the human's trust in the system changed over time, the human would adjust their behavior over the course of the experiment by changing their gait strategies. However, there were no significant differences in step characteristics and task error over time for trial types CT, CT+1, and B. (Table 2.1, Fig. 2.3). Ipsilateral minimum knee flexion and contralateral ankle plantarflexion did show a significant change over time, but the slope estimates were small and thus deemed not operationally relevant. The difference between trials when normalized by the standard deviations was less than 0.3, indicating small effect sizes (0.87° increase in ipsilateral knee flexion over CT trials with average standard deviation = 3.18°, 0.69° decrease in contralateral plantarflexion over CT trials with average standard deviation = 3.29°) (Table 2.2, Fig. 2.4). All other joint kinematics metrics did not change over the course of the experiment. This observation suggests trust was maintained throughout the study for this reliability of the system. If trust decreased, there may be greater hip flexion, ankle plantarflexion, and muscle activity about those joints across additional steps as the user anticipates the loss of torque and attempts to compensate. This study had catch trials for 1.68% of the strides. The frequency of catch trials should be increased in future studies to probe how gait strategies are modifications to characterize changes in users' trust.

2.3.3 Limitations and Future Work

This study supports that exoskeleton users adjust their joint kinematics and muscle activity to compensate for the absent exoskeleton torque to meet task performance goals, impacting human-exoskeleton fluency. A limitation of this study is the assumption that all participants were fully adapted to the exoskeleton after the 30-minute training period, as motor strategies may change during adaptation. Different and more complex systems may result in other observed strategies, as the exoskeleton in this study was intended to reduce energy consumption and only applied torques about the ankle. For instance, users may modify joint kinematics and muscle activity differently when experiencing errors with an exoskeleton that affects multiple joints. Our study also involved an exoskeleton algorithm that experienced errors 1.68% of all strides, which is equivalent to a 98.32% accuracy. Future work will introduce higher error rates to determine if there exists an error threshold where users will permanently alter gait strategies to anticipate errors when walking with an ankle exoskeleton, thus affecting system usability. This future study with various error rates will also

continue to explore if trust is impacted by imperfect exoskeleton algorithms and develop a quantitative measure for trust in exoskeletons.

2.4 Conclusion

This study explored the impact of missed exoskeleton actuations on users' human-exoskeleton fluency, task performance, muscle activity, and gait characteristics. Participants maintained acceptable task accuracy by increasing ipsilateral hip flexion and muscle activity when the exoskeleton did not provide an assistive torque. During the stride after a missed actuation, participants increased contralateral joint stiffness and plantarflexion torque to support task accuracy. Human-exoskeleton fluency was impacted by catch trials as ipsilateral hip and contralateral knee and ankle muscle activity increased in response to catch trials, but trust was maintained throughout the study since gait strategies did not change over time. Understanding the interactions between human-exoskeleton fluency and gait strategies will support defining the design requirements for acceptable error rates as well as developing adaptive algorithms for exoskeleton controllers. For instance, future controllers may modulate behavior based on quantitative measures of fluency and trust.

CHAPTER 3

Emergent Gait Strategies Defined By Cluster Analysis When Using Imperfect Exoskeleton Algorithms

In Chapter 2, random errors were introduced during exoskeleton operation by not applying an expected exoskeleton torque while participants completed a targeted stepping task. The study used an algorithm with approximately 2% error, or 98% accuracy, and found that step characteristics and task accuracy were not impacted by exoskeleton errors during missed actuations and strides with normal torque as users adapted their joint kinematics during errors to perform the stepping task. The level of error in the study was relatively low, so it is important to understand how more frequent exoskeleton errors will impact stepping strategies and task performance. For instance, it is possible that users will begin to increase muscle activation as they anticipate repeated errors, which is against the goals of the exoskeleton and would negatively impact human-exoskeleton fluency.

In this study, we introduce exoskeleton algorithms with defined error rates in order to understand how users respond to more frequent errors. We hypothesized that there would be time-dependent and algorithm-dependent changes in (1) joint kinematics, (2) muscle activity, and (3) task performance during the nominal steps. We also hypothesized that higher levels of error would cause larger changes in the above metrics. Our initial individual linear model analysis revealed various gait strategies across participants and error rates (Appendix B), so we utilized a k-means clustering to identify key behavior. Gait strategies were defined using a k-means cluster analysis on a reduced set of gait features involving joint kinematics, muscle activity, and task performance. These results will be interpreted in the context of human-exoskeleton fluency and can inform exoskeleton design requirements in operational environments. We also evaluated user perceptions of exoskeleton performance, task accuracy, and future exoskeleton usage probability (Appendix A).

3.1 Materials and methods

3.1.1 Participants

Participants (N = 22, age = 25.3±5.0 years (mean±SD), height = 1.67±0.30 m, mass = 68.0±9 kg, leg length = 903.0±43.7 mm, 12 female and 10 male) provided written informed consent. Participants were excluded if they had a lower extremity injury within the past 6 months or used an assistive walking device. The protocol was approved by the University of Michigan Institutional Review Board (HUM00217656).

3.1.2 Experimental Setup

Participants walked on a treadmill in a room equipped with a 10-camera optical motion capture system (Vicon Motion Systems Ltd, Oxford, UK). Reflective markers were placed on the participants according to the Vicon Plug-in Gait full-body model. Markers were adjusted for the exoskeleton by placing the lower limb markers on the lateral side of the exoskeleton when necessary. Electromyography (EMG) sensors (Cometa, Bareggio, Italy) were placed on the following 7 muscles on each leg: tibialis anterior (TA), soleus (SOL), medial gastrocnemius (GAS), biceps femoris (BF), rectus femoris (RF), tensor fasciae latae (TFL), and gluteus maximus (GMax). Motion capture and EMG data were collected at 100 and 2000 Hz, respectively. Study participants wore the Dephy ExoBoot on both legs (Fig. 2.1) (DpEb504, Dephy Inc, Maynard, MA, USA) [63]. The ExoBoot applied torque at the ankle at push-off during the stance phase of the gait cycle, learned from 25 strides, which is the same as Chapter 2 [106].

3.1.3 Protocol

Anthropometric measures were collected prior to walking with the exoskeleton. Leg length was measured as the distance from the anterior superior iliac spine to the medial malleolus. Participants were given a target stepping task, which was a 320 mm-long region marked along the sides of the treadmill, while walking at a fixed speed of 1.2 m/s. A targeted stepping task was chosen as foot placement is an important component of gait in an operational environment, such as stepping off a curb or avoiding an obstacle on the ground. Task accuracy may then be used to assess prioritization of the task with respect to coordinating with the exoskeleton. Participants were asked to aim their heel at the center-line of the target region at the end of each stride. The stepping target length was chosen to be the length of the largest exoskeleton boot size, a Men's size 13.

Participants underwent a training protocol where they walked with the stepping target for 15 minutes with the exoskeleton powered on and torque applied during each stride (Fig. 3.1). The Dephy exoskeleton applied a plantarflexion torque about the ankle during mid-late stance and reverted to a zero-torque control modality during the swing phase. The controller adjusts the torque-angle relationship as a function of estimated walking speed, where dorsiflexion stiffness and plantarflexion passive power increase as walking speed increases.

Participants were then separated into two groups ($N = 11$ per group), which experienced the exoskeleton control algorithm with fixed error rates in different orders. There were 5 different error rates: 0%, 2%, 5%, 7%, and 10% error. This translates to controller accuracies of 100%, 98%, 95%, 93%, and 90%, respectively. Errors were introduced randomly throughout each trial by not actuating the exoskeleton for a single stride. We chose errors of no exoskeleton assistance rather than adjustment of control parameters for this study, as it has been shown that individuals may exhibit different sensitivities toward parameters such as actuation timing [74], which may introduce additional confounding factors. The exoskeleton algorithm also included a recovery period after each error, where the exoskeleton gradually ramps up from 0% to 100% between the error stride and the third stride after.

Participants experienced each controller twice for a total of 10 trials in one of two fixed orders. A fully randomized order was not selected as it creates difficulty in disambiguating between order and participant effects. By selecting two fixed orders, we can begin to examine the effect of order separate from participant variability. Group 1 started with a 0% error controller, increased to 10% error, and then decreased to 0% error. Group 2 started with a 10% error controller, decreased to 0% error, and then increased to 10% error. Details on the groups and control algorithms are shown in Table A.1. The number of strides for 2% error trials was higher than other trials to ensure an adequate amount of errors within the trial, verified via power analysis.

3.1.4 Data Analysis

Gait cycles were segmented with a custom MATLAB script by using the heel marker data from motion capture to identify heel strikes. Absolute task error was calculated as the absolute value of distance between each heel strike and the center-line of the stepping target. Acceptable absolute task error was determined as ≤ 160 mm, which is half of the 320 mm-long target. Joint kinematics were calculated according to the Plug-in Gait model. Four metrics of interest were identified for each stride according to our previous study [106] – maximum hip flexion during swing, minimum knee flexion during loading response, maximum knee flexion during swing, and maximum ankle plantarflexion. These metrics were shown to be

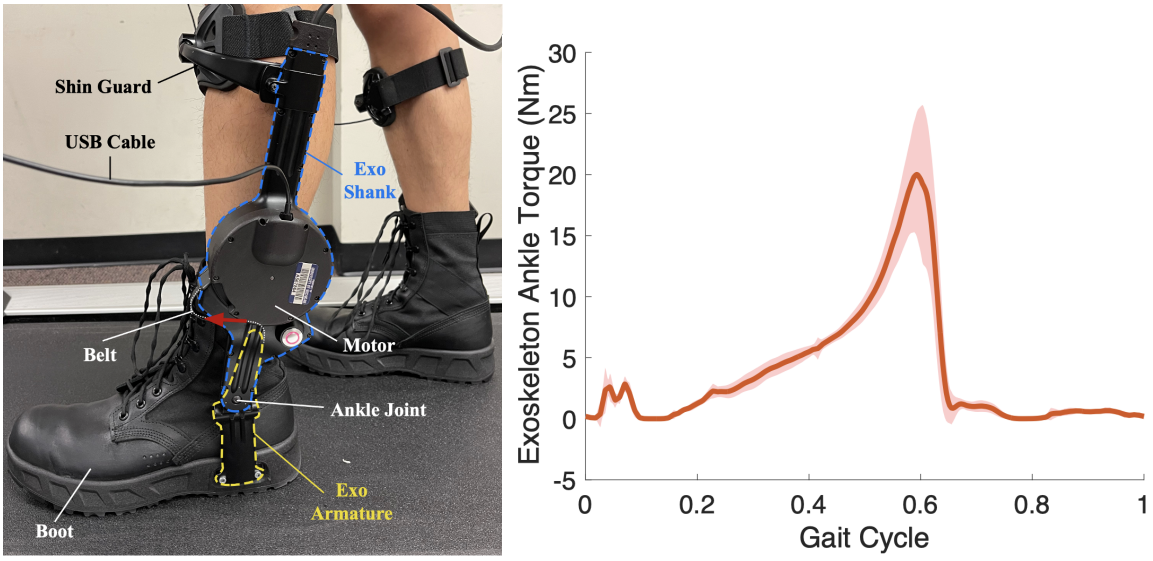

Figure 3.1: (a) Powered bilateral ankle exoskeleton, which provides assistance by applying torque via the inelastic belt attached to the exoskeleton armature (DpEb45, Dephy Inc) [74]. (b) Torque profile applied at strides with nominal torque, where the peak torque is applied at approximately 60% of the stride.

immediately impacted during strides with missed actuations, but did not change during strides with normal exoskeleton torque, which indicated that the users' gait strategies were not affected by 2% error in the previous study.

Only strides where the exoskeleton applied a normal torque were used in the analysis, as we were primarily interested in observing the effect of various error rates on gait strategies while the system was operating nominally over time. The joint kinematics metrics and task error of each trial were separated into 20 equal bins and averaged within each bin to observe time-dependent changes over a trial (20-length vector per metric).

EMG data were pre-processed using a high-pass 3rd-order Butterworth filter at 40 Hz, rectification, and a low-pass 3rd-order Butterworth filter at 10 Hz. Heel strikes identified from motion capture data was used to segment the EMG data to strides, then stance and swing were segmented using toe-off identified using the toe markers, respectively. The root-mean-square (RMS) values of each muscle in stance and swing were calculated for each stance and swing phase of each stride.

The mean of the RMS EMG values for last 60 strides of the training session was used as a baseline for each muscle. The RMS EMG values of each trial were normalized by subtracting the corresponding baseline value, then dividing by that baseline value, thus creating %RMS EMG values. Similar to joint kinematics and task performance, only strides without errors were used for the analysis. A mean %RMS EMG value for each muscle in stance and swing

Table 3.1: Trial order of each participant group

Trial	Group 1	Group 2	Order
1	0% (0/300)	10% (30/300)	1
2	2% (12/600)	7% (21/300)	1
3	5% (15/300)	5% (15/300)	1
4	7% (21/300)	2% (12/600)	1
5	10% (30/300)	0% (0/300)	1
6	10% (30/300)	0% (0/300)	2
7	7% (21/300)	2% (12/600)	2
8	5% (15/300)	5% (15/300)	2
9	2% (12/600)	7% (21/300)	2
10	0% (0/300)	10% (30/300)	2

Notes: The percentages represent the error rate of each control algorithm and the ratios in parentheses show the number of errors to the number of total strides within a trial. An error consists of not actuating the exoskeleton for a single stride. The order represents whether the trial is the first or second time that a participant experiences an error rate.

phases was calculated for each trial (14 values per leg).

3.1.5 Gait Features Matrix

A gait features matrix was created using the joint kinematics metrics, task error, and mean %RMS EMG values across all participants and trials. This analysis was inspired by a study from Rozumalski et al. [80], which used a k-means cluster analysis on a reduced set of gait features based on time-series kinematic data. Gait features vectors (114-length vector) were created for each trial-participant-leg combination by appending the four 20-length kinematics vectors, one 20-length task error vector, and 14 mean %RMS EMG values:

$$g_{s,t,l} = [(max\, hip_{1-20}),\ (min\, knee_{1-20}),\ (max\, knee_{1-20}),\ (max\, ankle_{1-20}),\ (task\, error_{1-20}),\ (\%RMS\, EMG_{1-14})] \quad (3.1)$$

where s is the participant number, t is the trial number, and l is the leg number.

All gait vectors were then vertically concatenated to form the gait features matrix:

$$G = \begin{bmatrix} g^1_{1,1,1} & \cdots & g^{114}_{1,1,1} \\ g^1_{1,2,1} & \cdots & g^{114}_{1,2,1} \\ & \vdots & \\ g^1_{22,10,2} & \cdots & g^{114}_{22,10,2} \end{bmatrix} \tag{3.2}$$

A total of 49 of 440 vectors were removed from the gait matrix due to issues with the EMG signals, potentially caused by EMG sensors detatching from skin during a trial or the exoskeleton cables hitting the sensors. The final gait matrix G was a 391x114 matrix.

3.1.6 Cluster Analysis

Principal component analysis (PCA) was performed to reduce the dimensionality of the data. The first 35 basis vectors accounted for 95% of the data's variability. Thus, the projection of the original gait matrix G onto the first 35 basis vectors, also known as the gait scores ($\tilde{G}$) were used to perform the cluster analysis, thus reducing the dimensionality by 69.3%. A k-means cluster analysis [36] was performed on $\tilde{G}$ to identify groups of gait strategies. The number of clusters was iteratively increased from 2 to 10 clusters and the Calinski-Harabasz (CH) index was calculated for each iteration. The CH index is a measure of the ratio between intra-cluster distances and inter-cluster distances [3] and was maximized to find the appropriate number of clusters.

3.1.7 User Perception of Fluency

A survey on user perception of exoskeleton system performance and task accuracy was conducted after each trial. The methodology and results are detailed by Wu et al. [**?**] in Appendix A. The question "Rate how you felt the exoskeleton supports your actions" was used to obtain a measure of user perception of human-exoskeleton fluency. The associated rating scale responses ranged from 1 (extremely hinders actions) to 5 (extremely supports actions).

3.1.8 Statistical Analysis

One-sample t-tests were performed within clusters across all metrics (kinematics, EMG, and absolute task error) with no p-value corrections ($\alpha = 0.05$). Cohen's d effect sizes (d) were calculated for all t-tests to provide context on effect size, where $0.2 < d < 0.5$ was considered small, $0.5 < d < 0.8$ was medium, and $d > 0.8$ was large. An ANOVA was performed for

the survey responses on exoskeleton supportiveness with a random factor of Participant and a fixed factor of Cluster (5 levels). Post-hoc analysis involved independent t-tests across Clusters with a Bonferroni correction.

3.2 Results

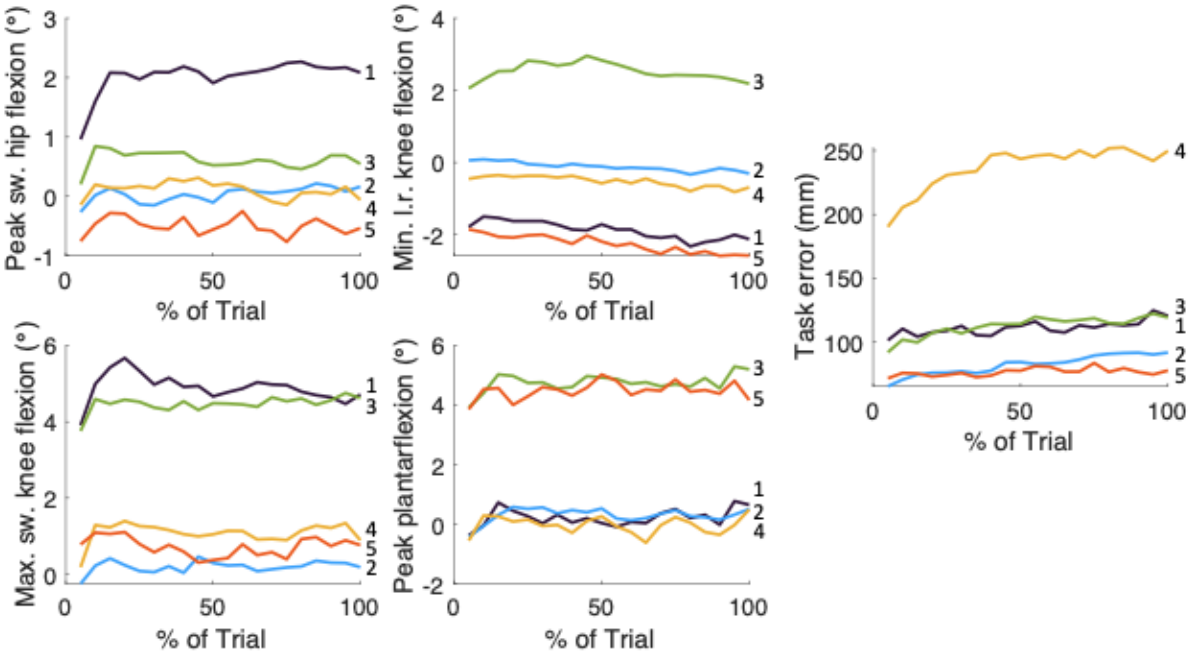

Figure 3.2: Mean joint kinematics metrics and abs. task error over a trial across five clusters. Joint kinematics metrics were mean-shifted by baseline values, calculated as the mean of each metric at the last 60 strides during the training session. Cluster assignment numbers are labeled on the right of each line.

3.2.1 Cluster Analysis

Five clusters were identified (CH index = 59.22) across all participant gait strategies (Figs. 3.2, 3.4). CH index values for other clustering k-values ranged from 47.98 to 57.76; thus, we selected the cluster number ($k = 5$) with the highest CH index. A t-SNE plot was created to illustrate the separation between gait strategies using the reduced gait matrix (Fig. 3.3). Four clusters exhibited different strategies that allowed the participant to accomplish the targeted stepping task ($\leq$160 mm error) and one cluster had increasingly poor task

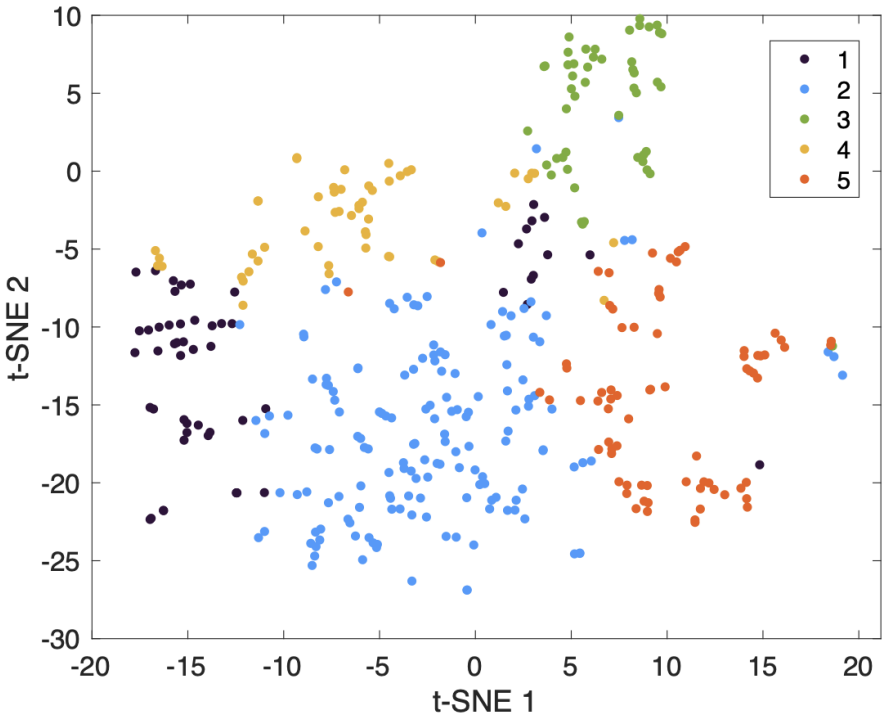

Figure 3.3: A t-SNE plot of $\tilde{G}$, the gait matrix projected onto the first 35 principal components identified using PCA dimensionality reduction.

performance (>160 mm error) over a trial. The mean joint kinematics metrics, task error, and RMS muscle activation are summarized in Tables 3.2 and 3.3.

Cluster 1 significantly increased hip flexion at swing (+1.95°, $d = 1.26$) compared to baseline in order to maintain acceptable task error (116.62 mm) (Fig. 3.2). At swing, participants in this cluster increased RF (+33.68%, $d = 0.48$) and TFL (13.14%, $d = 0.27$) activation and decreased GMax (-9.10%, $d = 0.21$) activation, thus supporting an increase in active hip flexion at swing (Fig. 3.4). Participants of Cluster 1 also decreased their minimum knee flexion during loading response (-1.83°, $d = -1.39$) and increased knee flexion during swing (4.49°, $d = 1.58$). Participants modulated their muscle activity during stance by decreasing GAS activation (-4.25%, $d = 0.30$), which may have impacted knee flexion at loading response. Participants also increased GAS activation at swing (20.95%), which may have contributed to increased knee flexion at swing. Cluster 1 participants did not have a significant change in plantarflexion across a trial (0.18°, $d = 0.07$).

Cluster 2 did not significantly ($p > 0.05$) change their joint kinematics metrics (hip flexion = 0.03° ($d = -0.03$), min. knee flexion at stance = -0.07° ($d = -0.09$), max. knee flexion at swing = 0.10° ($d = -0.04$)) and maintained acceptable task error (82.42 mm). Participants significantly increased plantarflexion (0.23°, $p < 0.001$) but with a very small effect size

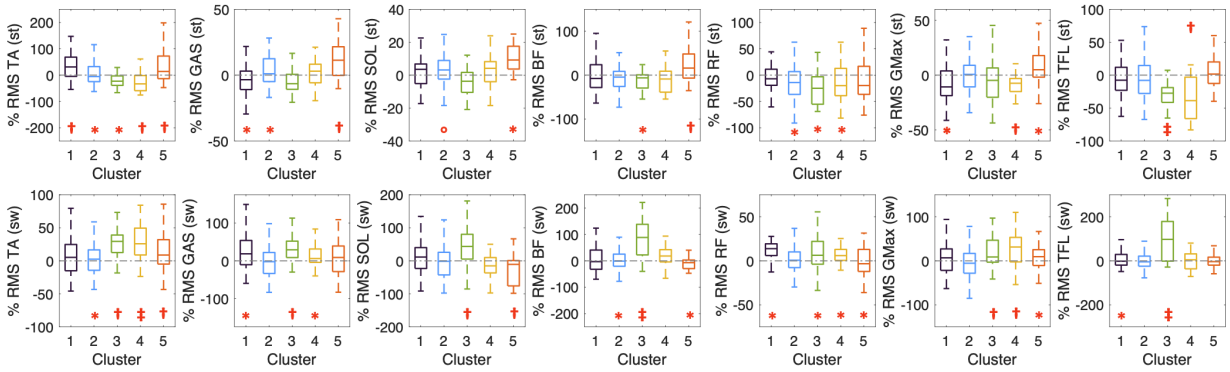

Figure 3.4: Boxplots of %RMS EMG of muscle activation during stance (top row) and swing (bottom row) phases across five clusters. %RMS EMG metrics were mean-shifted by baseline values, calculated as the mean of each metric at the last 60 strides during the training session, then divided by the baseline values. Each box includes 25th to 75th percentile and whisker length is 1.5*IQR. Significant changes in %RMS EMG compared to baseline are marked with red symbols, where ∘ represent very small effect sizes ($|d| < 0.2$), ∗ are small ($0.2 < |d| < 0.5$), † are medium ($0.5 < |d| < 0.8$), and ‡ are large ($|d| > 0.8$).

Table 3.2: Joint kinematics metrics and abs. task error across five clusters

	Cluster 1 (n=59)		Cluster 2 (n=161)		Cluster 3 (n=57)		Cluster 4 (n=57)		Cluster 5 (n=57)	
Max. hip flexion @ swing (°)	1.95 (1.74)	*	0.03 (1.42)		0.75 (1.63)	*	0.33 (1.58)		-0.50 (1.68)	*
Min. knee flexion @ l.r. (°)	-1.83 (1.54)	*	-0.07 (1.07)		2.74 (1.61)	*	-0.46 (1.38)	*	-1.75 (2.05)	*
Max. knee flexion @ swing (°)	4.49 (3.07)	*	0.10 (3.06)		4.97 (3.03)	*	1.38 (2.80)	*	0.66 (2.29)	*
Max. plantarflexion (°)	0.18 (2.77)		0.23 (1.89)	*	4.81 (2.50)	*	-0.20 (3.20)		4.39 (2.42)	*
Abs. task error (mm)	116.62 (52.58)		82.42 (41.80)		108.14 (53.94)		240.62 (47.39)		87.94 (51.11)	

Notes: Joint kinematics metrics (mean (SD)) were mean-shifted by baseline values, calculated as the mean of each metric at the last 60 strides during the training session. The n-values represent the number of gait vectors sorted to each cluster (391 total). The asterisks (*) mark significant changes from baseline.

($d = 0.18$). Muscle activation at stance and swing had small significant changes in most muscles ($|d| < 0.20$), with small increases in TA (12.44%, $d = 0.20$) and GAS (10.31%, $d = 0.29$) activation at stance.

Cluster 3 had significant changes ($p < 0.001$) at the knee and ankle compared to baseline and had acceptable task accuracy (108.14 mm). Participants increased minimum knee flexion during loading response (+2.74°, $d = 1.84$), maximum knee flexion during swing (+4.97°, $d = 1.67$), and maximum plantarflexion (+4.81°, $d = 2.14$). The changes in knee kinematics during stance were supported by decreases in antagonistic BF activation (-11.47%, $d = 0.47$) and RF activation (-15.65%, $d = 0.29$), creating a positive knee flexion moment between antagonistic muscles. Increases in knee flexion at swing corresponded to increases to BF (84.10%, $d = 1.15$) and GAS (26.88%, $d = 0.71$) activation at swing. The increase in

Table 3.3: %RMS EMG at swing and stance phases across five clusters

	Cluster 1 (n=59)		Cluster 2 (n=161)		Cluster 3 (n=57)		Cluster 4 (n=57)		Cluster 5 (n=57)	
TA @ stance (%)	41.66 (62.43)	*	12.44 (63.20)	*	-14.68 (38.15)	*	-24.09 (41.98)	*	37.41 (71.92)	*
GAS @ stance (%)	-4.25 (13.98)	*	10.31 (35.35)	*	-0.41 (32.61)		1.72 (9.04)		29.63 (57.64)	*
SOL @ stance (%)	-4.01 (22.74)		9.24 (51.46)	*	3.45 (56.53)		2.55 (19.34)		46.28 (111.97)	*
BF @ stance (%)	-1.94 (36.80)		-3.87 (30.05)		-11.47 (23.78)	*	2.71 (60.91)		23.60 (37.36)	*
RF @ stance (%)	-4.60 (29.89)		-9.95 (48.77)	*	-15.63 (53.28)	*	-12.04 (35.29)	*	-7.76 (44.00)	
GMax @ stance (%)	-7.78 (15.35)	*	3.14 (46.61)		-5.76 (20.28)		-7.47 (10.87)	*	23.31 (55.68)	*
TFL @ stance (%)	-6.51 (25.11)		-7.45 (38.62)	*	-27.69 (17.51)	*	-28.48 (47.34)	*	9.85 (47.08)	
TA @ swing (%)	7.01 (33.49)		8.65 (35.48)	*	42.19 (72.92)	*	30.88 (26.69)	*	20.01 (58.52)	*
GAS @ swing (%)	33.27 (68.41)	*	2.70 (52.41)		26.88 (37.13)	*	19.03 (40.78)	*	9.23 (62.22)	
SOL @ swing (%)	5.91 (56.91)		-0.54 (60.21)		44.53 (71.97)	*	-8.93 (45.10)		-24.16 (41.68)	*
BF @ swing (%)	2.89 (42.88)		12.13 (59.04)	*	84.10 (72.03)	*	12.00 (44.60)		-8.45 (29.99)	*
RF @ swing (%)	33.68 (50.23)	*	6.76 (45.84)		11.47 (23.24)	*	16.25 (57.68)	*	9.76 (36.21)	*
GMax @ swing (%)	9.10 (42.40)		3.82 (57.70)		19.39 (20.28)	*	26.46 (41.22)	*	19.11 (56.46)	*
TFL @ swing (%)	13.14 (47.41)	*	5.07 (69.11)		98.04 (98.46)	*	2.31 (46.13)		2.90 (41.51)	

Notes: %RMS EMG metrics (mean (SD)) were mean-shifted by baseline values, calculated as the mean of each metric at the last 60 strides during the training session, then divided by the baseline values. The %RMS EMG metrics were calculated during the stance phase (top half) and swing phases (bottom half). The n-values represent the number of gait vectors sorted to each cluster (391 total). The asterisks (*) mark significant changes from baseline.

plantarflexion were linked to increased GAS (26.88%, $d = 0.71$) and SOL (44.53%, $d = 0.61$) activation during swing. Participants in cluster 3 also moderately increased hip flexion (0.75°, $d = 0.50$), driven by a large increase in TFL activation at swing (98.04%, $d = 0.98$) and reduced by an antagonistic increase in BF activity (84.10%, $d = 1.15$).

Cluster 4 had mostly unchanged ($p > 0.05$) joint kinematics metrics (hip flexion = 0.33° ($d = 0.23$), plantarflexion = -0.20°, $d = 0.07$), with a small decrease in minimum knee flexion at loading response (-0.46°, $p = 0.01$, $d = 0.35$), a moderate increase in maximum knee flexion at swing (+1.38°, $p < 0.001$, $d = 0.52$), and unacceptable task error (240.62 mm). Participants increased GAS activation at swing (19.03%, $d = 0.46$), which may have contributed to the increase in knee flexion at swing. TA activation at swing also increased by 30.88% ($d = 1.14$), thus counteracting additional plantarflexion. Other muscles had small to moderate changes in activation (-28.48 to 24.09%, $-0.57 \leq d \leq 0.63$), with the no net change due to antagonistic muscle activity.

Cluster 5 primarily increased ankle plantarflexion (+4.48°, $d = 2.42$) and decreased minimum knee flexion at loading response (-2.26°, $d = 0.88$), with small changes to hip flexion (-0.50°, $d = 0.33$) and maximum knee flexion at swing (+0.72°, $d = 0.31$). Participants in this cluster also had acceptable task performance across the trial (76.32 mm). The increase in plantarflexion may have been driven by the increase in GAS (29.63%, $d = 0.51$) and SOL (46.28%, $d = 0.41$) activation at stance, as well as a small increase in GAS (9.23%, $d = 0.15$) swing. Antagonistic TA muscle activation also increased at stance (37.41%, $d = 0.51$) and

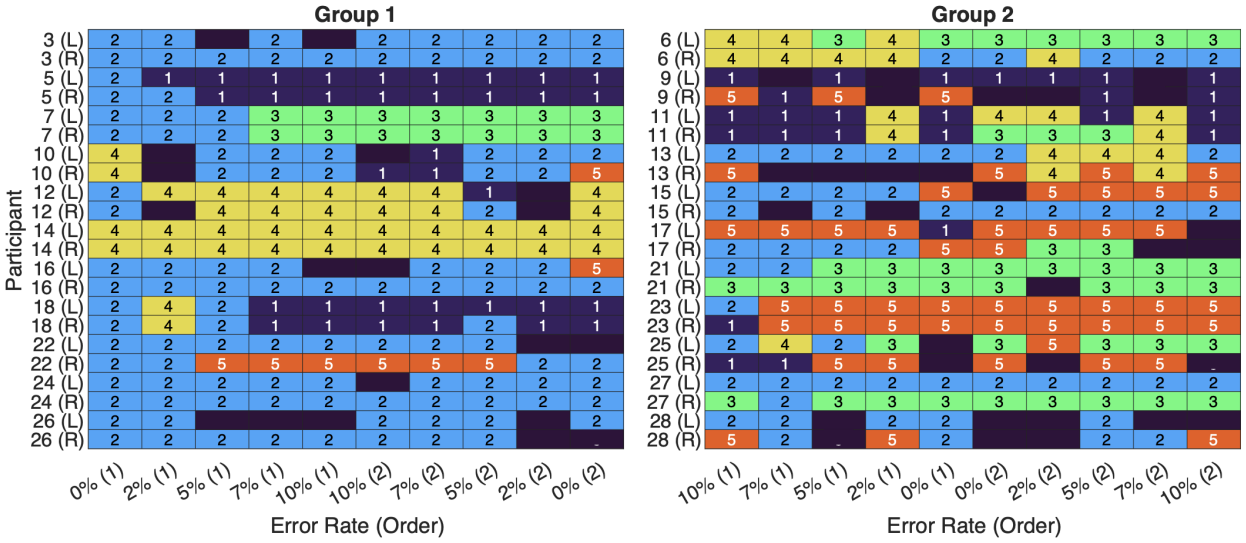

Figure 3.5: Cluster assignments for all participants and trials. 49 trials were excluded from analysis due to noisy or unusable EMG data and are marked using unlabeled black boxes. Participant number and leg (left or right) are marked on the left of each cluster map. Trial error rates and order (1st or 2nd exposure to the error rate) are shown on the x-axis.

swing (20.01%, $d = 0.34$). Notably, GMax activation at swing increased by 23.31% ($d = 0.41$) with little to no change in hip flexion, as antagonistic TFL activation also increased by 9.85% ($d = 0.21$).

3.2.2 Gait Strategies Across Trials

Cluster assignments for gait vectors were then sorted according to the participant number, group, trial number, and leg (Fig. 3.5). Group 1 trial strategies were most often sorted into Cluster 2 (108/201 trials), then to Cluster 4 (37/201 trials), Cluster 1 (34/201 trials), Cluster 3 (14/201 trials), and Cluster 5 (8/201 trials). Nine (81.8%) participants in Group 1 used strategies defined in Cluster 2 in the first trial and six (54.5%) of those participants changed strategies as they experienced different exoskeleton controllers with varying error rates. Two (18.2%) participants primarily used the Cluster 4 strategy and did not successfully complete the stepping task across trials.

Group 2 trial strategies were sorted into the clusters with the following frequencies: Cluster 2 (53/190 trials), Cluster 5 (49/190 trials), Cluster 3 (43/190 trials), Cluster 1 (25/190 trials), and Cluster 4 (20/190 trials). All 11 participants in Group 2 used strategies of various clusters when experiencing different controllers.

3.2.3 User Perception of Fluency

The Subject factor ($F(21, 388) = 23.61, p < 0.001$) and Cluster factor ($F(4, 388) = 2.66, p = 0.033$) were significant for perceived exoskeleton supportiveness. Perceived supportiveness in Cluster 2 (3.51 ± 0.90) was significantly higher than in Cluster 3 (3.06 ± 1.09). Responses in Clusters 1 (3.78 ± 0.98), 4 (3.84 ± 1.38), and 5 (3.71 ± 0.94) were not significantly different compared to Cluster 2.

3.3 Discussion

In this study, we introduced an exoskeleton algorithm with varying error rates (0%, 2%, 5%, 7%, and 10% error) to observe the effect of exoskeleton error levels on gait strategies during nominal operation periods. Participants were sorted into two groups that experienced each controller twice, but in different orders. A k-means clustering algorithm ($k = 5$) was used to define gait strategies across participants using metrics of joint kinematics, task error, and muscle activity. These clusters of strategies were then interpreted in the context of human-exoskeleton fluency.

3.3.1 Interpretation of Clusters

Gait strategies defined by the cluster analysis had varying impacts on human-exoskeleton fluency, which was maximized when users reduced muscle activity, as the goal of the Dephy exoskeleton is to reduce the metabolic cost of walking. Muscle activity was used to assess strategies as it has been shown to be linked to metabolic cost during walking [89]. Fluent strategies may involve minimal changes or decreases in muscle activity with respect to participants' initial adaptation to the exoskeleton at the end of training. Cluster 2 exhibited strategies that supported human-exoskeleton fluency while successfully completing the stepping task, even when errors were present throughout a trial. Participants in Cluster 2 were able to coordinate with the exoskeleton and utilize the exoskeleton's assistive torque during nominal steps to complete the task without significant modifications to joint kinematics and muscle activity (Tables 3.2 and 3.3). While participants in Cluster 4 were also fluent with the exoskeleton, they were unable to achieve acceptable task error ($\leq$160 mm), suggesting that users may have directed less attention to the task or were unable to match the treadmill speed and may have altered walking speed if they had been on a self-paced treadmill or were overground.

In comparison, Clusters 1, 3, and 5 increased muscle activation and modified joint kinematics about the hip (Cluster 1), knee (Clusters 3 and 5), and ankle (Clusters 3 and 5)

in order to complete the task with acceptable error (Fig. 3.2 and 3.4). Cluster 1 utilized a strategy observed in our previous study with a 2% error algorithm [106], where participants increased hip flexion and muscle activity about the hip to extend the leg and reach the stepping target during exoskeleton errors. This strategy was previously only observed during exoskeleton errors and participants were able to return to baseline behavior after errors. In this study, participants increased hip flexion and muscle activity even during nominal exoskeleton behavior, indicating that users may have expected the presence of errors and modified their strategies to accomplish the stepping task. Similarly, Clusters 3 and 5 may have increased plantarflexion and muscle activation about the ankle in anticipation of additional exoskeleton errors. The added plantarflexion may have generated a larger push-off force, which then followed with increased muscle activation and co-contraction in the hip and knee, possibly to stiffen the joints and prevent over-stepping the target. The strategies used by Clusters 1, 3, and 5 negatively impacted human-exoskeleton fluency as participants increased joint flexion and muscle activity, which increased energy usage and thus opposed the design goals of this exoskeleton. These strategies may also indicate that users in these clusters may have prioritized task performance over fluent gait strategies and lost trust in the exoskeleton to actuate correctly over time. Participants in Cluster 3 also perceived the exoskeleton as less supportive than those in Cluster 2, which may be linked to non-fluent strategies in Cluster 3. While participants in Clusters 1 and 5 also utilized non-fluent strategies, the increases in muscle activation supporting hip flexion and ankle plantarflexion occurred during stance. The increased muscle activation across all muscles during swing observed in Cluster 3 may be more salient, leading to lower supportiveness ratings.

3.3.2 Gait Strategies Across Trials

Most participants (18 of 22, 81.8%) changed gait strategies as they experienced additional exoskeleton algorithms with different error levels (Fig. 3.5). In Group 1, participants often began with gait strategies defined in Cluster 2 that were fluent with the exoskeleton's goals and accomplished the stepping task. Six participants (54.5%) were able to maintain fluent gait strategies (Cluster 2) on one or both legs during all trials. These participants may have trusted the exoskeleton to continue to support their actions, even when walking with algorithms with higher error frequencies. These six participants stated that they primarily focused on completing the stepping task and tried to coordinate with the exoskeleton's behavior, regardless of error rate. Three participants (27.3%) transitioned to strategies that increased hip or ankle flexion and muscle activity in order to maintain task accuracy (Clusters

1, 3, and 5), thus reducing human-exoskeleton fluency. These users may have lost trust in the exoskeleton once they encountered controllers with higher error, as they continued with these compensatory strategies when walking with 0% or 2% error controllers. The contrast between participant behavior within Group 1 may indicate that some users may be more heavily impacted by poor algorithm performance than others.

In Group 2, all participants changed strategies across trials and were more likely to increase hip and ankle flexion and underlying muscle activity (50% of strategies) than to utilize strategies that supported human-exoskeleton fluency (27.9% of strategies). Group 2 participants were also more likely to start with non-fluent strategies on at least one leg (90.9%) compared to Group 1 participants (18.2%). This behavior aligns with the order presented, as Group 2 began with the lower performing algorithm (10% error) after training, while Group 1 began with the algorithm with no errors, thereby impacting the strategies used during the first trial. However, when Group 2 participants transitioned to algorithms with lower error (0% or 2%) in later trials, most participants (90.9%) maintained increases in hip or ankle flexion as defined in Clusters 1, 3, and 5. This behavior is similar to users in Group 1 who were strongly impacted by poor controllers and modified their gait strategies for the remaining trials. These users may have updated their underlying internal models—representations of the dynamic properties of the limb in the environment [85]—when walking with an exoskeleton, leading to changes in walking strategies. Adaptation of internal models may occur in response to visual [105] or mechanical changes in the environment [93], which cause errors in movement. Algorithms with higher error rates induce a higher frequency of movement errors and may influence the dynamics within coupled human-exoskeleton system, thus prompting modifications of internal models and the resulting motor commands.

Participants who experience poor controllers earlier or are sensitive to exoskeleton errors were more likely to use gait strategies with increased muscle activity and joint flexion, thereby conflicting with the exoskeleton's goal. Users should first adapt to and use exoskeletons in settings where error frequency is low for an ample amount of time (i.e. steady-state walking in laboratory) before walking in more uncertain environments where errors may be more prevalent (i.e. uneven terrain, ramps, speed-variable walking) to build sufficient experience and trust in the exoskeleton. In this study, participants walked for 15 minutes with a 0% error controller at a fixed speed during the training session, which may have been too short and uniform for some participants to explore different speeds and develop a resilient and fluent gait strategy. Participants in Group 1 began to utilize less fluent walking strategies once algorithm errors increased to 5-7% of all strides. Participants who started with 10% error were less likely to exhibit fluent strategies throughout the experiment. Thus, it is recommended that researchers strive to have systems with errors below 5-7% error. We

acknowledge that this threshold may be larger if error types were less noticeable compared to this study (loss of assistive torque) or may be lower if gait stability or foot clearance were affected (i.e. early or late actuations).

It is currently unclear how long a system must operate correctly after a period of errors for the user to transition to more fluent strategies. A study involving the same Dephy exoskeleton found that some participants maintained a stepping strategy developed when adapting to the exoskeleton even when the exoskeleton was turned off for 5 minutes [2]. This suggests that some users may need at least 5 minutes of walking without exoskeleton errors before modifying their gait strategies. Due to time limitations of the study, none of the controllers other than 0% error had a period greater than 5 minutes without errors as each trial lasted between 10-15 minutes. It is also important to evaluate the impact of lower-limb exoskeletons on the entire kinematic chain of the leg rather on one specific joint, as the data shows increased muscle activity and modified kinematics about the hip and knee while walking with an ankle exoskeleton.

3.3.3 Limitations and Future Work

This study supports that users may utilize various gait strategies when given a targeted stepping task with a powered ankle exoskeleton in the presence of errors. Fluent strategies minimize changes in joint kinematics and muscle activity during nominal exoskeleton behavior. Users may increase hip or ankle flexion to support completing the task, thus negatively impacting human-exoskeleton fluency. A limitation of this study is the assumption that participants were fully adapted to the exoskeleton's normal operation within 15 minutes of training, which would impact our calculation of baseline joint kinematics and muscle activation. Clusters defined in this study did not show large decreases in GAS or SOL activation (an indication of post-training adaptation), though individual users may have continued to adapt to the system after training. A study estimated that users may need up to 109 minutes to fully adapt to a different ankle exoskeleton [75], which was not feasible for the duration of this study.

While this study introduced error rates in two fixed orders, randomized error rates may result in different user responses. For instance, if the randomized order began with a higher error, the user may increase muscle activation as they anticipate repeated errors (non-fluent strategy), even if the following controller had a low error rate. Future work may explore how the order of error rates may affect learning and adaptation to an exoskeleton to inform training protocols and operational use. Alternate exoskeletons and error types (i.e., changes in different control parameters) may also yield different responses across error ranges. Future

work may explore new algorithms that modulate exoskeleton behavior in response to gait strategies that reduce human-exoskeleton fluency.

3.4 Conclusion

In this study, we investigated the impact of imperfect exoskeleton algorithms (up to 10% error) on joint kinematics, muscle activation, and task error. Error rates were presented in two orders–Group 1 experienced controllers with low error (0-2%) before those with higher error rates (5-10%) and Group 2 experienced controllers with higher error before those with lower error rates. A k-means cluster analysis ($k = 5$) was used to define the emergent gait strategies. The fluent strategy minimized muscle activation and aligned with the exoskeleton's goal of reducing metabolic cost while maintaining acceptable task error. Three strategies had acceptable task error, but increased muscle activation about the hip or ankle, thus negatively impacting human-exoskeleton fluency. One strategy minimized muscle activity, but had unacceptable task performance. Participants in Group 2 who experienced 10% error first were more likely to use non-fluent gait strategies compared to those who walked with 0% error first. A subset of users across both groups transitioned from fluent to non-fluent gait strategies after using the controller with higher error rates. Exoskeleton users may build fluent and resilient gait strategies if they first walk with the exoskeleton in environments with low variability (i.e., treadmill walking) before transitioning to more uncertain environments where exoskeleton errors may be more prevalent. Understanding emergent gait strategies can inform the development of exoskeleton algorithms that support appropriate gait strategies and system use.

CHAPTER 4

Modeling Co-Adaptive Control of Ankle Exoskeletons

In Chapter 3, fluent and non-fluent gait strategies were identified and characterized as people walked with imperfect exoskeleton algorithms. While fluent strategies were defined as those that minimized muscle activation and aligned with the exoskeleton's goal of reducing metabolic cost, non-fluent strategies involved increased muscle activity about the hip or ankle, which would yield increased energy usage. It may be possible to induce different strategies in healthy users using exoskeletons. For example, Selinger et al. [84] showed that a knee exoskeleton applying resistive torque was able to guide users to new stepping frequencies by shifting the energetically optimal step frequency away from the normally preferred and optimal step frequency. A subset of users in Chapter 3 also transitioned from fluent to non-fluent strategies as we manipulated the system reliability using missed actuation errors (no torque applied at specified strides). Thus, modulating exoskeleton torque according to user behavior may encourage users to utilize fluent strategies.

Thus, it is important to develop a co-adaptive control algorithm that supports fluent strategies and modifies the torque assistance in response to non-fluent strategies to encourage convergence to fluent strategies. A previous study by Jackson et al. [47] found that a co-adaptive algorithm involving only ankle muscle activity and kinematics was able to reduce metabolic cost with a bilateral ankle exoskeleton by adjusting torque based on ankle metrics. However, we previously identified non-fluent strategies with nominal ankle behaviors and compensatory motions higher in the kinematic chain. The proposed algorithm incorporated joints and muscles along the lower-limb rather than only about the ankle to observe and react to compensatory behaviors higher in the leg's kinematic chain. For instance, in Chapter 3, users anticipated repeated errors and increased hip flexion and underlying muscle activity to compensate for the potential loss of torque. This behavior may cause the proposed algorithm to reduce peak torque in order to allow the user to adjust to a lower level of exoskeleton torque and lessen compensatory muscle activation.

In this study, we developed a co-adaptive control algorithm for an ankle exoskeleton and modeled the anticipated changes in resulting torque profiles depending on user behavior. The proposed co-adaptive algorithm modulated peak torque, which is the maximum amplitude of the torque profile, in response to user strategies. This study also highlighted the impact of incorporating additional inputs to the algorithm (muscle activity and joint kinematics about the hip and knee) and compared the generated torque profiles against an ankle-only co-adaptive controller with only ankle kinematics and muscle activity.

4.1 Algorithm Formulation

The proposed co-adaptive control algorithm utilizes muscle activity and joint kinematics measurements to guide the evolution of the exoskeleton torque assistance. In our proposed algorithm, electromyography (EMG) and joint angle measurements from the hip, knee, and ankle were incorporated, as our previous study [108] found non-fluent strategies involving increased muscle activity and deviations from baseline kinematics about the knee and hip. Similar to the Jackson et al. [47] co-adaptive controller, our algorithm used heuristic-based metrics calculated from the EMG and joint kinematic deviations and extended the work to include the hip and knee joints. The contributions from each metric were scaled and combined in a linear expression to drive the progression of the torque profile over strides. The exoskeleton torque output was be modified by changing key parameters of the torque profile.

The torque profile provided by the exoskeleton can be parameterized using four variables: peak torque, the time of peak torque, rise time, and fall time [110]. The proposed controller calculates peak torque applied at subsequent strides while holding the rise, fall, and peak torque times constant. Changing the peak torque also modifies the rising slope and falling slope, thus impacting the total torque and energy provided over each stride. Peak torque $\tau_{pk}(n)$ of the torque profile at stride n was calculated as the sum of the previous peak torque, $\tau_{pk}(n-1)$, and a specified change in peak torque, $d\tau_{pk}(n)$. The change in peak torque, $d\tau_{pk}(n)$, was expressed as linear combination of scaled metrics of (1) the EMG of major muscles at the ankle, knee, and hip, (2) the associated deviations in joint kinematics, and (3) the previous peak torque.

4.1.1 Proposed Control Algorithm

Our proposed algorithm calculates the total change in peak torque $d\tau_{pk}$ as a combination of the joint-specific components ($d\tau_{pk,ankle}$, $d\tau_{pk,knee}$, $d\tau_{pk,hip}$), as well as the peak torque applied

during the previous stride, $\tau_{pk}(n-1)$. The previous peak torque term is scaled by gain k_9 and provides negative feedback to the system, thus establishing an equilibrium point and stabilizing the system. At the equilibrium point, the algorithm assumes that muscle activity of the SOL, GAS, and TFL are minimized with low co-contraction about the knee and hip joints, along with no deviations from baseline ankle and hip kinematics. The magnitude of the gain k_9 shapes the equilibrium point, as larger k_9 values will result in lower equilibrium tau_{pk} and smaller values will result in larger τ_{pk}. The total change in peak torque at stride n is written in Eq. 4.1 as follows.

$$d\tau_{pk}(n) = d\tau_{pk,ankle}(n) + d\tau_{pk,knee}(n) + d\tau_{pk,hip}(n) - k_9 * \tau_{pk}(n-1) \tag{4.1}$$

The peak torque applied at stride n is the sum of the previous peak torque $\tau_{pk}(n-1)$ and $d\tau_{pk}$ if the magnitude of the $d\tau_{pk}$ is greater than a defined threshold, τ_{thres}, and 0 otherwise. The threshold requirement on $d\tau_{pk}$ exists to prevent small deviations in peak torque from the positive contributions of the plantarflexors and TFL terms, which may cause the peak torque to drift upwards and become unstable. We also bound $\tau_{pk}(n)$ between a minimum of 5 N-m and a maximum of $T_norm * m_{user}$, where T_norm is a scaling factor with units of N-m/kg and m_{user} is the user's mass in kg. The minimum boundary ensures that a small level of torque is applied during each stride even if the user exhibits continuous non-fluent strategies over the course of many strides and the peak torque is driven downwards from the negative contributions from muscle co-contraction and kinematic deviations. The peak torque is also limited by T_{norm} and the user's body mass to ensure the peak torque does not exceed the exoskeleton's motor capabilities or cause harm to the user. Finally, $\tau_{pk}(n)$ is formulated in Eq. 4.2 and 4.3 as follows.

$$\hat{\tau}_{pk}(n) = \tau_{pk}(n-1) + \text{sign}(d\tau_{pk}(n)) * \max(\text{abs}(d\tau_{pk}(n)) - \tau_{thres}, 0) \tag{4.2}$$

$$\tau_{pk}(n) = \begin{cases} 5 & \hat{\tau}_{pk}(n) \leq 5 \\ \hat{\tau}_{pk}(n) & 5 < \hat{\tau}_{pk}(n) < (T_{norm} * m_{user}) \\ (T_{norm} * m_{user}) & \hat{\tau}_{pk}(n) \geq (T_{norm} * m_{user}) \end{cases} \tag{4.3}$$

4.1.2 Ankle Contributions

The muscle activity of the soleus (SOL), medial gastrocnemius (GAS), and tibialis anterior (TA) contribute to the change in peak torque at subsequent strides. EMG metrics $SOL(n-1)$ and $GAS(n-1)$ are calculated from the SOL and GAS measurements from the previous

stride in Eq. 4.4 and 4.5.

$$SOL(n-1) = \text{RMS}\left(\frac{EMG_{SOL}(n-1)}{\langle EMG_{SOL}(n-1)\rangle^{m_{ankle}}}\right) \tag{4.4}$$

$$GAS(n-1) = \text{RMS}\left(\frac{EMG_{GAS}(n-1)}{\langle EMG_{GAS}(n-1)\rangle^{m_{ankle}}}\right) \tag{4.5}$$

EMG_{SOL} and EMG_{GAS} are the time-series EMG signals of the respective muscles across a stride and the $\langle\cdot\rangle$ operation finds the mean value of the time-series EMG. The means are raised to the power m_{ankle}, where $m_{ankle} \geq 1$ to reduce the contribution of higher GAS and SOL muscle activation, as the exoskeleton's goal is to reduce the muscle activity from the plantarflexors. Dividing the term by the mean EMG activation creates an inverse relationship between the EMG signal amplitude and the term's magnitude—as the amplitude of the SOL and GAS EMG signals increases, the magnitude of the terms decrease. Higher muscle activity from the plantarflexors may signify that the user may need more time adapting to the exoskeleton, while lower muscle activity indicates the user is working collaboratively with the exoskeleton and may benefit from increased torque. The terms $SOL(n-1)$ and $GAS(n-1)$ are thus expressed as the root-mean-squared (RMS) mean of the scaled muscle activity across a stride. Since SOL and GAS muscle activity work cooperatively with the exoskeleton torque to produce a plantarflexion moment, these terms contribute positively to $d\tau_{pk}(n)$. These SOL and GAS terms are also scaled by the gains k_1 and k_2, respectively.

The TA term, $TA(n-1)$, for the previous stride is expressed in Eq. 4.6, where EMG_{TA} is the time-series EMG signal of the TA muscle across a stride.

$$TA(n-1) = \text{RMS}\left(EMG_{TA}(n-1)\right) \tag{4.6}$$

Since the TA is responsible for ankle dorsiflexion and acts antagonistically to the plantarflexors and exoskeleton torque, the TA term contributes negatively to the change in peak torque. The TA term is scaled by the gain k_3 and reduces $d\tau_{pk}(n)$ as TA muscle activity increases over subsequent strides. The TA term is not scaled by the mean of the EMG signal, as increased TA activity should create a larger decrease in peak torque to slow the growth of the torque profile. The ratio between the TA, GAS, and SOL terms can act as an indicator of muscle co-contraction—a mechanism to control joint stiffness [38, 66]—as the these muscles form agonist-antagonist pairs driving ankle movement. A user strategy that relies on ankle co-contraction is characterized by larger magnitudes of the ankle muscle terms and may signify the user is not fluent with the system, as they may be stiffening their ankle to resist the motion of the exoskeleton. The gains k_1, k_2, and k_3 are thus scaled appropriately so these terms result in no change or a decrease in peak torque when ankle co-contraction is

high or the TA term dominates the ankle muscle contributions.

Deviations from baseline ankle kinematics contribute negatively to $d\tau_{pk}(n)$. The deviations are calculated during the push-off portion of gait, as our previous study in Chapter 3 [108] found non-fluent strategies involving increased plantarflexion with corresponding increase muscle activity. Baseline kinematics may be derived using a period of walking with the exoskeleton powered with a static torque profile or without exoskeleton torque. The ankle kinematics term, θ_{ankle}, is an indirect measure of significant deviations from peak baseline plantarflexion (Eq. 4.7). Incorporating the ankle kinematics term also accounts for strategies where the user increases plantarflexion without reducing plantarflexor muscle activity. In this scenario, the resulting peak torque would decrease to encourage the user to adapt to the exoskeleton with a reduced torque profile.

$$\theta_{ankle}(n-1) = \begin{cases} -k_4 & \text{abs}(\theta_{pushoff}(n-1) - \theta_b) \geq \theta_{threshold_a} \\ 0 & \text{otherwise} \end{cases} \tag{4.7}$$

The gain k_4 is included in the θ_{ankle} piece-wise expression, where θ_{ankle} is equal to $-k_4$ if the absolute value of deviation in peak plantarflexion at push-off compared to baseline exceeds a predefined threshold $\theta_{threshold_a}$ and is zero otherwise. The kinematic term was set to a specified value rather than a direct calculation from ankle angle to standardize the contribution of the kinematic term across participants. Using a direct calculation for the kinematic term resulted in unstable behaviors due to inter-subject variability in joint kinematics during the initial tuning of the gain k_4.

The total contribution from ankle muscle activity and kinematics can be expressed as:

$$d\tau_{pk,ankle}(n) = k_1 * SOL(n-1) + k_2 * GAS(n-1) - k_3 * TA(n-1) - \theta_{ankle}(n-1) \tag{4.8}$$

4.1.3 Knee Contributions

Muscle activity from the biceps femoris (BF) and rectus femoris (RF) are used to calculate the co-contraction index (CCI) of the knee joint. The BF and RF are bi-articular muscles responsible for knee flexion/extension and hip extension/flexion and act as an agonist-antagonist pair. While these muscles may induce motion about both the hip and knee, they are used to assess the knee contribution to $d\tau_{pk}$ in this study. Researchers are recommended to place EMG sensors closer to the knee on the RF and BF muscle body to accurately assess muscle activity contribution to knee motion. High levels of knee CCI contribute negatively to the change in peak torque, as it may suggest the user is stiffening their knee to resist the motions of the exoskeleton. The knee co-contraction metric is derived from Rudolph et al.

[81], which has been shown to correlate with joint stiffness for quadriceps-hamstring pairs for knee and hip stiffness [57].

$$CCI_{knee}(t) = \frac{\min(EMG_{BF}(t), EMG_{RF}(t))}{\max((EMG_{BF}(t), EMG_{RF}(t))} \left(EMG_{BF}(t) + EMG_{RF}(t)\right)) \tag{4.9}$$

$$d\tau_{pk,knee}(n) = -k_5 * \frac{1}{T} \sum_{t=0}^{T} CCI_{knee}(t, n-1) \tag{4.10}$$

Knee co-contraction, $CCI_{knee}(t)$, at each time point t along a stride is the product of the ratio between the lower and higher absolute EMG magnitude and the sum of both BF and RF activity at t. $CCI_{knee}(t)$ measurements range from [0,2], where 0 represents no activity from the antagonist muscle and 2 signifies that both muscles are contracting equally at maximum amplitude over the stride (assuming peak amplitude = 1). The contribution to $d\tau_{pk}$ is then calculated as the summation of CCI_{knee} across all time points along the stride divided by the number of total time points and scaled by gain k_5 (Eq. 4.10). We utilize a measure of knee CCI rather than a direct metric from BF and RF activation, similar to ankle muscle contributions, as knee motion cannot be mapped to cooperating or resisting the exoskeleton's plantarflexion torque as simply as ankle motion.

4.1.4 Hip Contributions

The muscle activity of the tensor fasciae latae (TFL) and gluteus maximus (GMax) are used to calculate EMG metrics. A direct measure of TFL activity of the previous stride, $TFL(n-1)$, was constructed similar to the GAS and SOL terms, as we previously identified a non-fluent strategy where users compensated for low system reliability by increasing hip flexion and TFL activity at swing in Chapter 3 [108]. TFL muscle activity can generate hip flexion and the TFL term is expressed as the RMS mean of the scaled TFL muscle activity across a stride, as shown in Eq. 4.11.

$$TFL(n-1) = \text{RMS}\left(\frac{EMG_{TFL}(n-1)}{\langle EMG_{TFL}(n-1)\rangle^{m_{hip}}}\right) \tag{4.11}$$

EMG_{TFL} is the time-series EMG signal of the TFL muscle across a stride and $\langle EMG_{TFL}\rangle$ is the mean of the TFL EMG signal, raised to the power m_{hip} where $m_{hip} \geq 1$. The term $TFL(n-1)$ is then scaled by gain k_6 and contributes positively to the change in peak torque for the following stride. When TFL activity is low, the magnitude of the term is larger, as this behavior may indicate that the user is properly adapting to the system and may benefit from greater torque assistance. The TFL term addresses the non-fluent strategy found in

Chapter 3 by reducing the magnitude of its contribution to $d\tau_{pk}$ when muscle activity is high and aligned with compensatory behavior.

Similar to the knee, a metric for hip co-contraction, CCI_{hip}, is derived using the Rudolph et al. [81] definition of CCI with the TFL and GMax muscles as the agonist-antagonist pair for hip flexion/extension. The hip CCI at each time point t along a stride ranges from [0,2], where 0 indicates no activity of the antagonistic muscle and 2 indicates equal maximal activity, assuming peak muscle activity is normalized to 1. The hip CCI term is scaled by gain k_7 and negatively contributes to $d\tau_{pk}$, where high levels of hip CCI may indicate the user is less fluent with the system and is stiffening their hip to resist the exoskeleton assistance.

$$CCI_{hip}(t) = \frac{\min(EMG_{TFL}(t), EMG_{GMax}(t))}{\max((EMG_{TFL}(t), EMG_{GMax}(t))} \left(EMG_{TFL}(t) + EMG_{GMax}(t)\right)) \tag{4.12}$$

$$CCI_h(n-1) = \frac{1}{T}\sum_{t=0}^{T} CCI_{hip}(t, n-1) \tag{4.13}$$

Deviations from baseline hip kinematics contribute negatively to the change in peak torque. The deviations are calculated during the swing phase, as we found in Chapter 3 that some users increased hip flexion during swing as a compensatory strategy when walking with imperfect control algorithms. Similar to ankle kinematics, baseline kinematics may be derived using a period of walking with the exoskeleton powered with a static, predefined torque profile or without exoskeleton torque. The hip kinematics term, θ_{hip} is a piece-wise function that is equal to $-k_8$ when deviations in hip kinematics during swing are larger than a specified threshold, $\theta_{threshold_h}$ (Eq. 4.14). When users utilize a strategy with increased hip flexion, the algorithm will decrease $d\tau_{pk}$ at subsequent strides until hip flexion at swing returns to baseline levels.

$$\theta_{hip}(n-1) = \begin{cases} -k_8 & \text{abs}(\theta_{swing}(n-1) - \theta_b) \geq \theta_{threshold_h} \\ 0 & \text{otherwise} \end{cases} \tag{4.14}$$

Thus, the total contribution from hip muscle activity, co-contraction, and kinematics can be written as:

$$d\tau_{pk,hip} = k_6 * TFL(n-1) - k_7 * CCI_h(n-1) - \theta_{hip} \tag{4.15}$$

4.1.5 Ankle-Only Control Algorithm

To assess the impact of incorporating major lower-limb joints to the co-adaptive controller, an ankle-only controller was developed based on heuristics defined in the Jackson et al. [47]. While the similar muscle activity and joint kinematic measurements were included in both

formulations of the ankle-only controller, the results may differ as our study utilizes metrics involving the RMS mean of EMG signals to calculate a change in peak torque rather than a direct mapping from EMG signals to the torque profile. The peak torque generated by the ankle-only controller, $\tau_{pk,ankle}(n)$, is defined using only the ankle contributions to $d\tau_{pk}$, the negative feedback term, and the previous peak torque (Eq. 4.17). We enforced the same minimum and maximum bounds on $\tau_{pk,ankle}(n)$ as those on τ_{pk} (Eq. 4.18).

$$d\tau_{ankle-only} = d\tau_{pk,ankle}(n) - k_{9,ankle-only} * \tau_{pk,ankle} \tag{4.16}$$

$$\hat{\tau}_{pk,ankle}(n) = \tau_{pk,ankle}(n-1) + \text{sign}(d\tau_{ankle-only}) * \max(\text{abs}(d\tau_{ankle-only}) - \tau_{thres}, 0) \tag{4.17}$$

$$\tau_{pk,ankle}(n) = \begin{cases} 5 & \hat{\tau}_{pk,ankle}(n) \leq 5 \\ \tau_{pk,ankle}(n) & 5 < \hat{\tau}_{pk,ankle}(n) < (T_{norm} * m_{user}) \\ (T_{norm} * m_{user}) & \hat{\tau}_{pk,ankle}(n) \geq (T_{norm} * m_{user}) \end{cases} \tag{4.18}$$

4.2 Simulating Torque Output

Muscle activity and joint kinematics data from Chapter 3 were used to model the evolution of peak torque over approximately 300 strides from 0% error trials, as these trials do not contain exoskeleton errors that produce immediate changes in kinematics and EMG. The proposed co-adaptive control algorithm and ankle-only algorithm were used to generate peak torque over strides according to user behavior. The performance of each controller was assessed based on the modulation of the peak torque as users exhibit fluent and non-fluent strategies.

The gains for muscle activity, co-contraction, and kinematics terms were hand-tuned using representative trials of each gait strategy found in Chapter 3 to dictate controller behavior. The model gains were tuned to ensure various characteristics, such as decreasing or constant peak torque as the user struggles with adapting to the system (e.g., increased muscle activity, non-fluent) and increasing torque as the user becomes fluent with the system (e.g., decreased ankle muscle activity). These gains were used across all users' data in this study, but may be adjusted according to the desired controller behavior and participant pilot data. We used the same procedure to set $m_{ankle} = 1.3$, $m_{hip} = 1.0$, $\theta_{threshold_a} = 1.5$ deg, $\theta_{threshold_h} = 1.25$ deg. The thresholds for ankle and hip angle deviations were chosen to align with the variability in ankle and hip kinematics found in Clusters 3/5 and 1, respectively. The hand-tuned gains are shown in Table 4.1.

Gains	Values
k_1	0.1
k_2	0.1
k_3	0.11
k_4	0.04
k_5	0.04
k_6	0.04
k_7	0.06
k_8	0.05
k_9	0.00845
$k_{9,ankle-only}$	0.009

Table 4.1: Model gains for proposed co-adaptive controller and ankle-only controller.

4.2.1 Data From Identified Strategies

In Chapter 3, fluent and non-fluent strategies were identified as users walked with predefined, fixed torque profiles with varying error rates. Three main strategies were selected for simulations:

1. Fluent strategy (Cluster 2): Users minimized muscle activity across the lower-limb with minimal to no deviations in ankle plantarflexion or hip flexion at swing.

2. Non-fluent strategy (Cluster 1): Users increased hip flexion at swing and underlying TFL muscle activity to compensate for potential errors in exoskeleton assistance (loss of torque over a stride).

3. Non-fluent strategy (Clusters 3 & 5): Users increased plantarflexion during push-off and underlying ankle muscle activity in anticipation of low system reliability. Knee kinematics also deviated from baseline with increased knee muscle activation and co-contraction.

A representative trial was selected for each strategy in this study and the initial peak torques $\tau_{pk}(0)$ were set to the mean peak torque of the static profile that users walked with in Chapter 3. The initial peak torques were (1) fluent strategy, $\tau_{pk}(0) = 23.88$ N-m; (2) non-fluent strategy, $\tau_{pk}(0) = 19.20$ N-m, and (3) non-fluent strategy, $\tau_{pk}(0) = 22.02$ N-m.

4.2.2 Simulated Adaptive Behaviors

Potential scenarios that may occur while using a co-adaptive controller, but were not identified in Chapter 3, were modeled by sampling the data from Chapter 3. The following

scenarios were constructed by scaling existing muscle activity and kinematics data from fluent strategies to simulate different trends (e.g., increasing or decreasing EMG).

- **A1 - Increasing GAS/SOL activity and ankle plantarflexion**: SOL and GAS muscle activity increased across all strides using a vector of evenly-spaced, linearly-increasing factors between 1 and 1.5. Scaling factors were generated using the MATLAB command `linspace(1,1.5,n)`, where n is the number of total strides. The EMG signals were thus scaled by 1 for the first stride and 1.5 for the last stride. An increase in ankle plantarflexion was simulated by adding a vector of evenly-spaced, linearly increasing offsets between 0 and 6 degrees (`linspace(0,6,n)`) to the ankle angle deviations at each stride. These scaling factors were chosen to align with identified muscle activity and joint kinematics changes in the Chapter 3 and induced noticable changes in the scenario's torque output.

- **A2 - Varying GAS/SOL activity and ankle plantarflexion**: SOL and GAS muscle activity increased for the first 50 strides, decreased for the next 50 strides, and remained unscaled for the remaining strides using the following MATLAB scaling vector `[linspace(1.25,1.5,50), linspace(1.5,1,50), linspace(1,1,n-100)]`. Ankle plantarflexion followed the same trend of varying ankle angle deviations using the offset vector `[linspace(0,6,50), linspace(6,0,50), linspace(0,0,n-100)]`.

- **K1 - Increased knee co-contraction**: BF and RF muscle activity increased across all strides using a scaling vector ranging from 1.25 to 2.5 (`linspace(1.5,2.5,n)`). The increase in muscle activity of the agonist-antagonist pair generated an increase in knee CCI.

- **H1 - Increased TFL/CCI and hip flexion**: TFL activity increased across all strides using a scaling vector ranging from 1.25 to 1.75 (`linspace(1.25,1.75,n)`). The increase in TFL activity increases the ratio of TFL activity to GMax activity, thus increasing hip co-contraction. Hip flexion deviations at swing increased using the offset vector ranging from 0 to 6 degrees (`linspace(0,6,n)`). Similar to Scenario A1, these scaling and offset values were selected according to cluster strategies identified in Chapter 3 and produced observable changes in torque output.

- **H2 - Varying TFL/CCI and hip flexion**: TFL activity increased for the first third of all strides, decreased for the next third of strides, and remained unscaled for the remaining strides using the following scaling vector `[linspace(1,1.5,n/3) , linspace(1.5,1,n/3), linspace(1,1,n/3)]`. Hip flexion at swing followed the

same trend of varying hip angle deviations using the offset vector `[linspace(0,6,n/3, linspace(6,0,n/3), linspace(0,0,n/3]`.

While different user strategies may manifest while walking with a co-adaptive controller, we decided to highlight the above scenarios as they may be representative of users who are struggling to adapt to the system (Scenarios A1, K1, and H1) and users that initially have difficulties adapting before becoming fluent with the system (Scenarios A2 and H2). The scenarios were created using data from the fluent strategy, thus the initial peak torque $\tau_{pk}(0)$ was set to 23.88 N-m for these potential simulated strategies.

4.3 Results

4.3.1 Data From Identified Strategies

The three identified strategies from Chapter 3 resulted in varying simulated behaviors modeled using the proposed co-adaptive controller and ankle-only controller (Fig. 4.1). The fluent strategy minimized ankle muscle activity of the GAS and SOL muscles after a period of adaptation, as the initial RMS muscle activations were reduced from 1.43 ± 0.43 (mean±SD) and 1.16 ± 0.11 across the first 10 strides to 1.05 ± 0.13 and 0.95 ± 0.09 across the last 10 strides, respectively. Deviations in ankle plantarflexion and hip flexion were centered about $-.43 \pm 1.05$ and 0.16 ± 0.95 degrees, respectively. When the user exhibits a fluent strategy, the proposed co-adaptive controller increased peak torque from $\tau_{pk}(0) = 23.88$ N-m and converged to a final peak torque of $\tau_{pk} = 26.08$. The ankle-only controller exhibited similar behavior and converged to a final peak torque of $\tau_{pk,ankle-only} = 27.59$.

When the user exhibits non-fluent strategies, the proposed co-adaptive algorithm and ankle-only controller differ in peak torque evolution. One of the non-fluent strategies was characterized by increased hip flexion (7.54 ± 2.78 degrees), TFL activation (0.96 ± 0.10), and hip co-contraction (0.78 ± 0.08). The proposed co-adaptive controller decreased peak torque from $\tau_{pk}(0) = 19.20$ N-m to a final peak torque of $\tau_{pk} = 15.21$ N-m, due to the negative contributions from the increased hip CCI and deviations in hip flexion. In contrast, the ankle-only controller resulted in increased final peak torque of $\tau_{pk,ankle-only} = 22.00$ N-m.

The second non-fluent strategy highlighted in this study exhibited increased GAS activation (1.34 ± 0.26), SOL activation (1.25 ± 0.16), and TA activation (1.22 ± 0.20), indicating increased co-contraction of the ankle. Ankle plantarflexion deviations also increased to 1.58 ± 2.18 degrees during the last 120 strides, which exceeded the predefined threshold $\theta_{threshold_a} = 1.50$ degrees. Knee and hip co-contraction also maintained larger values of 0.71 ± 0.07 and 1.04 ± 0.09. This non-fluent user behavior resulted in decreased peak torque

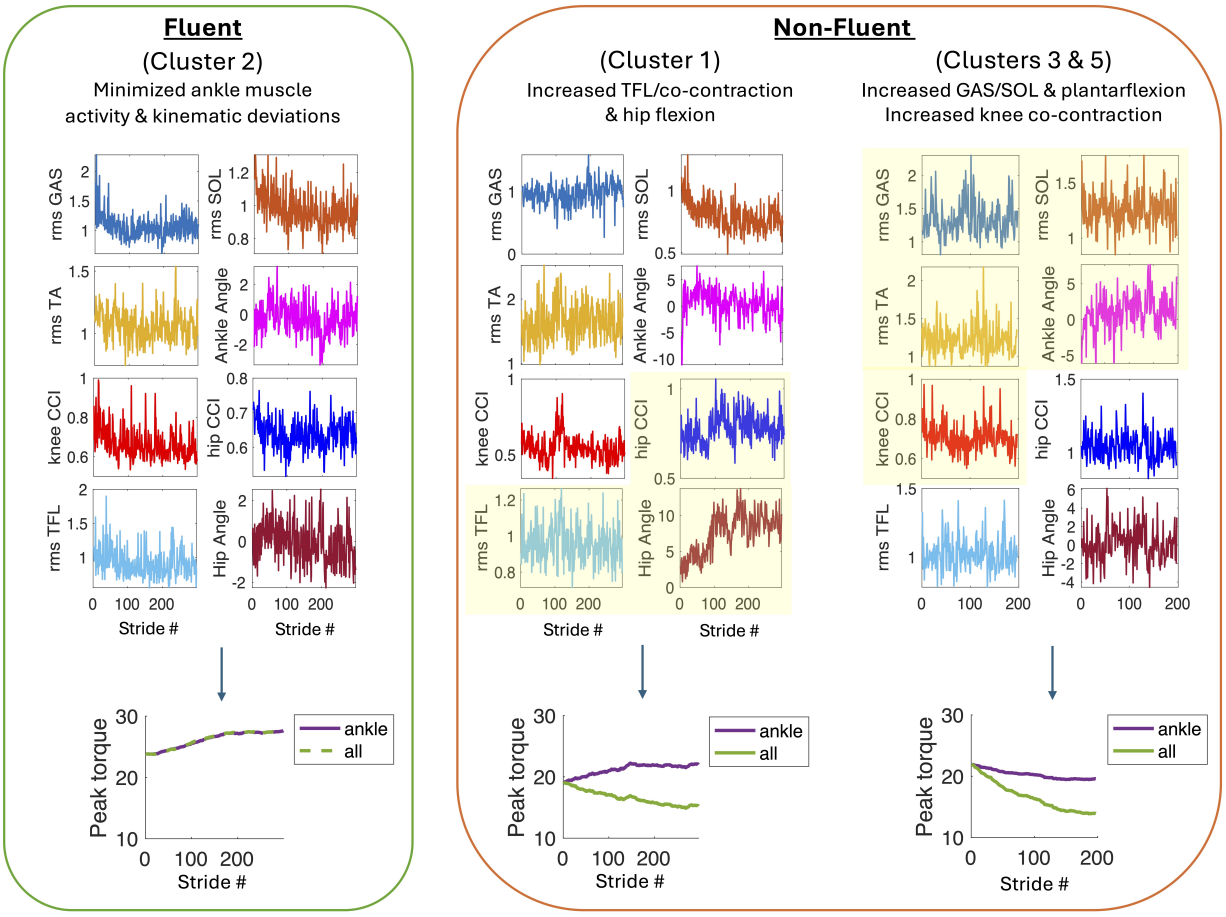

Figure 4.1: Representative data and resulting torque profiles using identified fluent and non-fluent strategies from Chapter 3.

from $\tau_{pk}(0) = 22.02$ N-m to a final value of $\tau_{pk} = 13.88$ N-m when using the proposed co-adaptive algorithm. The ankle-only controller resulted in a smaller decrease in peak torque with a final value of $\tau_{pk,ankle-only} = 19.59$ N-m.

4.3.2 Simulated Adaptive Behavior

Distinct controller behaviors from the proposed co-adaptive algorithm and ankle-only algorithm emerged from three of the five potential scenarios involving modifications in ankle, knee, and hip kinematics and muscle activity (Fig. 4.2). All scenarios were started at an initial peak torque of $\tau_{pk}(0) = 23.88$ N-m, as the underlying data was sampled from the fluent strategy described in Section 4.3.1.

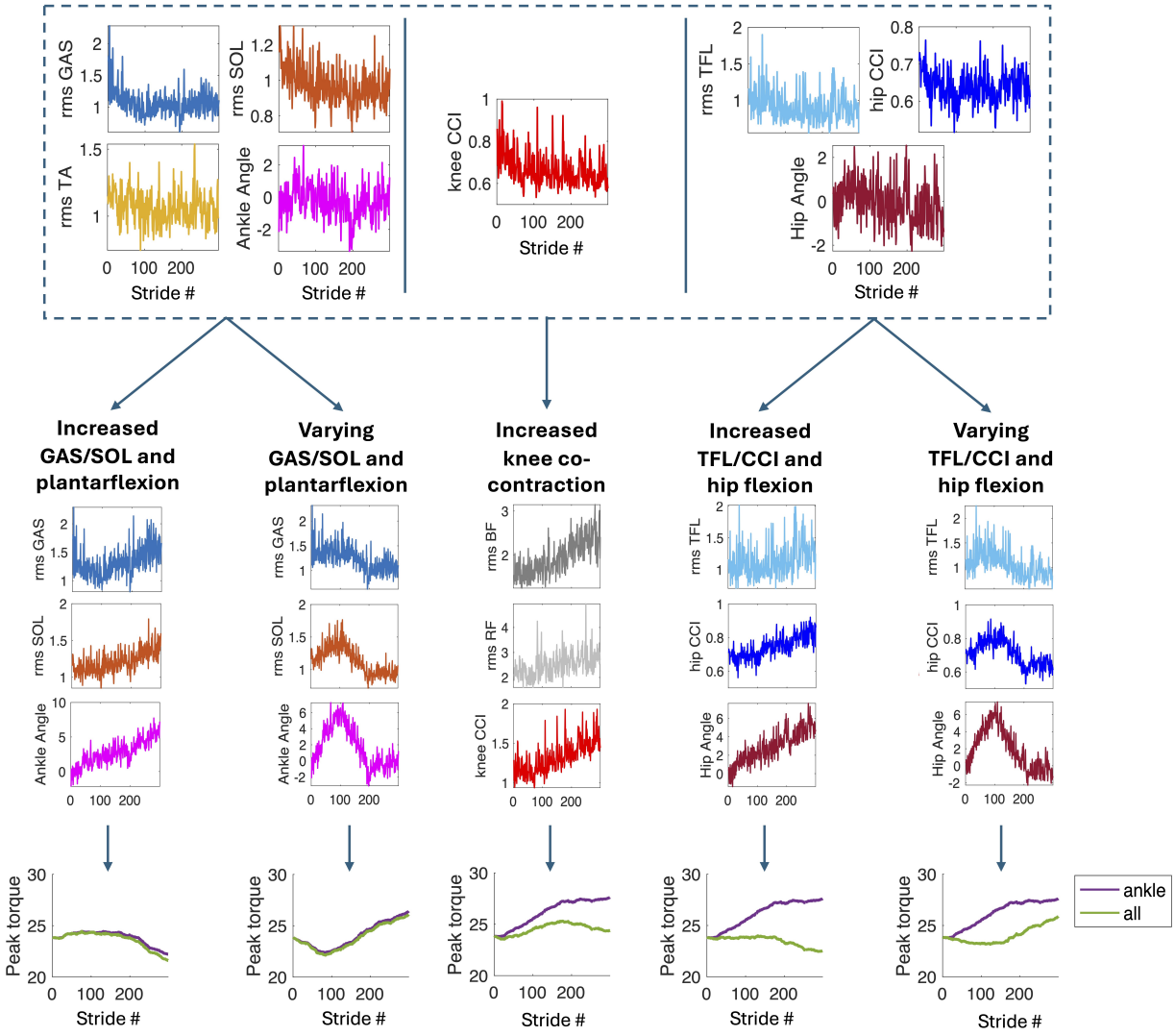

Figure 4.2: Simulated potential strategies with changes in ankle, knee, and hip behavior.

4.3.2.1 Modified Ankle Scenarios

Scenarios A1 and A2 comprised of strategies with modified ankle muscle activity and plantarflexion behavior. In Scenario A1, GAS and SOL activation increased from 1.43 ± 0.43 (mean±SD) and 1.16 ± 0.11 across the first 10 strides to 1.57 ± 0.19 and 1.43 ± 0.13 across the last 10 strides, respectively. Deviations in ankle plantarflexion also increased from 1.17 ± 0.10 to 5.78 ± 0.73 degrees across the first and last 10 strides, respectively. This user behavior prompted similar controller responses between the proposed and ankle-only algorithms, where the proposed controller resulted in a final peak torque of $\tau_{pk} = 21.58$ N-m and the ankle-only controller resulted in $\tau_{pk,ankle-only} = 22.22$ N-m.

At the first stride of Scenario A2, the initial RMS muscle activations of the GAS and SOL were 2.14 and 1.47, respectively. GAS and SOL activity increased to peak values of 1.93 and 1.77 at the 50th stride and then decreased until the 100th stride. Deviations in ankle plantarflexion followed the same trend—ankle angle deviation increased from 0.39 to 7.44 degrees across the first 50 strides, then decreased to 0.57 degrees across the next 50 strides. During the remaining strides, GAS activity, SOL activity, and ankle angle deviations were centered about 1.03 ± 0.16, 0.95 ± 0.09, and -0.44 ± 1.04 degrees, respectively. Similar to Scenario S1, the proposed co-adaptive controller and ankle-only controller resulted in comparable peak torque evolution. The peak torque simulated with the proposed algorithm initially decreased to $\tau_{pk} = 21.96$ N-m at stride 84, then increased and plateaued at a final peak torque of $\tau_{pk} = 26.75$ N-m. The ankle-only controller initially decreased peak torque to $\tau_{pk,ankle-only} = 22.22$ N-m at stride 84, then increased peak torque to $\tau_{pk,ankle-only} = 27.04$ N-m.

4.3.2.2 Modified Knee Scenario

Scenario K1 was driven by an increase in knee co-contraction due to an underlying increase in BF and RF muscle activation. BF activation increased from 1.56 ± 0.23 across the first 10 strides to 2.34 ± 0.37 across the final 10 strides. RF activation increased from 2.22 ± 0.23 to 2.96 ± 0.28 between the first and final 10 strides. The corresponding knee CCI thus increased from 1.12 ± 0.14 to 1.53 ± 0.10 between the first and final 10 strides. This user behavior resulted in differing strategies from the proposed and ankle-only algorithms. The proposed controller initially increased peak torque to a maximum value of $\tau_{pk} = 25.31$ N-m at stride 177, then decreased peak torque to a final value of $\tau_{pk} = 24.39$ N-m. In contrast, the ankle-only controller increased peak torque until reaching an equilibrium at $\tau_{pk,ankle-only} = 27.64$ N-m.

4.3.2.3 Modified Hip Scenario

Scenarios H1 and H2 involved modifications to hip muscle activity, co-contraction, and kinematics. In Scenario H1, TFL activity and corresponding hip CCI increased from 1.34 ± 0.28 and 0.82 ± 0.03 across the first 10 strides to 1.52 ± 0.23 and 0.87 ± 0.07 across the last 10 strides. GMax activity was not altered in this scenario. Deviations in hip flexion during swing increased from 0.33 to 4.60 degrees over simulated strides. Simulated peak torque with the proposed algorithm gradually decreased to a final value of $\tau_{pk} = 22.53$ N-m. The ankle-only controller resulted in increased peak torque with a final value of $\tau_{pk,ankle-only} = 27.64$ N-m.

In Scenario H2, TFL activity increased from 1.16 at stride 1 to 1.87 at stride 99, then decreased to 0.68 at stride 200. The mean RMS TFL activation for the remaining 99 strides was centered about 0.89 ± 0.19. The corresponding hip CCI followed a similar pattern, where CCI values increased from 0.71 to 0.83 across the first 99 strides, then decreased until stride 206 and plateaued about 0.64 ± 0.04. Hip flexion deviations at swing also increased from 0.33 degrees at stride 1 to 7.30 degrees at stride 102, then decreased and converged about -0.43 ± 0.92 degrees. The proposed controller initially reduced peak torque to a minimum value of $\tau_{pk} = 23.17$ N-m at stride 123 and then increased peak torque to a final value of $\tau_{pk} = 25.89$ N-m. The ankle-only controller produced the same peak torque pattern as Scenario H1, as no ankle kinematics or muscle activity were modified.

4.4 Discussion

4.4.1 Comparing Proposed vs. Ankle-Only Algorithm

User strategies involving changes in ankle muscle activity and plantarflexion resulted in similar controller behavior from the proposed co-adaptive algorithm and the ankle-only algorithm. The fluent strategy characterized by Cluster 2 had reduced GAS and SOL activation over time with minimal changes in plantarflexion, which led to to gradual increases in peak torque from the proposed and ankle only controllers (Fig. 4.1, left). Peak torque was designed to increase with minimized muscle activation and plantarflexion deviations, as lowered plantarflexor EMG signals indicated the user was leveraging the added exoskeleton torque while walking. When a user increased ankle EMG and plantarflexion deviations in Scenario A1, peak torque decreased over time for both controllers as larger muscle activity and plantarflexion levels may suggest that the user is struggling to adapt to the exoskeleton torque (Fig. 4.2). Modifications in only ankle behavior caused nearly identical peak torque evolution between the proposed and ankle-only controllers, as the hip and knee terms were not impacted in these strategies.

Gait strategies with increased knee or hip muscle activity and kinematic deviations, however, prompted reductions in peak torque over time when using the proposed co-adaptive controller compared to the ankle-only controller. Strategies found in Cluster 1 and simulated in Scenarios H1 and H2 led to decreased peak torque with the proposed controller when TFL activity, hip co-contraction, and hip flexion deviations were large (Figs. 4.1, 4.2). Similarly, when knee co-contraction and its underlying muscle activity increased in Scenario K1, peak torque decreased over time with the proposed algorithm. The changes in user behavior may be indicative of the user stiffening their knee or hip to resist the motions of the exoskeleton

(increased CCI) or anticipating and compensating for poor system performance (increased TFL and/or hip flexion). Thus, the proposed controller decreases peak torque to allow the user to adjust to a lower level of exoskeleton torque. In contrast, the ankle-only controller does not account for changes in hip or knee behavior and thus continues to increase peak torque over time until the specified equilibrium torque. The behavior of the ankle-only controller may inhibit adaptation to the exoskeleton if the user is uncomfortable and resists higher levels of torque.

Scenarios where users initially utilized non-fluent strategies before adapting to the exoskeleton were modeled using the proposed and ankle-only controller. Scenario A2 involved an initial non-fluent strategy of increasing ankle muscle activity and plantarflexion, then coordinating with the exoskeleton torque by lessening EMG and deviations in ankle angle (Fig. 4.2). The resulting peak torque profiles were nearly identical for both controllers, as only ankle behavior was modified. The peak torque initially decreased in the regions of rising EMG and ankle plantarflexion, then increased and plateaued to a larger final peak torque. In Scenario H2, hip muscle activity and kinematics were modulated to simulate an initial non-fluent strategy of increased hip EMG and flexion then adaptation to the exoskeleton with lowered hip EMG and flexion levels. The ankle-only algorithm generated the same peak torque evolution as Scenario A2, as the ankle behavior remained the same between Scenarios A2 and H2. The proposed algorithm, however, decreased peak torque in regions with increased hip EMG and flexion and increased peak torque when muscle activity and kinematic deviations were lessened. Thus, the proposed algorithm was able to adjust peak torque in response to signs of poor fluency and indicators of user adaptation, while the ankle-only exoskeleton did not respond to user strategies involving knee and hip angle and EMG modulation.

4.4.2 Considerations for Implementation

There exist various factors that should be considered for a real-time implementation of the proposed co-adaptive control algorithm. First, in this study, the gains for the muscle activity, CCI, and kinematics terms were hand-tuned according to previously collected data of people walking with the Dephy exoskeleton. These gains were used across different participants' data and generated peak torques aligned with controller behavior designed to support adaptation to the exoskeleton and fluency. In future studies, these gains may be tuned on pilot data of users walking with or without the powered exoskeleton in order to induce the desired controller output. The tuning of the gains may be conducted by hand or using a learning or optimization algorithm formulated to the the parameters. For instance, the gains can

be scaled by the same factor to cause smaller or larger changes in peak torque over each stride with respective changes in EMG and joint angles. The gains can also be scaled with respect to each other (e.g. larger gains for ankle contribution compared to hip contribution) to prioritize the effect of different joint or muscle behavior on peak torque. Different lower-extremity exoskeletons may require varying hand-tuned weights depending on the desired torque output in response to user behavior.

Our proposed control algorithm was designed for level-ground walking with minimal obstacles. The controller may be extended to different and more complex environments, such as uneven terrain or stair ascent/descent, by modifying certain aspects of the algorithm. When users are walking in uneven terrain or environments with obstacles, they may increase joint co-contraction to stiffen their joints for stability and alter their joint kinematics to ensure accurate foot placement for obstacle avoidance [98, 62, 17]. The proposed controller would thus decrease exoskeleton torque output, which may be desirable as it allows the user to have more control of their movements with lower exoskeleton assistance. Stair and ramp ascent/descent require different joint angle profiles and muscle activation compared to level-ground walking [76, 82, 13]. The proposed controller could be modified to a mode-based controller, where baseline joint trajectories and EMG profiles could be stored for each mode (e.g., stair ascent, descent) for calculations of kinematic deviations and EMG normalization.

The data used in this study was constrained to trials with approximately 300 strides per leg (5-10 minutes), which is a relatively short period compared to shifts performed by industry workers or military personnel. In operational settings, users may don the exoskeleton for longer periods of time, which may cause changes in EMG signals due to fatigue. Thus, we may incorporate a fatigue model to the proposed algorithm to offset potential changes in EMG signals. Two common measures of muscle fatigue using the Joint Analysis of Spectrum and Amplitude (JASA) method are the median frequency (MDF) and root-mean-square (RMS) or electrical activity (EA) of the EMG signals [29, 23]. The MDF is used to characterize the EMG power spectral distribution and the RMS of the EMG signal is a measure of signal amplitude. Muscle fatigue can be assessed as a decrease in MDF and an increase in RMS EMG with the same joint kinematics. Our proposed algorithm currently calculates EMG terms based on the RMS of the direct or scaled EMG signals. We can thus easily incorporate the MDF and RMS measures to our controller by calculating these measures across strides. When a shift in MDF and a corresponding increase in muscle activity is detected, the EMG signals can be re-normalized using a higher EMG signal in order to account for fatigue. Using this model, the torque profile provided by the co-adaptive controller will sustain a similar peak torque regardless of fatigue, assuming the user does not compensate using non-fluent hip or knee behavior.

4.4.3 Limitations

This study presented a formulation for a co-adaptive controller involving the major lower-limb joints and muscles and assessed its performance on existing and simulated muscle activity and joint kinematics data. A limitation of this study is that the controller has not been implemented in real-time on the Dephy exoskeleton, so it has not been determined if a change in peak torque would be sufficient to encourage fluent strategies. A co-adaptive algorithm [47] mapped ankle EMG signals and joint kinematics to the torque profile of an ankle exoskeleton, rather than the peak torque, and were able to reduce metabolic cost across multiple users. Future studies could explore shifting the torque profile's timing parameters in addition to peak torque in order to support reductions in muscle activity and energy expenditure. Additionally, this study modeled the controller behavior on a set of representative user behaviors from Chapter 3. Future work could apply the proposed algorithm to all available data from Chapter 3 and additional potential strategies to refine the fitted gains used in the controller.

4.5 Conclusion

In this study, we developed and modeled a co-adaptive control algorithm for ankle exoskeletons that incorporated muscle activity and joint kinematics measurements from the hip, knee, and ankle. The proposed controller modulated the peak torque of the exoskeleton torque profile in response to user gait strategies to support human-exoskeleton fluency. We modeled the controller behavior in multiple scenarios informed by strategies identified in Chapter 3 and simulated potential unseen strategies of non-fluency and user adaptation. The proposed co-adaptive controller was able to adjust peak torque over strides in response to indicators of low fluency (e.g., increased SOL/GAS activation, increased knee and hip co-contraction) and adaptation (e.g., minimized ankle muscle activity, minimal deviations in joint angles). The performance of our controller was compared to an ankle-only control algorithm, which was unable to adjust torque output in response to user strategies involving changes in knee and hip muscle activity and kinematics. This work is one of the first approaches to utilize measurements from joints higher in the leg kinematic chain for a co-adaptive ankle control algorithm.

CHAPTER 5

Conclusions and Future Work

The overarching goal of this work was to investigate strategies that people use when interacting with imperfect exoskeletons in the presence of foot placement goals and develop control algorithms to support human-exoskeleton fluency, which is maximized when the user and exoskeleton's goals are aligned (e.g. metabolic cost reduction). This thesis expands the existing literature on lower-limb exoskeletons, human factors, and co-adaptive control, through the following three main aims:

1. Characterize the immediate effects of exoskeleton errors on human gait strategies and trust in exoskeletons

2. Characterize the residual effects of exoskeleton errors on gait strategies in terms of human-exoskeleton fluency

3. Develop a co-adaptive exoskeleton algorithm that incorporates all major lower-limb joints and muscles to support human-exoskeleton fluency

The first aim was addressed in Chapter 2, which investigated the immediate effects of exoskeleton errors (loss of torque for select strides) and informed our understanding of motor strategies formed when walking with an exoskeleton, which aligned with the internal model hypothesis. Chapter 2 was the first study to define early direct measures for user trust in exoskeletons. Chapter 3 characterized the residual effects of selected fixed levels of exoskeleton errors on gait strategies and task performance via k-means clustering. Then, in Chapter 4, we developed and modeled a co-adaptive control algorithm using hip, knee, and ankle angle and muscle activity, as well as compared its performance against an ankle-only controller.

5.1 Summary of Results

We briefly summarize the key results from each chapter of this thesis prior to defining the major contributions to the literature.

5.1.1 Immediate Effects of Exoskeleton Errors on Gait Strategies

In Chapter 2, we found that exoskeleton users maintained acceptable targeted stepping task accuracy by increasing ipsilateral hip flexion and muscle activity when there was a loss of torque. Contralateral joint stiffness and plantarflexion torque were also increased to support task accuracy for the targeted stepping task. During catch trials, users had decreased ipsilateral plantarflexion and increased ipsilateral knee flexion, which indicated that users may have decreased muscle-generated plantarflexion torque. This ankle and knee behavior aligns with an internal model developed when adapting to an exoskeleton that provided plantarflexion assistance. We determined that human-exoskeleton fluency was impacted by missed actuations, as ipsilateral hip activity and contralateral knee and ankle activity increased in response to errors. A preliminary assessment of trust in exoskeletons was maintained throughout the study since gait strategies did not change over the course of the trials.

5.1.2 Emergent Gait Strategies When Using Imperfect Exoskeleton Algorithms

Chapter 3 utilized a k-means clustering analysis to define five emergent gait strategies as users walked with imperfect exoskeleton algorithms with fixed error rates up to 10% error. Our initial individual linear model analysis revealed various strategies across participants and error rates, so we utilized a k-means clustering to identify key behavior. We assessed user strategies in terms of muscle activation, joint kinematics, and stepping task performance. The resulting clusters were significantly different from baseline muscle activity and joint kinematics (evaluated using t-tests) and were aligned with compensatory behavior found in Chapter 2. One of the identified strategies was considered fluent, where users minimized muscle activity and aligned with the exoskeleton's goal of reducing metabolic cost while maintaining acceptable task performance. Three strategies had acceptable task error but involved increased hip or ankle muscle activity, thus negatively impacting human-exoskeleton fluency. Users may have anticipated poor system performance and thus utilized compensatory strategies by extending their leg further during swing (increased hip flexion and EMG) or increasing plantarflexion to supplement propulsive energy during push-off in case of missed actuations. We also found that participants who experienced 10% error first

(Group 2) were more likely to utilize non-fluent strategies compared to those who walked with 0% error first (Group 1). Some users also transitioned from fluent to non-fluent strategies when using controllers with poor reliability (5-10% error). While this study had a small sample size (N=22), the observed behaviors and changes in response to exoskeleton errors warrant further investigation to understand how people interact with imperfect algorithms with longer exposure periods and different systems.

5.1.3 Modeling Co-Adaptive Control of Ankle Exoskeletons

Chapter 4 presented the design of a co-adaptive control algorithm for an ankle exoskeleton that incorporated muscle activity and kinematics measurements from the hip, knee, and ankle joints. The controller was developed to support human-exoskeleton fluency by modifying the peak torque of the exoskeleton torque profile in response to user behavior. We modeled the proposed controller output in various scenarios informed by strategies identified in Chapter 3 and simulated potential unidentified strategies of non-fluency and user adaptation. The proposed co-adaptive controller was able to adjust peak torque evolution in response to signs of poor fluency (e.g., increased ankle EMG, increased joint co-contraction) and indicators of adaptation to the exoskeleton (e.g., lowered SOL/GAS activation, decreased co-contraction). The performance of the our controller was also compared against an ankle-only control algorithm, which was unable to adjust torque behavior in response to user strategies involving knee and hip angle and EMG modulation.

5.2 Contributions

This thesis makes several contributions to the existing literature on human-exoskeleton systems:

1. Immediate compensatory actions were identified when there was a loss of exoskeleton torque about the ankle, where users walking with the Dephy exoskeleton increased hip flexion and underlying muscle activity to maintain stepping task accuracy.

2. Trust in ankle exoskeletons was quantified by the change in gait strategies over time, as modifications may indicate a change in trust.

3. Objective measures of fluency were developed using user joint kinematics and muscle activity.

4. Emergent gait strategies that people may utilize when walking with imperfect exoskeleton algorithms were identified and characterized as fluent and non-fluent. Users may

transition between fluent and non-fluent strategies as they use controllers with higher error rates, as their perception of system reliability is impacted by repeated errors.

5. User perceptions of exoskeleton algorithm performance and probability of future exoskeleton usage were correlated with actual system performance.

6. Experimental methods of assessing the impact of exoskeleton errors on user performance were introduced and may be extended to different systems and error modes. These methods may be used to determine exoskeleton performance thresholds for proper usage.

7. A co-adaptive control algorithm that modifies torque assistance based on muscle activity and joints along the lower limbs was developed to support human-exoskeleton fluency.

8. Recommendations for implementing co-adaptive control in complex environments (e.g., stair ascent, ramps) and addressing fatigue during long use times were defined for future studies.

5.3 Connecting to Existing Literature

In Chapter 2, we extended our understanding of the underlying internal models developed when people walk with ankle exoskeletons. We introduced pseudo-random catch trials in the form of missed actuations, which aligned with methods in existing motor control literature [11, 12]. During catch trials, users had immediate decreases in ankle plantarflexion with the loss of exoskeleton torque, which indicated that users may have formed internal models involving reduced muscle-generated plantarflexion as they adapted to exoskeleton torque during push-off. These findings align with the modified internal model described by Hybart et al. [41], where users may form internal models that combine their own biological system dynamics with robotic dynamics. In Chapter 3, we characterized five emergent gait strategies while walking in with imperfect exoskeleton algorithms. Studies have begun to assess gait variability as people walk with exoskeletons in different environments [41] and during early adaptation to exoskeletons [2]. The different gait strategies extends our understanding of the variability in how people use exoskeletons with varying error frequencies and a foot placement task.

We also developed a preliminary measure of trust in exoskeletons, where we hypothesized that changes in user trust may manifest in changes in gait strategies over time. For instance, if a user perceived that the exoskeleton's actions were unreliable and thus decreased trust

in the system, the user may increase compensatory hip behaviors during baseline strides with normal torque in anticipation of poor exoskeleton performance. Our hypothesis aligns with the established definition of trust in human-automation systems, where trust is "the attitude that another entity will help achieve a person's goals in a situation characterized by uncertainty and vulnerability" and humans calibrate trust according to the perceived reliability of the system [54]. In Chapter 2, participants did not modify their baseline gait strategies when walking with an exoskeleton algorithm with errors in approximately 2% of all strides, which may indicate users maintained trust levels with 2% error. In Chapter 3, however, we identified three non-fluent strategies involving changes in hip and ankle behavior after exposure to poor exoskeleton performance, which may signal that users decreased trust in the system.

We developed a co-adaptive controller for ankle exoskeletons in Chapter 4, which modified torque assistance based on major lower-limb joint angles and muscle activation. This algorithm adds to existing literature on heuristic-based co-adaptive control and the simulation-based findings compare its performance against a controller that utilizes only ankle behavior, which is common for control of ankle exoskeletons. Jackson et al. [47] previously proposed and evaluated a co-adaptive controller for a bilateral ankle exoskeleton that directly maps ankle muscle activity and kinematics to torque profiles. The ankle-only controller in Chapter 4 is analogous to the Jackson controller, as both algorithms modify the exoskeleton torque profile using TA activation, plantarflexor muscle activity, and ankle plantarflexion. Additionally, we modulated peak torque in response to different hip, knee, and ankle strategies, but there exist four parameters that can describe the exoskeleton torque profile used in this thesis (rise time, fall time, peak torque, peak torque time) [110]. Future studies may investigate controllers that adjust timing parameters in response to user behavior to support coordination between the human and exoskeleton. Overall, the formulation of our proposed co-adaptive controller can inform future algorithm design for ankle exoskeletons and may potentially map to different systems.

The construct of fluency enables researchers to assess collaboration between a human and exoskeleton through direct measures of user behavior, as well as support effective exoskeleton usage through algorithms that encourage fluent human-exoskeleton interactions. While our co-adaptive control algorithm utilizes metrics defined to quantify various aspects of human-exoskeleton fluency, it may be possible to encourage fluency with different algorithm formulations without heuristic-based metrics. Since fluency has been defined as maximized when the exoskeleton and user's goals align, user behavior that is deemed as fluent depends on the system and its design goals. In this thesis, we have defined fluent behavior as the reduction of plantarflexor muscle activity and minimal deviations from baseline kinematics as

people walk with an assistive ankle exoskeleton for metabolic cost reduction. For a rehabilitative gait exoskeleton, fluent strategies may involve significant changes in joint trajectories [7] or increases in energy expenditure [22] as people with motor deficits follow the desired exoskeleton joint trajectories to encourage healthy gait patterns. Thus, one control method for gait training exoskeletons may encourage fluency by minimizing interaction forces between the human and exoskeleton to support healthy gait patterns using impedance-based control [97, 8]. Exoskeleton designers can support safe and goal-based human-robot interaction by supporting fluent behaviors through control algorithm formulations.

5.4 Applications and Recommendations

The co-adaptive control scheme with hip, knee, and ankle measurements for lower-limb exoskeletons is one of the main immediate applications of this work. The controller adapts to user behavior and modulates the exoskeleton torque profile to support fluent strategies and user adaptation to the system. While the control algorithm currently uses hand-tuned gains that dictate controller behavior, these gains can be used across multiple users once they have been adjusted based on representative data, as shown in Chapter 4. We have also given recommendations on extending the control algorithm into operational settings in Section 4.4.2, where the environment may necessitate different modes of locomotion (e.g., ramps, stairs) and the terrain may be uneven or contain obstacles. Baseline muscle activity and kinematics measurements may be defined in each locomotion mode to account for intentional and necessary changes in gait strategies.

This work has also operationalized human-exoskeleton fluency using gait strategies as people walk using an ankle exoskeleton. Fluent behaviors involve reductions in muscle activity and minimal deviations in kinematics, while users with low fluency may increase joint stiffness via muscle co-contraction and modify their joint angles to resist or compensate for exoskeleton torque. While we have only assessed fluency with ankle exoskeletons, fluency can be defined based on the desired exoskeleton system and its goals. For instance, a rehabilitative exoskeleton can be used to encourage normal and symmetrical muscle recruitment and joint trajectories. An interpretation of human-exoskeleton fluency for the rehabilitative robot may thus involve increased muscle activation and significant modifications in joint kinematics, which opposes our definition of fluency for the assistive Dephy ankle exoskeleton. Fluency can be incorporated into the design process of exoskeleton controllers, similar to our proposed co-adaptive algorithm, and used as an evaluation metric for human-exoskeleton team performance.

We observed in Chapter 3 that participants who experienced exoskeleton controllers with

poor performance first (Group 2) were more likely to utilize non-fluent strategies than users who walked with high performing controllers first (Group 1). Users in Group 2 may have modified their underlying internal model or used a different strategy in anticipation of repeated exoskeleton errors with 5-10% error controllers to utilize compensatory strategies, such as increased hip flexion and TFL activation. In comparison, multiple participants in Group 1 were able to maintain fluent strategies even after walking with controllers with higher error rates. We hypothesized that experiencing controllers with lower error may encourage users to build robust internal models supporting fluent strategies. Users that experienced higher error controllers may have lost trust in the exoskeleton, as the perceived system performance lowered due to repeated errors, and utilized compensatory non-fluent strategies. Thus, we recommend that users should first adapt to and use exoskeletons in settings where error frequency is low (e.g., steady-state walking in laboratory) prior to walking in more complex environments where errors may be more prevalent (e.g., uneven terrain, variable speed walking). Training in a controlled environment allows users to build sufficient experience and trust in the exoskeleton before using the system in uncertain, operational settings.

The results of Chapter 3 also suggest there may exist a threshold for exoskeleton performance where users will transition from fluent to non-fluent strategies. Users were more likely to use strategies with increased hip or ankle muscle activity and joint flexion when the frequency of missed actuations exceeded 5-7%. It is important to define the minimum performance requirements for an exoskeleton system to ensure user behavior is likely to align with the goals of the exoskeleton. Our experimental protocols in Chapters 2 and 3 provide an approach to evaluating the immediate and residual effects of errors on user performance, and may be adapted to different systems and error modalities. For instance, a knee exoskeleton applies a different torque profile during gait compared to an ankle exoskeleton, so deviations in the torque parameters may incur varying responses in user strategies. Exoskeleton performance must be robust to a specified threshold prior to use in operational settings to support user adoption.

5.5 Potential Future Work

This thesis lies in the intersection of exoskeleton control algorithms, human factors, and human motor control and investigated key questions involving interactions between users and exoskeletons and algorithm design. Here, we will detail other existing related areas and topics that we did not address in this thesis, as well as promising areas and studies for future development.

5.5.1 Implementation of the Co-Adaptive Controller

A direct extension of this thesis is the implementation of the proposed co-adaptive controller on an ankle exoskeleton. In this thesis, we utilized the Dephy exoskeleton, which applies a plantarflexion torque about the ankle, and thus developed the controller for a similar assistive exoskeleton. The algorithm could be directly mapped to exoskeletons with analogous torque profiles, where the torque ramps to a peak value then decreases for predictable, cyclic motions. Depending on the task and exoskeleton goal, peak torque or other parameters may be modulated in response to user behavior. Exoskeletons that apply torques that do not subscribe to a defined profile or assist tasks that do not have cyclic motions (e.g., upper limb exoskeletons) require additional modifications to the control algorithm prior to implementation. While the controller was designed for exoskeletons with one degree of freedom, increasing actuation to multiple degrees of freedom would allow for different tasks or assistance profiles while adding to algorithm complexity. Greater degrees of freedom would benefit exoskeletons that exert more control or assistance to support the user's actions, such as gait rehabilitation robots that guide patients to normal gait trajectories.

Following the implementation of a co-adaptive controller on a physical exoskeleton system, the impact of co-adaptive control on user strategies should be compared to that of a fixed torque controller, as controllers with fixed, predefined torque profiled are a common control method for exoskeletons. Users should walk with both the fixed torque controller and the co-adaptive controller in order to evaluate the impact of changing peak torque on user adaptation. The experimental design of future studies should account for learning effects by randomizing the order of controllers across participants. It is recommended that users walk with each controller for at least 30 minutes, which is the time provided during the training protocol in Chapter 2, and additional experience with longer walking periods may encourage further adaptation to the exoskeleton. Future studies may assess the rate of adaptation between using the co-adaptive and fixed torque controller by using measures of muscle activity across key lower-limb muscles, where user adaptation may manifest as decreased plantarflexor muscle activity (e.g. gastrocnemius, soleus) and minimal deviations in joint kinematics compared to walking without an exoskeleton. Users may also converge to different gait strategies when using a co-adaptive or fixed controller, so it is important to also evaluate the progression of user behavior as they adapt to the control algorithms. While we found that some users transitioned from fluent to non-fluent strategies while using imperfect fixed torque controllers in Chapter 3, it may be possible that users may converge to more fluent strategies if given additional time to walk with the fixed controller.

5.5.2 Repeatability of User Strategies

We identified five different gait strategies in Chapter 3, where users modulated joint kinematics and muscle activity while walking with a powered ankle exoskeleton and completed a targeted stepping task. It is important, however, to assess if these strategies would arise repeatedly while people interact with ankle exoskeletons and develop algorithms to support collaboration with exoskeletons. We developed experimental methods in Chapter 3 involving various fixed error frequencies, which allowed us to probe different user behavior and may be extended to different error modalities and systems. Future studies can investigate the repeatability of user strategies by utilizing similar experimental methods over multiple sessions, where the participants walk with the same controllers and error frequencies multiple times over the course of days or weeks. Resulting user strategies could be sorted to the defined clusters from Chapter 3 by transforming the data using the same identified principal components and assigning cluster membership based on proximity to cluster centroids. It may also be possible that strategies that were not identified in Chapter 3 may arise due to additional exposure to the exoskeleton over multiple sessions or variability across different users. Overall, it is important to understand variations in user gait strategies in order to develop algorithms which support collaboration between the human and exoskeleton, as users have individual and differing adaptation rates [2] and strategies as identified in Chapter 3.

5.5.3 Long-Term User Adaptation

Similar to many lower-limb exoskeleton studies, the training periods in Chapters 2 and 3 typically involved 15-30 minutes of steady-state treadmill walking, as the length was restricted due to time constraints of the experimental protocol. A key assumption is that users have undergone an initial adaptation to the exoskeleton after the training protocol and baseline measures of performance may be calculated based on the end of training. It has been shown, however, that adaptation to a bilateral ankle exoskeleton may take up to 109 minutes for healthy expert exoskeleton users [75]. The study by Poggensee et al. [75] also noted that high variability training with a human-in-the-loop controller that continuously optimized during training may have sped up adaptation rates. Thus, researchers should explore if longer training times with the co-adaptive controller that also varies torque parameters (peak torque) would encourage users to converge to fluent strategies at a different rate with varying reductions in muscle activity and metabolic cost.

Longitudinal studies, where participants utilize the exoskeleton for periods over the course of days or weeks, could reveal long-term user adaptation to exoskeletons. Many exoskeleton studies involving metabolic cost reduction or rehabilitative robots assess changes in user

performance over one to two sessions in controlled laboratory settings, as the equipment is typically restricted to the laboratory. A longitudinal study where users walk with the exoskeleton in various environments over multiple sessions may deepen our understanding of user adaptation. It may be possible that users can learn multiple gait strategies and underlying internal models and utilize specific strategies depending on the environment. These experiments are also important prior to adoption of exoskeletons in industry or medicine, as the results may reveal long-term effects of exoskeleton assistance on workers and patients.

5.5.4 Feedback Modalities to Encourage Fluency

Incorporating different types of feedback modalities may be utilized to encourage different behavior when interacting with the exoskeleton. Our previous study found that gait-synchronized haptic cues could induce changes in gait speed and stride length as users walked with an ankle exoskeleton [107]. We had observed reductions in feedback benefits when the exoskeleton was powered on as people balanced collaborating with the exoskeleton and the haptic cues, but were still able to modulate speed in response to different cue timing. Auditory and visual cues have also been used during gait training for individuals with Parkinson's Disease to encourage specific stepping strategies, such as increased stride length [88], gait cadence [4], and postural control [68]. Thus, it may be possible to use auditory and/or haptic feedback to encourage certain gait strategies and variability during training protocols.

Training protocols may also be a key tool to support adaptation and convergence to optimal strategies when using exoskeletons. Many studies investigating human adaptation to exoskeletons instruct users to walk with the powered exoskeleton at a predetermined speed and duration [32, 70, 26] and found reductions in energy expenditure across grouped participant data. On an individual scale, however, users may not adapt to the exoskeleton by reducing the underlying muscle activity as expected [2], resulting in minimal changes to metabolic cost. Thus, it is important to investigate if incorporating feedback that encourages exoskeleton users explore different strategies when using the exoskeleton will support adaptation to optimal strategies.

Guided exploration during training has been shown to improve adaptation to novel environments. Selinger et al. [84] used an exoskeleton to apply torques that resisted motion in order to shift people's energetically optimal step frequencies to those higher or lower than preferred. When users underwent a training protocol with auditory metronome cues that enforced large variations in step frequency, they were able to reach the new energetically optimal step frequency that could not be found with normal gait variability. Mapping this exploration framework to augmentative exoskeletons that apply torques that assist motion

during gait, we can also encourage exploration during training that may improve adaptation. For instance, during guided training, users would walk at various speeds and step frequencies by matching metronome cues similar to [84], which can support convergence to a new preferred walking strategy with an assistive exoskeleton. For instance, metronome cues of varying frequencies may be used as auditory feedback to guide the user's gait cadence to prompt higher variability during exoskeleton training, which may speed up adaptation and expose the user to different gait strategies.

5.5.5 Linking Fluency to Additional Metrics

In addition to muscle activity and joint kinematics measurements, human-exoskeleton fluency can be linked to additional metrics, such as direct measures that align with the exoskeleton's goal (e.g., metabolic cost) and user perception measures. Studies involving lower-limb assistive exoskeletons often involve measures of metabolic rate through respiratory indirect calorimetry, so future work can investigate the relationship between different gait strategies, fluency, and metabolic cost. User perceptions of exoskeleton performance may be assessed through surveys and used to form perception-based measures of fluency. In Chapter 3, we used the survey question "Rate how well the exoskeleton supports your actions" to obtain a measure of user perception of human-exoskeleton fluency. Participants who utilized one of the three non-fluent strategies perceived lower exoskeleton supportiveness than those who used a fluent strategy, which may indicate a connection between direct measures of fluency and the perception-based measure. Future work can implement specific inquiries on system reliability and performance to build additional user perception measures of fluency.

5.5.6 Measures of Human-Exoskeleton Trust

We developed a preliminary direct measure of user trust in exoskeletons in Chapter 2, where changes in trust may manifest as modifications in gait strategies over time. For example, users may lower their trust in the system due to poor system reliability or predictability, which may be observed through sustained increases in ankle or hip muscle activation as the user anticipates exoskeleton errors. Future work could assess our defined trust metric or other potential measures by establishing a relationship between quantitative and user perception-based measures of trust. Surveys involving user perception of trust and system performance may inform perception measures, as perceived system reliability is linked to trust [54]. Similar to Section 5.5.4, trust may then be linked to other metrics of user performance, such as metabolic cost, in addition to muscle activity and joint kinematics.

5.5.7 Different Error Modalities

The experimental protocols in Chapters 2 and 3 were used to assess the impact of missed actuations on gait strategies and stepping task performance and may be mapped to different error modalities and systems. For an assistive ankle exoskeleton, errors in actuation timing, such as early or late actuations, may result in misalignment between muscle-generated plantarflexion and exoskeleton torque and may impede food clearance. The resulting changes in user behavior may differ between errors in actuation timing and peak torque (e.g., loss of torque, unexpected reduction of torque). Additionally, we identified a threshold of 5-7% error where a subset of users would transition between fluent and non-fluent strategies. The experimental methods in Chapter 3 may be used to determine minimum performance metrics for various error types prior to adoption in operational settings.

5.6 Concluding Remarks

This thesis explored defined aspects of exoskeleton design, from how people interact with exoskeletons to a proposed co-adaptive control algorithm. At the beginning of this thesis, we highlighted the question of how users would interact with exoskeleton errors that may occur in operational settings. This question was addressed for missed actuation errors in Chapter 2, in which immediate hip compensatory behaviors were identified in response to loss of plantarflexion torque to maintain acceptable stepping task accuracy. We then characterized the residual effects of exoskeleton errors, where users utilized different strategies involving changes in muscle activity and joint kinematics. We also established a definition for human-exoskeleton fluency—alignment of user and exoskeleton goals—that can be used to evaluate user behavior when interacting with exoskeletons and as a design metric for control algorithms. A co-adaptive control algorithm was then designed to support fluency through torque profile modulation in response to user strategies during level-ground walking. We also provided recommendations for implementation and extending the work to different environments and systems. Throughout this thesis, we investigated how humans and exoskeletons may affect one another as a tightly-coupled system. In the future, designers of exoskeletons and other wearable robots should continue to account for human behavior and perceptions to support human-exoskeleton interactions and teams.

APPENDIX A

Impact of Imperfect Exoskeleton Algorithms on Step Characteristics, Task Performance, and Perception of Exoskeleton Performance

A.1 Introduction

Lower-limb exoskeletons have the potential to assist a human user's motor performance in laboratory environments by decreasing energy expenditure [70, 110]. In order for exoskeletons to be adopted in operational settings, they must be robust in uncertain environments. However, while exoskeleton control algorithms are continuously being developed and improved [86, 48], they are unlikely to be perfect and will experience errors. For instance, if gait phase estimation is inaccurate, the exoskeleton may miss an actuation during a stride and affect gait strategies. Gait outcomes arise from the interaction between the human and exoskeleton. As the coordinated meshing of actions between the human and robot is defined as fluency [39], we can consider that human-exoskeleton fluency occurs when the human and exoskeleton's goals align. For example, the human decreasing muscular activity for exoskeletons designed to reduce energy expenditure. Thus, it is important to understand how exoskeleton errors impact gait strategies and human-exoskeleton fluency in order to inform performance requirements for exoskeleton algorithms.

Previous work has begun exploring the impact of imperfect control algorithms when walking with a lower-limb exoskeleton. Wu et al. [106] introduced random errors in exoskeleton operation by not applying an expected exoskeleton torque while participants completed a targeted stepping task. The study used an algorithm with approximately 2% error, or 98% accuracy, and found that step characteristics and task accuracy were not impacted by errors due to adaptations in joint kinematics. The level of error in the study was relatively low, so it is important to understand how more frequent exoskeleton errors will impact stepping strategies and task performance. For instance, it is possible that users will begin to in-

crease muscle activation as they anticipate repeated errors, which is against the goals of the exoskeleton and would impact human-exoskeleton fluency.

The adoption of exoskeletons in real-world environments also depends on the user's perception of the exoskeleton's performance and benefits. Perceived usefulness of technology has been correlated with the current and future usage in the technology acceptance model [19], which has been shown to be applicable to various forms of technology [50]. Similarly, when users interact with exoskeletons, the algorithm's performance informs their perceptions of system usefulness, thus impacting their willingness to adopt the technology. Studies have begun to characterize the perception of exoskeleton performance, such as control parameters [74] and metabolic benefit [67], under nominal laboratory conditions. It is also necessary to understand user perception of exoskeleton usefulness when exposed to exoskeleton errors similar to operational settings.

In this study, we introduce exoskeleton algorithms with defined error rates in order to understand how users respond to more frequent errors. We hypothesized that there would be time-dependent and algorithm-dependent changes in (1) step characteristics (step length and width), (2) task performance (task error), and (3) perception of exoskeleton performance (survey ratings). We also hypothesized that higher levels of error would cause larger changes in the above metrics. These results will be interpreted in the context of perceived exoskeleton usefulness and human-exoskeleton fluency.

A.2 Methods

A.2.1 Participants

Participants (N = 22, age = 25.3±5.0 years (mean±SD), height = 1.67±0.30 m, mass = 68.0±9 kg, leg length = 903.0±43.7 mm, 12 female and 10 male) provided written informed consent. A subset of N = 12 were analyzed in this study. Participants were excluded if they had a lower extremity injury within the past 6 months or used an assistive walking device. The protocol was approved by the University of Michigan Institutional Review Board (HUM00217656).

A.2.2 Experimental Setup

Participants walked on a treadmill in a room equipped with a 10-camera optical motion capture system. Reflective markers were placed on the participants according to the Vicon Plug-in Gait full-body model. Markers were adjusted for the exoskeleton by placing the lower limb markers on the lateral side of the exoskeleton when necessary. Motion capture

data were collected at 100 Hz. Study participants wore the Dephy ExoBoot on both legs (Fig. A.1) (DpEb504, Dephy Inc, Maynard, MA, USA) [63]. The ExoBoot applied torque at the ankle at push-off during the stance phase of the gait cycle, learned from 25 strides, which is the same as our previous study [106].

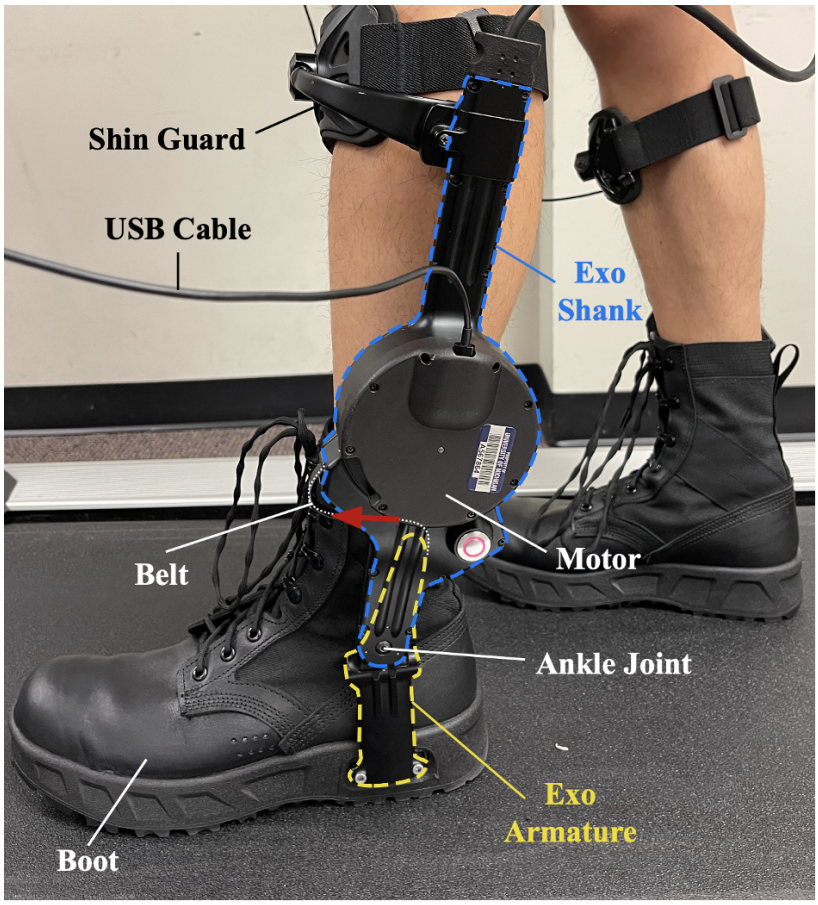

Figure A.1: Powered bilateral ankle exoskeleton, which provides assistance by applying torque via the inelastic belt attached to the exoskeleton armature (DpEb45, Dephy Inc) [74].

A.2.3 Protocol

Anthropometric measures were collected prior to walking with the exoskeleton. Leg length was measured as the distance from the anterior superior iliac spine to the medial malleolus. Participants were given a target stepping task, which was a 320 mm-long region marked along the sides of the treadmill, while walking at a fixed speed of 1.2 m/s. Participants were asked to aim their heel at the center-line of the target region at the end of each stride. The length of the stepping target was chosen to be the length of the largest exoskeleton boot

size, a Men's size 13.

Participants underwent a training protocol where they walked with the stepping target for 15 minutes with the exoskeleton powered on and torque applied during each stride. Then, participants were separated into two groups (N=6 per group), which experienced the exoskeleton control algorithms in different orders. There were 5 different controllers with 0%, 2%, 5%, 7%, and 10% error. This translates to controller accuracies of 100%, 98%, 95%, 93%, and 90% respectively. Errors were introduced randomly throughout each trial by not actuating the exoskeleton for a single stride. The exoskeleton algorithm also included a recovery period after each error, where the exoskeleton ramps up from 0% to 50% of the normal torque on the first stride after each error, then 80% on the second stride after a error, and finally back to 100% from the third stride onward.

Participants experienced each controller twice for a total of 10 trials. Group 1 started with a 0% error controller, increased to 10% error, and then decreased to 0% error. Group 2 started with a 10% error controller, decreased to 0% error, and then increased to 10% error. Details on the groups and control algorithms are shown in Tables A.1 and A.2.

Trial	Group 1	Group 2	Order
1	0%	10%	1
2	2%	7%	1
3	5%	5%	1
4	7%	2%	1
5	10%	0%	1
6	10%	0%	2
7	7%	2%	2
8	5%	5%	2
9	2%	7%	2
10	0%	10%	2

Table A.1: Trial order of each participant group, where the percentages represent the error rate of each control algorithm. The order represents whether the trial is the first or second time that a participant experiences an error rate.

A.2.4 Survey

Participants were given a survey after every trial to rate their perceptions of the control algorithms. The questions analyzed in this study and the associated Likert scales of 1 to 5 are described below:

- Rate how you felt the exoskeleton supports your actions.

Error Rate	# of Catch Trials	Total # of Strides
0%	0	300
2%	12	600
5%	15	300
7%	21	300
10%	30	300

Table A.2: The number of catch trials and total strides for each error rate, where a catch trial consists of not actuating the exoskeleton for a single stride.

(1 = extremely hinders actions, 3 = neither hinders nor supports actions, 5 = extremely supports actions)

- Rate your accuracy in completing the stepping task.
  (1 = not at all accurate, 3 = moderately accurate, 5 = extremely accurate)
- Rate the predictability of the exoskeleton's actions.
  (1 = not at all predictable, 3 = moderately predictable, 5 = extremely predictable)
- Rate the probability that you would use this controller again. (1 = not probable, 3 = neutral, 5 = very probable)

A.2.5 Data Analysis and Statistical Analysis

Gait cycles were segmented with a custom MATLAB script by using the heel marker data from motion capture to identify heel strikes. Normalized step length (NSL), normalized step width (NSW), and task error were calculated using heel marker positions and treadmill velocity. NSL and NSW were calculated as the distance between anterior and lateral foot fall locations, normalized by leg length. Absolute task error was calculated as the absolute value of distance between each heel strike and the center-line of the stepping target. Acceptable absolute task error was determined as ≤ 160 mm, which is half of the 320 mm-long target.

Linear mixed-effects models were fit to NSL, NSW, and task error data with the following factors: Participant (random, 12 levels), Step Number (continuous, [1, 600 or 1200]), Group (2 fixed levels), and Order (2 fixed levels). The models were fit using a custom R script and significance level was set to $\alpha = 0.05$. Operationally relevant changes were identified as significant changes in each metric between the beginning and end of a trial that were greater than the mean standard deviation across the trial.

ANOVAs were fit to the responses of each survey question with the factors of Participant (random) and Error Rate (5 fixed levels) with significance level set to $\alpha = 0.05$. Spearman's

rank correlation coefficients (r_s) were calculated for the survey results to assess if survey scores were monotonically related.

A.3 Results

	0% Error		2% Error		5% Error		7% Error		10% Error	
	Estimate	p	Estimate	p	Estimate	p	Estimate	p	Estimate	p
Participant	0.675	<0.001	0.685	<0.001	0.673	<0.001	0.670	<0.001	0.668	<0.001
Step Num	<0.001	<0.001	<0.001	0.125	<0.001	<0.001	<0.001	<0.001	<0.001	<0.001
Order 1 vs 2	0.021	<0.001	-0.056	<0.001	0.007	0.001	<0.001	0.728	0.005	<0.001
Group 1 vs 2	0.020	<0.001	0.017	<0.001	0.023	<0.001	0.023	<0.001	0.020	0.0145
Step N*Order 2	<0.001	0.062	<0.001	<0.001	<0.001	0.849	<0.001	0.220	<-0.001	0.0349
Step N*Group 2	<-0.001	0.301	<0.001	0.211	<0.001	0.387	<0.001	0.294	<-0.001	0.497
Order 2*Group 2	-0.017	<0.001	0.054	<0.001	-0.003	0.384	0.011	<0.01	0.007	0.025
Step N*O2*G2	<-0.001	0.090	<-0.001	<0.001	<-0.001	0.272	<-0.001	0.006	<-0.001	0.713

Table A.3: Summary of statistics for linear mixed-effects models (N=12) fitted to normalized step length (NSL) across all error rates. O2 represents Order 2 and G2 represents Group 2.

	0% Error		2% Error		5% Error		7% Error		10% Error	
	Estimate	p	Estimate	p	Estimate	p	Estimate	p	Estimate	p
Participant	0.136	<0.001	0.133	<0.001	0.135	<0.001	0.133	<0.001	0.143	<0.001
Step Num	<0.001	0.699	<0.001	0.813	<-0.001	0.8687	<0.001	0.045	<-0.001	<0.001
Order 1 vs 2	<-0.001	0.778	0.022	<0.001	-0.006	0.003	0.001	0.510	-0.010	<0.001
Group 1 vs 2	-0.001	0.557	0.003	0.065	0.004	0.092	0.010	<0.001	0.003	0.130
Step N*Order 2	<-0.001	0.149	<-0.001	<0.001	<0.001	0.001	<-0.001	0.010	<0.001	<0.001
Step N*Group 2	<-0.001	0.201	<-0.001	0.490	<-0.001	0.954	<-0.001	0.001	<0.001	0.048
Order 2*Group 2	<0.001	0.802	-0.025	<0.001	-0.005	0.112	-0.016	<0.001	<0.001	0.924
Step N*O2*G2	<0.001	0.164	<0.001	<0.001	<-0.001	0.345	<0.001	<0.001	<-0.001	0.007

Table A.4: Summary of statistics for linear mixed-effects models (N=12) fitted to normalized step width (NSW) across all error rates. O2 represents Order 2 and G2 represents Group 2.

A.3.1 Step Characteristics

While there were significant main effects of Participant, Step Number, Order, Group, and interaction effects on normalized step length (NSL) across select error rates (Table A.3), most were not operationally relevant. Pooled NSL across all participants at all error rates are shown in Fig. A.2 (left). Using the definition of operationally relevant changes, only participants in Group 2 increased NSL at an error rate of 2% at Order 1 (mean=15.2% increase, SD=5.7%), despite significant factors in the linear-mixed effects models.

There were significant main effects of the Participant, Step Number, Order, Group, and interaction effects for normalized step width (NSW) across select error rates, shown in Table

	0% Error		2% Error		5% Error		7% Error		10% Error	
	Estimate	p	Estimate	p	Estimate	p	Estimate	p	Estimate	p
Participant	79.64	<0.001	135.75	<0.001	118.55	<0.001	112.12	<0.001	101.95	<0.001
Step Num	0.06	<0.001	0.01	<0.001	0.05	<0.001	0.04	<0.001	0.06	<0.001
Order 1 vs 2	41.03	<0.001	7.28	0.005	-15.99	<0.001	14.11	0.002	10.07	<0.001
Group 1 vs 2	38.87	<0.001	-10.47	<0.001	1.99	0.582	-7.40	0.102	-4.00	0.130
Step N*Order 2	0.02	0.075	-0.02	<0.001	0.02	0.033	0.01	0.468	-0.03	<0.001
Step N*Group 2	-0.08	<0.001	-0.01	0.051	-0.02	0.087	0.02	0.131	0.04	0.048
Order 2*Group 2	-34.80	<0.001	-14.49	<0.001	13.50	0.008	48.69	<0.001	22.77	0.924
Step N*O2*G2	-0.002	0.857	0.03	<0.001	-0.02	0.191	0.01	0.544	-0.08	0.007

Table A.5: Summary of statistics for linear mixed-effects models (N=12) fitted to absolute task error across all error rates. O2 represents Order 2 and G2 represents Group 2.

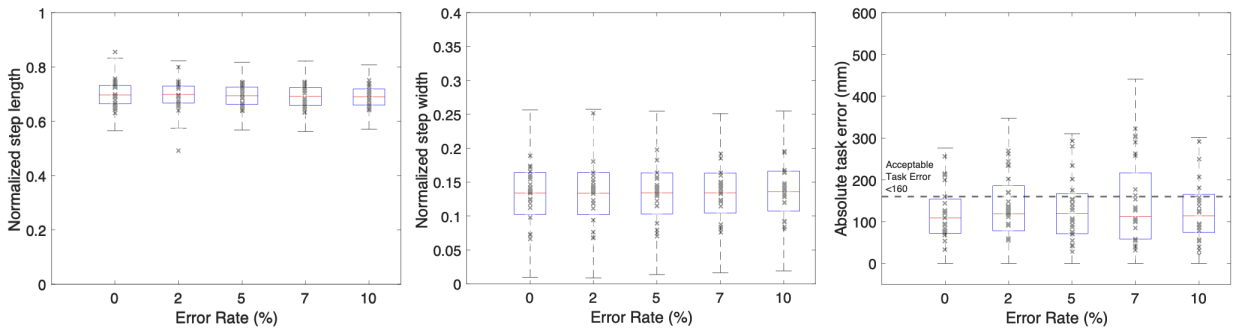

Figure A.2: (left) Normalized step length (NSL), (middle) normalized step width (NSW), and (right) absolute task error pooled from all participants (N=12) across all error rates. For the right figure, each 'x' marker represents the mean abs. task error of a single trial for one participant. Each box includes 25th to 75th percentile and whisker length is 1.5*IQR.

A.4. Pooled NSW across all participants at all error rates are shown in Fig. A.2 (middle). When using the definition of operational relevance, there were no relevant changes in NSW across all error rates despite significant fitted slopes in the linear models.

A.3.2 Task Accuracy

There were significant main effects of Participant, Step Number, Order, Group, and interaction effects on absolute task error, shown in Table A.5. While most participants were able to achieve acceptable task accuracy ($\leq$160 mm), some participants (6 of 12, 50%) had significantly higher task error (Table A.6). A majority of participants (8 of 12, 67%) also experienced a relevant operational change in task accuracy over time (A.7), as defined in Section II.E. A plot of the absolute task error across all error rates is shown in Fig. A.2 (right).

		Order 1		Order 2	
Error	$\leq$ 160mm?	N	$\overline{\lvert TaskError \rvert}$	N	$\overline{\lvert TaskError \rvert}$
0	Y	10	89.58 mm	9	103.44 mm
	N	2	213.16 mm	3	223.45 mm
2	Y	8	97.14 mm	9	94.94 mm
	N	4	217.88 mm	3	240.22 mm
5	Y	10	104.23 mm	9	94.67 mm
	N	2	264.41 mm	3	201.94 mm
7	Y	9	79.25 mm	7	89.27 mm
	N	2	235.89 mm	5	219.82 mm
10	Y	10	101.29 mm	8	89.27 mm
	N	2	233.40 mm	4	285.29 mm

Table A.6: Table of absolute task error data for acceptable ($\leq$160 mm) and non-acceptable ($>$160 mm) task performance. N represents the amount of participants in each group and $\overline{\lvert TaskError \rvert}$ is the mean absolute task error per group.

	Order 1		Order 2	
Error	N	$\Delta\lvert TaskError \rvert$	N	$\Delta\lvert TaskError \rvert$
0	6	+65.58 mm	5	+66.83 mm
2	5	+47.67 mm	3	+48.82 mm
5	6	+54.99 mm	3	+63.61 mm
7	5	+48.38 mm	6	+66.57 mm
10	6	+87.74 mm	3	+52.55 mm

Table A.7: Table of operationally relevant changes in task error across all error rates. N is the amount of participants that experienced changes and $\Delta\lvert TaskError \rvert$ is the mean change in abs. task error for each error rate and Order.

Error	Support	Accuracy	Predictability	Usage Prob.
0%	4.08 (0.65)	4.00 (0.78)	4.13 (1.03)	4.17 (0.96)
2%	3.79 (1.02)	3.75 (0.85)	3.21 (1.18)	3.33 (1.52)
5%	3.63 (1.10)	3.54 (0.72)	2.63 (1.21)	2.88 (1.48)
7%	3.58 (1.14)	3.46 (0.88)	2.50 (1.14)	2.88 (1.54)
10%	3.38 (1.31)	3.50 (0.88)	2.41 (1.17)	2.58 (1.56)

Table A.8: Summary of survey responses, where users rated the exoskeleton's supportiveness, perceived task accuracy, algorithm predictability, and possibility of future usage on a scale from 1 (low) to 5 (high). The mean and standard deviation are reported across all error rates (mean (SD)).

A.3.3 Survey Results

The mean and standard deviation of the survey responses across all error rates are shown in Table A.8. The factor of Error Rate was significant for perceived algorithm predictability ($F(4, 104) = 17.95$, $p < 0.001$), exoskeleton supportiveness ($F(4, 104) = 15.41$, $p < 0.001$), probability of future usage ($F(4, 104) = 15.41$, $p < 0.001$), and perceived task accuracy ($F(4, 104) = 4.24$, $p = 0.003$). There was a moderate negative correlation between perceived predictability and error rates ($r = -0.46$, $p < 0.001$), a very weak negative correlation between supportiveness and error rate ($r = -0.18$, $p = 0.051$), and a strong positive correlation between perceived predictability and supportiveness ($r = 0.73$, $p < 0.001$) (Fig. A.3).

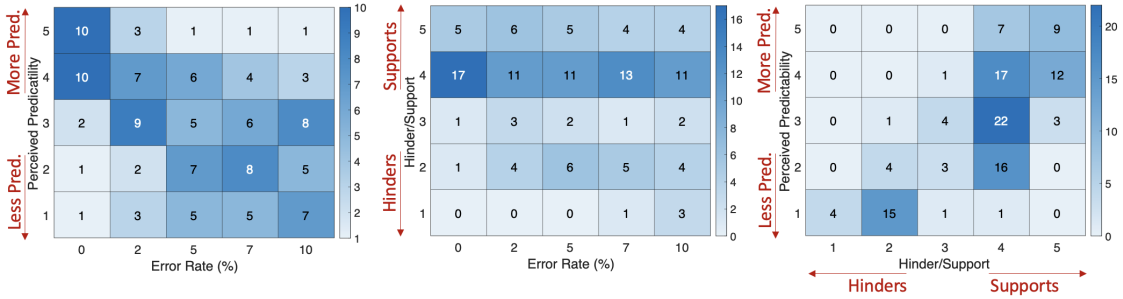

Figure A.3: (left) Perceived predictability vs. trial error rate ($r = -0.46$, $p < 0.001$), (middle) perceived supportiveness vs. trial error rate ($r = -0.18$, $p = 0.05$), and (right) perceived predictability vs supportiveness for all participants and trials ($r = 0.73$, $p < 0.001$). The numbers are the count of data-points for each combination of predictability, supportiveness, and error rate.

A.4 Discussion

This study explored the effect of imperfect algorithms on step characteristics, task performance, and perceptions of exoskeleton performance. We introduced algorithms with 0%, 2%, 5%, 7%, and 10% error, which corresponds to 100%, 98%, 95%, 93%, and 90% accuracy, respectively. Participants were also sorted into two groups which experienced each controller twice, but in different orders. We evaluated the impact of each error rate with respect to the participant's group, if it was their first or second exposure to the algorithm (order), and over the time of each trial (step number). Operationally significant changes were defined as changes in metrics over time that were greater than the standard deviation.

Overall, participants were able to maintain their step characteristics across error rates for the assessed Orders and Groups. The data do not support the first hypothesis that there would be time-dependent changes in step characteristics. Only participants within Group

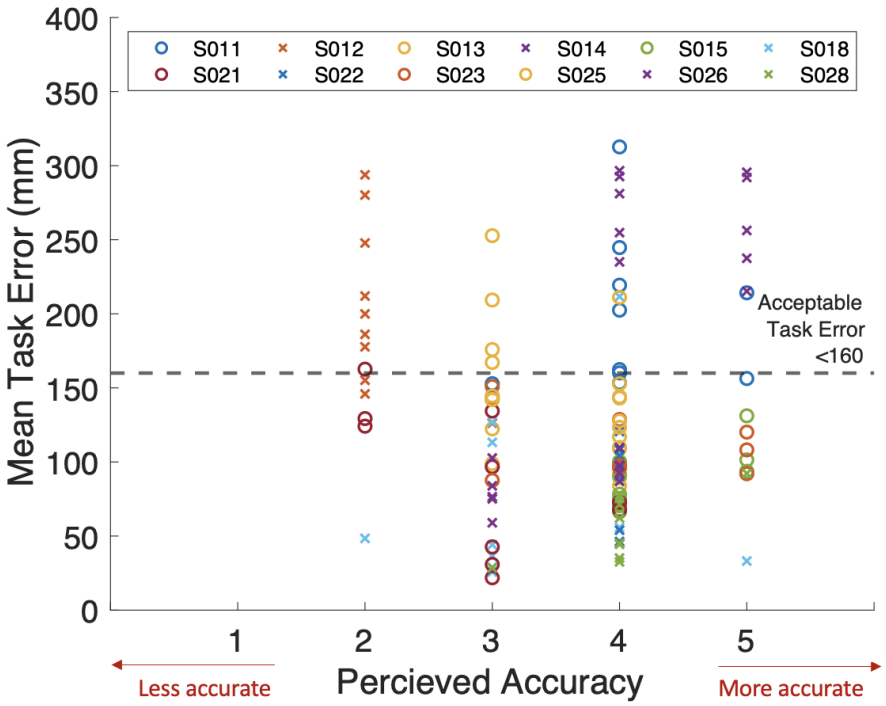

Figure A.4: Mean absolute task error plotted against the users' rating of perceived task accuracy, where 1 represents low accuracy and 5 represents high accuracy. Each marker represents the data from one trial for one participant.

2 during the first exposure to 2% error increased NSL by 15.2%. This change in NSL may have been motivated by the relatively low error rate compared to the previous 5%-10% error controllers that the Group 2 participants experienced first. Participants may have relearned to trust the exoskeleton when it performed with lower error, which allowed for improved collaboration with the exoskeleton torque and thus increased NSL over time. The data had no observed significant changes in NSW, which can be considered an indicator of mediolateral stability [5] and may indicate that errors up to 10% do not impact this stability metric.

Our second hypothesis predicted that there would be time-dependent changes to task accuracy and was supported by these data. There was a significant increase in absolute task error over each trial. The changes in task accuracy were observed in multiple participants (67%), regardless of their mean absolute task error, Group, and the Order (Table A.6). Multiple participants (50%) were also unable to achieve acceptable absolute task accuracy of $\leq$160 mm (Table A.7). The changes in task error with the consistent NSL and NSW indicates that participants may be adjusting their position on the treadmill over time rather than changing NSL to reach the stepping target. Participants with significant increases in task error likely shifted further back along the treadmill. The significant task error changes

may suggest that users directed less attention to completing the stepping task or were unable to match the treadmill speed and may have slowed down if they had been on a self-paced treadmill or were overground.

The trend in task accuracy is different from our previous study [106], where participants were able to consistently achieve acceptable task accuracy when walking with a controller with 2% error. The difference in task performance between studies may arise as this study's participants had experience with controllers with relatively poorer accuracy, impacting their overall trust in the system and human-exoskeleton fluency. If participants were less trusting of the system, they may either focus more on coordinating with the exoskeleton's torque, adjust their kinematics in anticipation of errors, or begin to fight the system by stiffening their muscles to restrict joint movement, thus leading to deviations in task performance. Changes in trust may be linked to the perception of exoskeleton performance, which was qualitatively assessed through post-trial surveys.

Survey responses on exoskeleton performance and future usage were impacted by the frequency of controller errors, which supports our third hypothesis of algorithm-dependent changes in survey responses. As error rates increased, the average score for supportiveness, predictability, and future usage probability significantly decreased (Table A.8). At 0% error, participants on average felt that the exoskeleton moderately supports their actions with a very predictable control algorithm that they would likely use again, enabling them to achieve very accurate task performance. When errors were more frequent, users' perceptions of the exoskeleton become more neutral and tended towards negative. At 10% error, participants on average felt that the exoskeleton neither hindered nor supported their actions; users found the algorithm to be slightly to moderately predictable and rated it slightly improbable that they would use the controller in the future. As perceived predictability of the exoskeleton's algorithm decreased, users also reported that the exoskeleton no longer supported their actions (Fig. A.3). The transition to feeling neutral about the predictability and future usage of the exoskeleton was observed as errors increase from 2% to 5%. The transition from positive to negative perception of exoskeleton performance between 2 to 5% error should inform minimum accuracy requirements for exoskeletons designed to support gait.

Users' perception of task accuracy was consistently between moderate and very accurate across all error rates (Table A.8). The data shows otherwise, with 6 participants (50%) with a mean task error of >160 mm across all controllers, indicating that some users may overestimate their task performance. Additionally, 8 participants (67%) significantly increased task error over trials across all controllers. The misaligned perceived and actual task accuracy may prevent users from making accurate adjustments to their stepping strategies to support acceptable task accuracy.

Overall, participants maintained step characteristics when walking with an exoskeleton controlled by imperfect algorithms, but task accuracy and perceptions of exoskeleton performance and future usage were impacted. Multiple participants were not able to achieve acceptable task accuracy and some participants showed increases in absolute task error over time as the exoskeleton experienced errors. Users also reported that they perceived exoskeleton algorithms as less predictable and less likely to be used in the future as the frequency of errors increased. It is important to note that users' survey responses are dependent on their interpretation of terms such as "predictability" and "supportiveness." For instance, it is possible that users felt that the exoskeleton was supportive if they were able to feel the applied torque, regardless of if the exoskeleton assisted or opposed their motions. Further research should explore differences between actual and perceived exoskeleton goals and the emergent torques. Alternate exoskeletons may also yield different responses across error ranges. Future work will involve analyzing the joint kinematics and muscle activity data collected with this dataset to understand the underlying adaptations across the range of exoskeleton error frequency collected. The analysis will also help further define algorithm accuracy requirements for gait-assist exoskeleton controllers.

A.5 Conclusion

This study explored the impact of imperfect exoskeleton algorithms with up to 10% error on step characteristics, task performance, and perceived exoskeleton performance. Users were able to maintain step characteristics, but multiple participants were not able to achieve acceptable task accuracy and also increased task error over time across all error rates. Users' perception of exoskeleton performance was negatively impacted as the frequency of errors increased, thus decreasing the probability of future usage. Understanding the effect of the various exoskeleton error rates will inform minimum exoskeleton algorithm accuracy to support human-exoskeleton fluency and system performance.

APPENDIX B

Initial Individual Linear Mixed Effects Models Fit To Joint Kinematics

Our initial analysis in Chapter 3 involved individual linear mixed effects models to assess changes in joint kinematics (peak hip flexion during swing, minimum knee flexion during loading response, peak plantarflexion) across error rates and groups. The model utilized factors of Error (fixed, 0, 2, 5, 7, 10% error), Leg (fixed, left or right), Order (fixed, the first or second exposure to the error rate), and Stride Num (continuous, the stride number associated with each measurement, used as a measure of time). Interaction effects were calculated across all factors and levels. The intercept fit to each model was evaluated at the first level of each fixed factor (0% error, left leg, first exposure to 0% error). The model was fit for each participant and the results (fitted estimates and p-values) have been summarized in Tables B.1 to B.20. Each table includes a note contextualizing the results of the fitted model with respect to gait strategies over time.

Table B.1: S003 linear mixed effects model fit to joint kinematics

	Hip Estimate	Hip P value	Knee Estimate	Knee P value	Ankle Estimate	Ankle P value
(Intercept)	4.49E-01	0.108406	-0.058379017	0.739299555	0.276861769	0.232590348
error2	-2.10E+00	5.90E-05	0.105625184	0.747388156	-0.209671082	0.628645347
error5	1.06E+00	0.042368	0.294512622	0.366087163	1.130219327	0.008728445
error7	-1.35E+00	0.046439	0.349078491	0.411267814	0.007704408	0.989054389
error10	-1.87E+00	0.008608	0.143521551	0.747716641	-0.049746204	0.932789498
leg2	-4.92E-01	0.213525	0.230254177	0.353384528	2.69337844	3.10E-16
order2	-9.70E-01	0.014155	-1.639990618	4.30E-11	1.475873677	6.90E-06
stride_num	-3.00E-03	0.064014	0.000389193	0.701022168	-0.001845745	0.168456402
error2:leg2	8.62E-01	0.203729	0.797253719	0.060989395	-3.011282983	9.16E-08
error5:leg2	1.56E-01	0.87516	-1.227723659	0.049130474	-5.978427742	5.21E-13
error7:leg2	4.08E-01	0.659843	-2.042397723	0.00044401	-5.212639397	1.35E-11
error10:leg2	1.34E+00	0.173054	-1.010144442	0.100811542	-4.983772487	1.01E-09
error2:order2	1.17E+00	0.113672	0.530725302	0.252915175	0.266934552	0.663545823
error5:order2	-2.44E+01	2.00E-16	4.421964943	7.50E-22	-1.771848073	0.00337827
error7:order2	8.54E+00	2.00E-16	-8.801091296	2.58E-47	9.955370464	2.14E-35
error10:order2	1.77E+00	0.078535	2.168311995	0.000595909	-1.663947673	0.046115877
leg2:order2	1.54E+00	0.005842	0.358898554	0.306176507	-6.061971964	4.23E-38
error2:stride_num	7.68E-03	0.000336	-0.000806725	0.54775538	0.001747913	0.324531438
error5:stride_num	-2.56E-02	8.93E-14	0.001084147	0.612922424	-0.016464379	6.77E-09
error7:stride_num	2.00E-03	0.656491	-0.00218175	0.438682975	0.000187756	0.959791288
error10:stride_num	7.00E-03	0.05137	-0.001426491	0.526498963	0.002130626	0.4742442
leg2:stride_num	3.28E-03	0.151255	-0.001535028	0.28430612	-0.017955856	5.00E-21
order2:stride_num	3.96E-03	0.082667	0.002402966	0.092945289	0.001217371	0.519597753
error2:leg2:order2	-1.62E+00	0.09221	-0.22625444	0.707072329	3.705579709	3.35E-06
error5:leg2:order2	2.12E+01	2.00E-16	-1.456791738	0.097995668	8.007154907	7.09E-12
error7:leg2:order2	-9.76E+00	1.13E-13	10.4744351	1.89E-36	-2.276614244	0.035862214
error10:leg2:order2	-1.33E+00	0.33969	-1.854270087	0.033190971	6.420592056	2.59E-08
error2:leg2:stride_num	-4.32E-03	0.123574	-0.004082351	0.020265227	0.014655778	3.23E-10
error5:leg2:stride_num	1.88E-02	0.000554	0.000769391	0.821454121	0.036387743	9.52E-16
error7:leg2:stride_num	2.40E-05	0.996534	0.004660962	0.17801337	0.024202789	1.29E-07
error10:leg2:stride_num	-2.75E-03	0.632428	0.005415467	0.133003485	0.022526622	2.36E-06
error2:order2:stride_num	-4.57E-03	0.130285	-0.001123835	0.553188425	-0.001700024	0.497429452
error5:order2:stride_num	1.01E-01	2.00E-16	-0.016077891	5.92E-08	0.019174969	9.94E-07
error7:order2:stride_num	-1.10E-01	2.00E-16	0.111896142	2.22E-155	-0.124275609	1.13E-113
error10:order2:stride_num	-8.00E-03	0.115344	-0.00409859	0.197992351	-0.0003882	0.926504794
leg2:order2:stride_num	-5.69E-03	0.07838	0.00107727	0.594709806	0.016715262	4.79E-10
error2:leg2:order2:stride_num	7.88E-03	0.046778	0.001365877	0.582400028	-0.01538396	2.91E-06
error5:leg2:order2:stride_num	-8.64E-02	2.00E-16	0.002579291	0.589227694	-0.042844231	1.37E-11
error7:leg2:order2:stride_num	1.13E-01	2.00E-16	-0.114653303	3.27E-112	0.089137191	5.00E-42
error10:leg2:order2:stride_num	4.19E-03	0.606112	0.003041213	0.55064804	-0.02300558	0.000645002

Notes: S003 decreased peak hip flexion by ±2 degrees at 2, 5, 7, and 10% error when compared to 0% error. Minimum knee flexion at loading response generally did not change across error rates at the first exposure, but varied at 5 and 7% error during the second exposure. Peak plantarflexion was significantly different across legs and order, which interacted with error rate.

Table B.2: S005 linear mixed effects model fit to joint kinematics

	Hip Estimate	Hip P value	Knee Estimate	Knee P value	Ankle Estimate	Ankle P value
(Intercept)	-0.07494	0.648592	1.741931	1.99E-16	-0.01108	0.965238
error2	-0.48467	0.115708	-3.46619	2.59E-18	0.254116	0.593626
error5	-0.88013	0.004481	-2.13181	8.17E-08	0.491901	0.303913
error7	-0.40517	0.308963	-2.13635	2.91E-05	1.03688	0.092193
error10	0.129017	0.7586	-1.83092	0.000673	0.664684	0.305799
leg2	0.052947	0.820044	-1.28429	1.71E-05	-1.07777	0.00276
order2	1.943722	1.25E-16	-4.44481	2.57E-48	4.50591	6.00E-35
stride_num	0.0005	0.599043	-0.01161	2.78E-21	7.39E-05	0.959898
error2:leg2	-1.01424	0.010694	2.905022	1.24E-08	1.396629	0.022975
error5:leg2	2.674444	5.74E-06	2.485452	0.000996	-1.30735	0.15093
error7:leg2	2.10302	0.000115	1.735799	0.012923	-0.061	0.942239
error10:leg2	0.920308	0.111478	1.111221	0.133716	-0.05066	0.954798
error2:order2	-1.35917	0.001425	4.938385	2.39E-19	-2.81338	1.97E-05
error5:order2	0.615522	0.154167	3.243457	5.08E-09	-3.41615	3.29E-07
error7:order2	-0.53579	0.341778	1.942046	0.007199	-3.3331	0.000133
error10:order2	-1.59579	0.006742	3.777629	5.80E-07	-3.44447	0.000156
leg2:order2	0.94827	0.004129	-1.03217	0.01483	0.740252	0.14735
error2:stride_num	0.000712	0.571502	0.01172	4.46E-13	-0.00069	0.724498
error5:stride_num	0.005211	0.012463	0.007902	0.003116	-0.00753	0.01958
error7:stride_num	0.001408	0.593774	0.002984	0.377927	-0.00069	0.866737
error10:stride_num	0.001266	0.548748	0.001106	0.68256	0.002103	0.519399
leg2:stride_num	-0.00035	0.793586	0.008552	7.65E-07	0.007209	0.000543
order2:stride_num	-0.00042	0.759859	0.012398	1.44E-12	-0.00581	0.00575
error2:leg2:order2	1.143938	0.040427	-0.77881	0.276164	-3.04605	0.000419
error5:leg2:order2	-2.92921	0.000412	-0.33087	0.75533	0.945823	0.460267
error7:leg2:order2	-3.0088	9.65E-05	0.991644	0.315426	-1.53251	0.198433
error10:leg2:order2	0.149302	0.8545	0.604188	0.562551	-0.27274	0.828446
error2:leg2:stride_num	0.003205	0.051506	-0.01128	9.46E-08	-0.00866	0.000672
error5:leg2:stride_num	-0.00946	0.003589	-0.00865	0.03758	0.00818	0.103068
error7:leg2:stride_num	0.001163	0.719929	-0.01145	0.00593	-0.00328	0.513312
error10:leg2:stride_num	-0.00032	0.923431	-0.00785	0.069972	-0.00851	0.103469
error2:order2:stride_num	0.003582	0.040852	-0.0159	1.71E-12	0.009545	0.000428
error5:order2:stride_num	-0.00981	0.000552	-0.01271	0.00048	0.015992	0.000272
error7:order2:stride_num	-0.00711	0.057309	0.000253	0.957949	0.006469	0.263346
error10:order2:stride_num	-0.00011	0.970939	-0.00768	0.04158	0.00518	0.254467
leg2:order2:stride_num	0.003196	0.097264	-0.0072	0.003569	-0.0038	0.202656
error2:leg2:order2:stride_num	-0.00748	0.001317	0.008749	0.003373	0.00925	0.010181
error5:leg2:order2:stride_num	0.006766	0.134872	0.001984	0.732185	-0.01722	0.013846
error7:leg2:order2:stride_num	0.005134	0.264253	0.013147	0.025726	0.000819	0.908282
error10:leg2:order2:stride_num	-0.01098	0.021014	0.003411	0.575711	0.005597	0.446484

Notes: S005 decreased minimum knee flexion during loading response across error rates when compared to 0% error and maintained peak hip flexion and plantarflexion. There was a significant effect of order, which suggests there was a difference in gait strategies between the first and second exposure to error rates.

Table B.3: S006 linear mixed effects model fit to joint kinematics

	Hip Estimate	Hip P value	Knee Estimate	Knee P value	Ankle Estimate	Ankle P value
(Intercept)	-1.34063	2.17E-13	0.569804	0.00488	1.338908	9.04E-12
error2	-0.0614	0.857043	0.878455	0.020507	-0.7773	0.033937
error5	1.209161	0.00028	-0.66289	0.073022	0.613422	0.086158
error7	0.964722	0.027819	-0.61705	0.205624	0.091732	0.845662
error10	2.057183	9.05E-06	-1.91675	0.000198	0.653718	0.188855
leg2	-0.84169	0.001081	0.462569	0.10599	-2.04302	1.91E-13
order2	-0.52863	0.039816	-0.15835	0.579636	1.450381	1.63E-07
stride_num	-0.00123	0.240238	-0.00092	0.433778	-0.00228	0.044121
error2:leg2	1.743464	8.08E-05	-1.83454	0.000191	0.879459	0.064096
error5:leg2	-0.00314	0.996105	0.66937	0.350054	-1.9183	0.005628
error7:leg2	1.885676	0.001713	-0.19886	0.765985	-0.94926	0.141721
error10:leg2	0.592843	0.353025	-0.0326	0.963361	-0.12363	0.857012
error2:order2	3.254229	1.71E-11	-2.82769	1.40E-07	1.539471	0.00298
error5:order2	-1.02567	0.029574	1.160751	0.026806	-0.43596	0.38948
error7:order2	-1.65122	0.007915	0.904957	0.190382	0.628614	0.346734
error10:order2	-1.36365	0.037579	2.209574	0.002454	-1.12333	0.111003
leg2:order2	0.842103	0.020704	1.00855	0.012722	0.444116	0.256251
error2:stride_num	0.003077	0.027104	-0.00324	0.036272	0.002441	0.102883
error5:stride_num	0.003192	0.131992	0.00091	0.699442	-0.00447	0.049767
error7:stride_num	0.004769	0.102702	-0.00364	0.262402	-0.00066	0.833198
error10:stride_num	-0.00221	0.345122	0.008942	0.000583	-0.00578	0.021485
leg2:stride_num	0.002279	0.125424	0.001534	0.353557	0.000661	0.679236
order2:stride_num	0.011676	4.69E-15	-0.00083	0.613043	0.001347	0.398196
error2:leg2:order2	-3.95286	2.87E-10	1.979951	0.004406	-1.37227	0.041142
error5:leg2:order2	-0.96724	0.289418	-0.72412	0.475667	1.373926	0.161581
error7:leg2:order2	0.154146	0.856506	-0.15378	0.871126	-0.79107	0.38803
error10:leg2:order2	-0.62683	0.487868	0.087568	0.930548	-0.15153	0.876028
error2:leg2:stride_num	-0.00534	0.003418	0.002542	0.209923	-0.00272	0.164726
error5:leg2:stride_num	0.000362	0.916912	-0.00806	0.036826	0.011718	0.001704
error7:leg2:stride_num	-0.00912	0.011121	-0.00123	0.757399	0.005063	0.189403
error10:leg2:stride_num	0.000738	0.843406	-0.00644	0.121319	0.008187	0.04166
error2:order2:stride_num	-0.01794	1.18E-19	0.008996	3.94E-05	-0.00417	0.048472
error5:order2:stride_num	-0.01194	7.72E-05	-0.00453	0.177022	0.00577	0.075328
error7:order2:stride_num	-0.00534	0.195811	-0.00027	0.953461	-0.00066	0.882005
error10:order2:stride_num	-0.00993	0.002641	-0.00907	0.013551	0.010987	0.001978
leg2:order2:stride_num	-0.00852	5.23E-05	-0.00711	0.002366	-0.00016	0.943886
error2:leg2:order2:stride_num	0.015636	1.50E-09	0.001192	0.677745	0.00466	0.092909
error5:leg2:order2:stride_num	0.009743	0.047885	0.010611	0.052662	-0.01023	0.053244
error7:leg2:order2:stride_num	0.004504	0.37575	0.005655	0.317277	0.003422	0.531291
error10:leg2:order2:stride_num	-0.00027	0.959594	0.010532	0.073239	-0.0088	0.121549

Notes: S006 significantly modified peak hip flexion and minimum knee flexion at select error rates and across legs, but to a small margin (±2 degrees). While plantarflexion was not affected across error rates, it was significantly different between legs and order.

Table B.4: S007 linear mixed effects model fit to joint kinematics

	Hip Estimate	Hip P value	Knee Estimate	Knee P value	Ankle Estimate	Ankle P value
(Intercept)	-1.34063	2.17E-13	0.569804	0.00488	1.338908	9.04E-12
error2	-0.0614	0.857043	0.878455	0.020507	-0.7773	0.033937
error5	1.209161	0.00028	-0.66289	0.073022	0.613422	0.086158
error7	0.964722	0.027819	-0.61705	0.205624	0.091732	0.845662
error10	2.057183	9.05E-06	-1.91675	0.000198	0.653718	0.188855
leg2	-0.84169	0.001081	0.462569	0.10599	-2.04302	1.91E-13
order2	-0.52863	0.039816	-0.15835	0.579636	1.450381	1.63E-07
stride_num	-0.00123	0.240238	-0.00092	0.433778	-0.00228	0.044121
error2:leg2	1.743464	8.08E-05	-1.83454	0.000191	0.879459	0.064096
error5:leg2	-0.00314	0.996105	0.66937	0.350054	-1.9183	0.005628
error7:leg2	1.885676	0.001713	-0.19886	0.765985	-0.94926	0.141721
error10:leg2	0.592843	0.353025	-0.0326	0.963361	-0.12363	0.857012
error2:order2	3.254229	1.71E-11	-2.82769	1.40E-07	1.539471	0.00298
error5:order2	-1.02567	0.029574	1.160751	0.026806	-0.43596	0.38948
error7:order2	-1.65122	0.007915	0.904957	0.190382	0.628614	0.346734
error10:order2	-1.36365	0.037579	2.209574	0.002454	-1.12333	0.111003
leg2:order2	0.842103	0.020704	1.00855	0.012722	0.444116	0.256251
error2:stride_num	0.003077	0.027104	-0.00324	0.036272	0.002441	0.102883
error5:stride_num	0.003192	0.131992	0.00091	0.699442	-0.00447	0.049767
error7:stride_num	0.004769	0.102702	-0.00364	0.262402	-0.00066	0.833198
error10:stride_num	-0.00221	0.345122	0.008942	0.000583	-0.00578	0.021485
leg2:stride_num	0.002279	0.125424	0.001534	0.353557	0.000661	0.679236
order2:stride_num	0.011676	4.69E-15	-0.00083	0.613043	0.001347	0.398196
error2:leg2:order2	-3.95286	2.87E-10	1.979951	0.004406	-1.37227	0.041142
error5:leg2:order2	-0.96724	0.289418	-0.72412	0.475667	1.373926	0.161581
error7:leg2:order2	0.154146	0.856506	-0.15378	0.871126	-0.79107	0.38803
error10:leg2:order2	-0.62683	0.487868	0.087568	0.930548	-0.15153	0.876028
error2:leg2:stride_num	-0.00534	0.003418	0.002542	0.209923	-0.00272	0.164726
error5:leg2:stride_num	0.000362	0.916912	-0.00806	0.036826	0.011718	0.001704
error7:leg2:stride_num	-0.00912	0.011121	-0.00123	0.757399	0.005063	0.189403
error10:leg2:stride_num	0.000738	0.843406	-0.00644	0.121319	0.008187	0.04166
error2:order2:stride_num	-0.01794	1.18E-19	0.008996	3.94E-05	-0.00417	0.048472
error5:order2:stride_num	-0.01194	7.72E-05	-0.00453	0.177022	0.00577	0.075328
error7:order2:stride_num	-0.00534	0.195811	-0.00027	0.953461	-0.00066	0.882005
error10:order2:stride_num	-0.00993	0.002641	-0.00907	0.013551	0.010987	0.001978
leg2:order2:stride_num	-0.00852	5.23E-05	-0.00711	0.002366	-0.00016	0.943886
error2:leg2:order2:stride_num	0.015636	1.50E-09	0.001192	0.677745	0.00466	0.092909
error5:leg2:order2:stride_num	0.009743	0.047885	0.010611	0.052662	-0.01023	0.053244
error7:leg2:order2:stride_num	0.004504	0.37575	0.005655	0.317277	0.003422	0.531291
error10:leg2:order2:stride_num	-0.00027	0.959594	0.010532	0.073239	-0.0088	0.121549

Notes: Hip flexion was significantly higher at 5-10% error compared to 0% error and varied across leg and order. Minimum knee flexion and peak plantarflexion had small significant changes at select error rates. Plantarflexion levels differed between legs and order of controller exposure.

Table B.5: S009 linear mixed effects model fit to joint kinematics

	Hip Estimate	Hip P value	Knee Estimate	Knee P value	Ankle Estimate	Ankle P value
(Intercept)	1.113093	8.81E-10	0.642674	0.01029	0.246537	0.294459
error2	-0.4523	0.182427	-1.84299	8.67E-05	0.170478	0.698751
error5	-0.33317	0.313965	-0.31641	0.489157	1.085566	0.011564
error7	2.578377	4.50E-09	0.764851	0.207125	1.524829	0.007443
error10	-0.10174	0.825795	0.89387	0.16199	1.056888	0.078384
leg2	-0.85622	0.000835	-1.22272	0.00056	-0.87192	0.008777
order2	1.421925	3.03E-08	-1.91601	6.68E-08	0.40025	0.228784
stride_num	0.001176	0.260941	-0.00332	0.021789	0.000532	0.695422
error2:leg2	1.151562	0.008843	0.064654	0.91529	-0.33976	0.551788
error5:leg2	1.377759	0.031671	-0.02273	0.97954	-1.66021	0.046194
error7:leg2	-0.76714	0.201691	0.094701	0.909232	1.167877	0.134505
error10:leg2	0.63234	0.320489	0.846808	0.33594	-0.65377	0.428998
error2:order2	-0.94075	0.049922	2.573363	0.000106	0.227498	0.714973
error5:order2	0.434472	0.353148	0.429811	0.50646	-2.01169	0.000941
error7:order2	-1.05833	0.086976	5.354404	4.24E-10	-1.05444	0.189119
error10:order2	0.093012	0.886645	-1.28417	0.154672	0.102731	0.903507
leg2:order2	0.710822	0.049715	-0.49805	0.319888	0.047221	0.920018
error2:stride_num	-0.00148	0.285719	0.00467	0.014792	-0.00124	0.488907
error5:stride_num	-0.00545	0.009749	0.001212	0.677673	-0.00533	0.051833
error7:stride_num	-0.01349	3.61E-06	-0.00117	0.771195	-8.48E-05	0.982077
error10:stride_num	-0.00603	0.009516	-0.00433	0.177733	-0.00318	0.292625
leg2:stride_num	0.00296	0.045521	-0.008	9.32E-05	-0.00201	0.294816
order2:stride_num	-0.00436	0.003222	0.006133	0.002734	-0.00139	0.468983
error2:leg2:order2	-0.57118	0.358266	-1.16131	0.176761	-0.19748	0.806784
error5:leg2:order2	-3.00605	0.000923	0.221217	0.859909	2.89561	0.01396
error7:leg2:order2	2.041114	0.017474	1.670928	0.15927	-2.00784	0.071787
error10:leg2:order2	1.428431	0.113582	3.311195	0.008005	-0.64148	0.584217
error2:leg2:stride_num	-0.0041	0.02379	0.005643	0.024518	0.004975	0.034796
error5:leg2:stride_num	-0.00318	0.356859	0.003471	0.467456	0.012398	0.005751
error7:leg2:stride_num	0.008871	0.013392	0.003181	0.521092	-0.00672	0.149145
error10:leg2:stride_num	-0.00312	0.401151	0.008959	0.081584	0.014349	0.002994
error2:order2:stride_num	0.005653	0.003925	-0.01065	8.52E-05	-0.002	0.432823
error5:order2:stride_num	-0.00097	0.746046	-0.0039	0.34374	0.005548	0.152046
error7:order2:stride_num	0.001638	0.685966	-0.02602	3.56E-06	-0.00546	0.299936
error10:order2:stride_num	0.002688	0.413577	0.002688	0.55421	-0.01233	0.00391
leg2:order2:stride_num	-0.00242	0.248141	0.00375	0.194903	-0.00023	0.931828
error2:leg2:order2:stride_num	0.002757	0.28265	0.005247	0.139184	0.002681	0.421108
error5:leg2:order2:stride_num	0.025878	1.26E-07	0.020716	0.002181	-0.01377	0.030083
error7:leg2:order2:stride_num	-0.00479	0.352784	0.007927	0.265871	0.014361	0.031925
error10:leg2:order2:stride_num	0.013191	0.013194	0.006898	0.348376	-0.00283	0.681894

Notes: S009 peak hip flexion was significantly higher at 7% error and differed between the first and second exposures. Minimum knee flexion decreased at 2% error and peak plantarflexion increased by approximately 1.5 degrees at 5-7% error. Changes to joint kinematics were significant but relatively small in magnitude.

Table B.6: S010 linear mixed effects model fit to joint kinematics

	Hip Estimate	Hip P value	Knee Estimate	Knee P value	Ankle Estimate	Ankle P value
(Intercept)	-0.02244	0.922795	-0.53746	0.397303	-0.54062	0.209845
error2	0.640076	0.186303	-0.87209	0.511276	3.859629	1.90E-05
error5	1.937308	6.23E-06	-0.33599	0.774656	6.085323	2.90E-14
error7	1.495789	0.008919	0.787113	0.615526	4.509156	2.32E-05
error10	3.191379	1.15E-07	0.608083	0.711937	4.521039	5.38E-05
leg2	0.020464	0.95018	0.143716	0.872839	0.111908	0.85435
order2	2.122958	1.70E-10	-0.06165	0.945891	5.693491	4.72E-20
stride_num	0.000143	0.910969	0.003423	0.328769	0.003443	0.147961
error2:leg2	-0.4514	0.455795	-0.99441	0.548997	-1.71655	0.12765
error5:leg2	2.06559	0.013408	-0.3246	0.887234	-3.70462	0.017187
error7:leg2	1.7458	0.025698	-1.02552	0.63255	-0.73464	0.613904
error10:leg2	-2.67378	0.001259	-0.30266	0.893981	-0.41193	0.789341
error2:order2	-1.54618	0.018645	1.81955	0.312421	-4.95247	5.24E-05
error5:order2	-0.55779	0.359669	-0.88568	0.595745	-4.1005	0.000301
error7:order2	2.487257	0.002152	-0.85026	0.701821	-4.51242	0.002783
error10:order2	2.085953	0.01446	-31.5411	2.12E-40	-5.27418	0.000898
leg2:order2	0.292886	0.53214	-3.12605	0.015053	-0.05842	0.94662
error2:stride_num	-0.00302	0.118692	0.00178	0.737547	-0.00572	0.11283
error5:stride_num	-0.00305	0.255051	0.000609	0.933894	-0.0047	0.345078
error7:stride_num	0.002714	0.472037	0.002276	0.825918	-0.02437	0.000528
error10:stride_num	-0.00925	0.00208	-0.00292	0.723154	-0.01387	0.013147
leg2:stride_num	-0.00013	0.94253	-0.00092	0.85349	-0.00071	0.832263
order2:stride_num	-0.007	0.000191	0.002305	0.653529	-0.01151	0.000969
error2:leg2:order2	0.071205	0.932079	2.519947	0.271301	3.279066	0.03504
error5:leg2:order2	-5.62982	2.13E-06	6.820448	0.035935	2.836769	0.198669
error7:leg2:order2	-3.38478	0.002272	2.055672	0.498657	2.535883	0.218962
error10:leg2:order2	-1.46741	0.212258	32.70465	8.25E-24	0.650919	0.766236
error2:leg2:stride_num	0.003266	0.177527	-0.00142	0.830302	0.003791	0.400344
error5:leg2:stride_num	-0.00975	0.028252	0.000369	0.975864	0.006941	0.401478
error7:leg2:stride_num	-0.0123	0.007961	-0.00432	0.733724	0.008647	0.315859
error10:leg2:stride_num	0.010609	0.027751	-0.00177	0.89327	0.007998	0.372569
error2:order2:stride_num	0.006491	0.014472	-0.00506	0.48695	0.007744	0.116911
error5:order2:stride_num	-0.00603	0.117078	0.006776	0.520266	-0.01775	0.013165
error7:order2:stride_num	-0.01684	0.001692	-0.00268	0.85521	0.015058	0.131251
error10:order2:stride_num	-0.00388	0.363924	0.843677	0	0.019607	0.013775
leg2:order2:stride_num	-0.01724	9.42E-11	-0.00604	0.406358	-0.00124	0.800987
error2:leg2:order2:stride_num	0.016814	7.74E-07	0.006229	0.503461	-0.00493	0.435394
error5:leg2:order2:stride_num	0.045654	7.50E-13	-0.0153	0.378779	0.001772	0.880696
error7:leg2:order2:stride_num	0.040988	5.33E-10	0.0108	0.549494	-0.01186	0.333203
error10:leg2:order2:stride_num	0.021451	0.001757	-0.83893	0	-0.00016	0.989836

Notes: S010 significantly increased peak plantarflexion across 2-10% error compared to 0% error and the effects of error level interacted with exposure order. The participant also increased peak hip flexion at swing when walking with 5-7% error compared to 0% error.

Table B.7: S011 linear mixed effects model fit to joint kinematics

	Hip Estimate	Hip P value	Knee Estimate	Knee P value	Ankle Estimate	Ankle P value
(Intercept)	-0.50426	0.000927	-1.45914	2.00E-09	1.732141	6.19E-16
error2	-0.31895	0.262118	0.723678	0.110633	-1.55358	9.83E-05
error5	-0.41161	0.142924	1.548794	0.000552	-3.31694	5.21E-17
error7	1.342948	0.000271	2.590178	1.07E-05	-0.94501	0.067172
error10	1.222689	0.001657	1.86998	0.002553	1.318874	0.015402
leg2	0.778502	0.000304	1.572732	4.82E-06	0.071904	0.811602
order2	0.482271	0.025044	0.828951	0.015736	-2.95997	1.89E-22
stride_num	0.000588	0.503816	0.003395	0.015481	-0.0002	0.873584
error2:leg2	0.793296	0.031639	-0.26217	0.655967	1.449668	0.005073
error5:leg2	-1.56013	0.004008	0.779459	0.367045	1.471675	0.052597
error7:leg2	-1.57555	0.00178	-3.27072	4.80E-05	1.60155	0.023328
error10:leg2	-1.61595	0.002535	-1.52923	0.073064	-1.94009	0.009658
error2:order2	-0.51044	0.204445	-0.40696	0.525768	1.348858	0.016717
error5:order2	-0.05642	0.88649	-1.79756	0.004368	4.834189	3.98E-18
error7:order2	-1.94371	0.000194	-2.47429	0.002921	0.545062	0.455226
error10:order2	-1.27732	0.020098	-6.56415	8.58E-14	-1.42304	0.064482
leg2:order2	0.092092	0.762335	-0.33067	0.495939	8.353011	1.04E-80
error2:stride_num	0.00059	0.612115	-0.00673	0.000294	0.001922	0.238585
error5:stride_num	0.003254	0.074989	-0.0023	0.430949	0.004833	0.059093
error7:stride_num	-0.00427	0.080499	-0.01414	0.000288	-0.00197	0.564599
error10:stride_num	-0.00582	0.002918	-0.00451	0.14728	-0.00661	0.015712
leg2:stride_num	0.001731	0.165044	-0.00048	0.81029	0.001609	0.356845
order2:stride_num	-0.00235	0.058521	-0.0036	0.069595	-0.00247	0.15677
error2:leg2:order2	-0.43148	0.408381	0.274493	0.741538	-2.63977	0.00031
error5:leg2:order2	2.296252	0.002711	-0.67839	0.57827	-3.53699	0.000979
error7:leg2:order2	1.442921	0.043145	3.407613	0.002757	-0.96198	0.335734
error10:leg2:order2	1.232135	0.103395	3.646552	0.00252	1.341562	0.205563
error2:leg2:stride_num	-0.00296	0.053006	0.00205	0.399862	-0.00118	0.581682
error5:leg2:stride_num	0.003478	0.236668	-0.01095	0.019469	0.001215	0.767939
error7:leg2:stride_num	0.003069	0.306628	0.016576	0.000541	-0.0049	0.244313
error10:leg2:stride_num	0.004523	0.14809	-0.0028	0.574099	0.007009	0.109633
error2:order2:stride_num	0.003	0.06842	0.003978	0.1297	0.000831	0.718552
error5:order2:stride_num	-0.00315	0.216189	-0.0025	0.537135	-0.00939	0.008465
error7:order2:stride_num	0.0081	0.019114	0.003262	0.553784	0.009463	0.050634
error10:order2:stride_num	0.010003	0.000297	0.013567	0.002085	0.011508	0.002959
leg2:order2:stride_num	-0.00206	0.24255	0.002158	0.442732	0.001455	0.555569
error2:leg2:order2:stride_num	0.002018	0.34998	-0.00261	0.448639	0.002033	0.501518
error5:leg2:order2:stride_num	-0.007	0.090445	0.011363	0.084657	0.008927	0.123065
error7:leg2:order2:stride_num	-0.00383	0.368547	-0.01182	0.081556	-0.00323	0.587995
error10:leg2:order2:stride_num	-0.00925	0.036522	-0.00573	0.416197	-0.01627	0.008649

Notes: Participant S011 initially decreased peak plantarflexion at lower error rates (2-5% error), then increased peak hip flexion at swing at higher error rates (7-10%), potentially signalling a change in strategy across error levels. Minimum knee flexion also increased at 5-10% error.

Table B.8: S012 linear mixed effects model fit to joint kinematics

	Hip Estimate	Hip P value	Knee Estimate	Knee P value	Ankle Estimate	Ankle P value
(Intercept)	0.067896	0.687195	0.681882	0.000574	0.108996	0.653935
error2	0.305328	0.333774	-0.78492	0.034247	-0.97292	0.032732
error5	1.486446	1.47E-06	-0.60012	0.096983	-3.98762	4.65E-19
error7	-1.04823	0.009917	-1.49214	0.001761	-2.69428	4.40E-06
error10	-1.39356	0.001218	-2.09722	3.37E-05	-2.9779	1.68E-06
leg2	0.191967	0.420821	-0.45978	0.100376	-0.0326	0.924461
order2	-0.88087	0.000224	-0.35898	0.199516	-2.45586	1.12E-12
stride_num	-0.00045	0.642242	-0.00455	7.13E-05	-0.00073	0.605002
error2:leg2	0.265869	0.513735	0.085989	0.857138	1.486496	0.011374
error5:leg2	-1.10522	0.064187	0.990835	0.157246	3.093924	0.00033
error7:leg2	0.896859	0.107348	2.563041	8.92E-05	3.35624	2.99E-05
error10:leg2	-1.95307	0.000994	-0.00865	0.990079	-0.13839	0.87137
error2:order2	-1.46623	0.00104	-0.88969	0.08968	3.289796	3.45E-07
error5:order2	-0.83579	0.055651	-0.07449	0.88439	6.21778	1.09E-22
error7:order2	0.636746	0.269019	-0.87342	0.196296	5.818101	2.98E-12
error10:order2	0.162176	0.789936	0.471485	0.509214	5.203275	3.39E-09
leg2:order2	-3.90205	2.25E-30	0.885662	0.025252	5.839438	1.53E-32
error2:stride_num	0.000763	0.554379	0.001887	0.212547	-0.00036	0.847982
error5:stride_num	-0.00911	3.62E-06	0.002129	0.355508	0.015169	9.00E-08
error7:stride_num	-0.00502	0.063688	0.006223	0.050219	0.009084	0.020031
error10:stride_num	-0.00102	0.637415	0.005347	0.035336	0.007888	0.011544
leg2:stride_num	-0.00128	0.353023	0.003065	0.058026	0.000217	0.912891
order2:stride_num	-0.00348	0.011671	0.002319	0.151558	0.001605	0.41911
error2:leg2:order2	1.133181	0.049754	0.824491	0.223622	-7.28475	3.34E-18
error5:leg2:order2	1.050937	0.214188	-1.55978	0.116149	-9.52696	7.62E-15
error7:leg2:order2	1.229017	0.119558	-1.81571	0.050015	-7.28855	1.73E-10
error10:leg2:order2	4.203742	5.58E-07	-1.04606	0.28755	-4.88541	5.42E-05
error2:leg2:stride_num	-0.00168	0.31721	-0.00082	0.679635	0.000387	0.873445
error5:leg2:stride_num	0.000364	0.910037	-0.00226	0.548645	-0.00898	0.052962
error7:leg2:stride_num	-0.00968	0.003622	-0.01831	2.81E-06	-0.01895	7.88E-05
error10:leg2:stride_num	-0.0024	0.489214	-0.0052	0.200818	0.00358	0.473612
error2:order2:stride_num	0.004791	0.00867	0.000373	0.8618	-0.00332	0.207595
error5:order2:stride_num	0.007288	0.008711	-0.00212	0.516158	-0.02123	1.22E-07
error7:order2:stride_num	0.010988	0.004136	0.000383	0.932074	-0.01322	0.016703
error10:order2:stride_num	0.003202	0.295669	-0.00605	0.092113	-0.0055	0.212932
leg2:order2:stride_num	-0.001	0.607718	-0.00344	0.132066	-0.00308	0.272642
error2:leg2:order2:stride_num	0.000441	0.853334	0.001872	0.503734	0.01073	0.001829
error5:leg2:order2:stride_num	0.005718	0.208926	0.005947	0.26533	0.021264	0.001201
error7:leg2:order2:stride_num	0.003623	0.442066	0.016175	0.003461	0.013148	0.053063
error10:leg2:order2:stride_num	0.003748	0.444243	0.011825	0.039723	-0.01897	0.007275

Notes: Participant S012 significantly decreased peak plantarflexion at 2-10% error with decreases in minimum knee flexion at higher error levels (5-10%). The participant also increased hip flexion at 5% error, then decreased hip flexion at 7-10% error. Hip flexion and plantarflexion were also affected by order of error exposure.

Table B.9: S013 linear mixed effects model fit to joint kinematics

	Hip Estimate	Hip P value	Knee Estimate	Knee P value	Ankle Estimate	Ankle P value
(Intercept)	-0.02966	0.769063	-0.90887	7.62E-13	0.91819	5.34E-09
error2	0.299844	0.113129	-0.40748	0.085087	-0.36863	0.209876
error5	-0.52603	0.004398	0.112821	0.624945	0.209183	0.465691
error7	0.152261	0.533644	0.888663	0.003687	-0.58509	0.123683
error10	-0.0987	0.701911	1.140846	0.000408	1.001983	0.012419
leg2	1.113729	8.48E-15	-0.11807	0.50859	-1.35327	1.20E-09
order2	-0.52114	0.000265	-0.24405	0.171511	0.990604	8.16E-06
stride_num	0.003826	6.40E-11	-0.00256	0.000464	-1.53E-06	0.998651
error2:leg2	-1.4354	4.44E-09	-0.27162	0.373323	-0.28616	0.450306
error5:leg2	1.398728	9.83E-05	0.418158	0.351181	0.52531	0.345856
error7:leg2	-1.01764	0.002364	-1.52197	0.000277	0.267537	0.606638
error10:leg2	-0.15323	0.666073	0.602907	0.174512	-0.46005	0.404276
error2:order2	0.638506	0.017055	-0.31664	0.343882	1.009947	0.015144
error5:order2	0.345435	0.185673	-0.56352	0.084234	1.117945	0.005851
error7:order2	-0.30389	0.379636	-1.37495	0.001488	1.276163	0.017592
error10:order2	-0.7989	0.028518	-1.7223	0.000161	0.490799	0.386278
leg2:order2	0.206584	0.30633	-0.48866	0.053004	0.587339	0.061229
error2:stride_num	-0.00373	1.49E-06	0.001929	0.045963	0.003512	0.003458
error5:stride_num	0.001086	0.355709	-0.0001	0.944064	0.002415	0.1864
error7:stride_num	-0.00491	0.002491	-0.00083	0.683755	0.002297	0.362049
error10:stride_num	-0.00385	0.003002	-0.00143	0.376691	-0.00315	0.118321
leg2:stride_num	0.000294	0.721545	0.000936	0.364261	0.004287	0.000837
order2:stride_num	-0.00088	0.286368	0.001827	0.075959	0.004142	0.001215
error2:leg2:order2	0.545446	0.114901	0.419966	0.331572	0.854956	0.111669
error5:leg2:order2	0.458598	0.394564	-0.5531	0.411507	-2.03365	0.015126
error7:leg2:order2	1.224528	0.009666	1.144553	0.053016	0.433341	0.555361
error10:leg2:order2	-0.10624	0.832432	0.000307	0.999609	4.510646	8.03E-09
error2:leg2:stride_num	0.000483	0.632502	-0.00027	0.83198	-0.00522	0.000882
error5:leg2:stride_num	-0.00718	0.000197	-0.00132	0.584051	-0.00963	0.001308
error7:leg2:stride_num	0.004255	0.032759	0.002591	0.29838	-0.00398	0.198076
error10:leg2:stride_num	-0.00748	0.000317	-0.00515	0.047317	0.000708	0.826232
error2:order2:stride_num	-0.00188	0.084515	-0.00068	0.619697	-0.00716	2.47E-05
error5:order2:stride_num	-0.00391	0.018757	0.000835	0.687946	-0.00517	0.045268
error7:order2:stride_num	-0.00012	0.95999	0.003876	0.17649	-0.00342	0.33688
error10:order2:stride_num	0.003366	0.066407	0.003226	0.159266	-0.00173	0.542506
leg2:order2:stride_num	0.000925	0.427663	-0.00114	0.433908	-0.00633	0.000479
error2:leg2:order2:stride_num	0.000834	0.559084	0.001148	0.520129	0.007729	0.0005
error5:leg2:order2:stride_num	-0.00322	0.286062	0.003612	0.337829	0.015959	0.00066
error7:leg2:order2:stride_num	-0.00412	0.143211	-0.00203	0.563581	0.00699	0.110236
error10:leg2:order2:stride_num	0.00905	0.002056	0.004359	0.234804	-0.01245	0.006354

Notes: S013 exhibited small but significant changes in hip flexion (5% error), knee flexion (7-10% error), and peak plantarflexion (10% error) at select error levels. Hip flexion and plantarflexion metrics were also different across legs and exposure order. Interaction effects between error levels, leg, and stride number were also observed.

Table B.10: S014 linear mixed effects model fit to joint kinematics

	Hip Estimate	Hip P value	Knee Estimate	Knee P value	Ankle Estimate	Ankle P value
(Intercept)	-0.09301	0.395282	0.400104	2.77E-07	-0.0622	0.803481
error2	-1.2558	9.23E-10	-0.64305	9.85E-06	-0.25512	0.585103
error5	-1.06749	9.95E-08	-0.7967	2.18E-08	1.001657	0.028376
error7	0.207912	0.430318	0.059803	0.749412	-6.91447	6.33E-30
error10	-1.01817	0.000271	0.081458	0.681345	-8.07344	7.82E-36
leg2	-0.5377	0.000522	-0.122	0.26735	0.406595	0.250517
order2	0.7642	8.23E-07	-0.56884	2.39E-07	1.944762	4.06E-08
stride_num	0.00062	0.326717	-0.00267	3.13E-09	0.000415	0.774034
error2:leg2	1.568711	3.75E-09	0.36248	0.054526	-0.48025	0.42836
error5:leg2	1.30813	0.000742	0.3315	0.228309	-2.36935	0.007465
error7:leg2	0.904477	0.012363	0.236214	0.357417	7.669745	2.78E-20
error10:leg2	2.225957	7.84E-09	-0.06331	0.816725	8.755062	4.79E-23
error2:order2	0.998595	0.000562	0.45294	0.027516	4.175431	3.00E-10
error5:order2	0.700837	0.013227	0.826826	3.92E-05	-2.54417	8.37E-05
error7:order2	-1.52041	4.64E-05	0.195561	0.460172	7.507645	1.94E-18
error10:order2	0.457806	0.246516	0.341094	0.224095	8.157007	2.68E-19
leg2:order2	3.092324	5.32E-44	0.167353	0.281768	-1.86883	0.00019
error2:stride_num	7.82E-05	0.925574	0.00194	0.001108	0.001093	0.567458
error5:stride_num	-0.00188	0.140375	0.002675	0.00313	-0.00352	0.227025
error7:stride_num	-0.00327	0.06246	0.001168	0.349185	-0.00612	0.127308
error10:stride_num	0.0013	0.354851	0.001293	0.195073	0.000518	0.871858
leg2:stride_num	0.003599	6.07E-05	0.000807	0.204873	-0.00272	0.18443
order2:stride_num	-0.00385	1.73E-05	-0.00171	0.007034	-0.00099	0.62895
error2:leg2:order2	-1.46371	9.78E-05	-0.91251	0.000624	-2.82497	0.000994
error5:leg2:order2	-1.52526	0.005394	1.178575	0.00247	4.517306	0.000312
error7:leg2:order2	-1.03082	0.043747	-0.91125	0.012089	-7.10565	1.29E-09
error10:leg2:order2	-3.87311	1.32E-12	-0.15029	0.697243	-8.71879	2.77E-12
error2:leg2:stride_num	-0.00279	0.011204	-0.00099	0.206086	0.001978	0.430562
error5:leg2:stride_num	-0.00049	0.815283	-0.00162	0.275947	0.009519	0.046118
error7:leg2:stride_num	0.001927	0.372046	-0.00436	0.004492	0.006281	0.202889
error10:leg2:stride_num	-0.0026	0.247923	-0.00331	0.038052	0.002526	0.622911
error2:order2:stride_num	0.002542	0.031794	0.001301	0.12163	-0.02058	3.54E-14
error5:order2:stride_num	-0.00068	0.707506	-0.00103	0.419698	0.012091	0.003335
error7:order2:stride_num	0.01007	5.17E-05	0.00069	0.695971	0.01011	0.075013
error10:order2:stride_num	-0.00056	0.778752	0.000663	0.638417	-0.00124	0.784744
leg2:order2:stride_num	0.001896	0.13429	0.002499	0.005464	0.012429	1.78E-05
error2:leg2:order2:stride_num	-0.0009	0.561887	0.000152	0.890053	0.008578	0.015589
error5:leg2:order2:stride_num	0.001766	0.549741	-0.00159	0.448115	-0.0289	1.89E-05
error7:leg2:order2:stride_num	-0.0075	0.013997	0.003158	0.145213	-0.02086	0.0028
error10:leg2:order2:stride_num	0.002836	0.37239	0.001345	0.55155	-0.01075	0.138913

Notes: Participant S014 decreased peak hip flexion by approximately 1 degree across error rates of 2, 5, and 10% compared to 0% error. Peak plantarflexion increased at 5% error and decreased at higher levels of 7-10% error. Joint kinematics were also significantly different across exposure order and interaction effects between error levels, leg, and order were observed.

Table B.11: S015 linear mixed effects model fit to joint kinematics

	Hip Estimate	Hip P value	Knee Estimate	Knee P value	Ankle Estimate	Ankle P value
(Intercept)	-1.99575	4.08E-58	-0.00144	0.991798	3.39486	1.84E-52
error2	0.51022	0.022659	0.29529	0.251349	-0.01419	0.971845
error5	1.033988	2.28E-06	-0.27129	0.280149	0.343613	0.38128
error7	0.470859	0.102613	-0.17283	0.602382	-1.60582	0.001962
error10	1.842364	1.30E-09	-0.18814	0.589086	-3.04404	2.40E-08
leg2	-0.22296	0.195096	0.316336	0.110038	-0.26182	0.397182
order2	0.579923	0.000648	0.024614	0.899759	1.223969	6.23E-05
stride_num	0.00486	5.94E-11	-6.57E-05	0.938488	0.00097	0.465595
error2:leg2	-0.24336	0.402343	0.328578	0.325629	-0.6453	0.216634
error5:leg2	-1.0415	0.013808	0.391027	0.421395	-2.05408	0.006897
error7:leg2	0.200498	0.611288	0.175129	0.699544	2.257599	0.001464
error10:leg2	0.356032	0.394077	-0.28701	0.550317	1.283935	0.087297
error2:order2	-0.51977	0.09895	-0.46309	0.201216	-0.26499	0.639677
error5:order2	-1.3486	1.26E-05	0.254828	0.472523	-0.04863	0.93008
error7:order2	-1.86773	4.60E-06	-0.69165	0.139591	0.610383	0.403969
error10:order2	-6.50909	1.27E-50	-0.40974	0.404547	3.734148	1.21E-06
leg2:order2	-0.7262	0.002522	0.581168	0.035524	0.049667	0.908417
error2:stride_num	-0.00333	0.000449	-0.00078	0.474202	-0.00164	0.335248
error5:stride_num	-0.00325	0.021197	0.001011	0.532582	-0.00466	0.066028
error7:stride_num	0.002193	0.254546	-0.00136	0.538564	0.005081	0.141845
error10:stride_num	-0.00439	0.004612	0.000118	0.947354	0.00802	0.003958
leg2:stride_num	-1.02E-05	0.992215	0.000156	0.897028	-0.00237	0.208283
order2:stride_num	-0.00348	0.000564	0.000288	0.804097	-0.00259	0.153294
error2:leg2:order2	1.058644	0.009663	-1.07471	0.022371	-0.71829	0.32838
error5:leg2:order2	3.2848	3.87E-08	-0.49432	0.471023	-1.13938	0.287627
error7:leg2:order2	0.654409	0.239717	0.014973	0.98134	-3.44664	0.000576
error10:leg2:order2	3.044993	1.22E-07	0.815699	0.216946	-5.3056	2.90E-07
error2:leg2:stride_num	0.00126	0.314787	-0.0024	0.095621	0.002791	0.215238
error5:leg2:stride_num	0.005163	0.02462	-0.00276	0.295863	0.014948	0.000297
error7:leg2:stride_num	-0.00545	0.021539	-0.00055	0.838871	-0.00451	0.28992
error10:leg2:stride_num	-0.00039	0.875463	-0.00053	0.853167	-0.00393	0.375233
error2:order2:stride_num	0.002257	0.085659	0.000722	0.632366	0.002639	0.263434
error5:order2:stride_num	0.003146	0.113458	-0.00251	0.272548	0.003978	0.265406
error7:order2:stride_num	-0.01785	4.99E-11	0.004832	0.120806	0.000191	0.968615
error10:order2:stride_num	0.00742	0.000638	-0.00034	0.890227	-0.0079	0.04282
leg2:order2:stride_num	0.004896	0.000605	-0.0053	0.001249	0.001403	0.584049
error2:leg2:order2:stride_num	-0.00483	0.005208	0.006772	0.000662	0.000518	0.867486
error5:leg2:order2:stride_num	-0.01298	6.04E-05	0.005498	0.139287	-0.00272	0.639623
error7:leg2:order2:stride_num	0.011179	0.000798	-0.00051	0.893966	0.004014	0.502512
error10:leg2:order2:stride_num	-0.00664	0.044736	0.001223	0.747796	0.012846	0.030691

Notes: S015 increased peak swing hip flexion across 2-5% error in comparison to 0% error while decreasing peak plantarflexion at higher levels of error (7-10%). No significant changes in knee behavior were observed. There was a significant main effect of order for hip flexion and plantarflexion, as well as interaction effects between error level, order, and leg.

Table B.12: S017 linear mixed effects model fit to joint kinematics

	Hip Estimate	Hip P value	Knee Estimate	Knee P value	Ankle Estimate	Ankle P value
(Intercept)	0.506965	0.04024	-0.13158	0.683972	-3.57779	6.84E-15
error2	-1.80664	7.79E-06	0.10421	0.843483	4.051798	6.08E-08
error5	-1.49749	0.000151	1.193879	0.020866	3.062736	2.81E-05
error7	-1.67445	0.000993	1.565698	0.01857	4.153678	1.02E-05
error10	-1.45288	0.006625	1.079526	0.12295	6.216395	3.78E-10
leg2	-0.63116	0.071648	-1.81168	7.90E-05	2.191768	0.000726
order2	-0.88457	0.005539	-0.89511	0.031887	6.759966	2.00E-16
stride_num	0.004872	0.023016	-0.00743	0.008077	0.022748	1.04E-08
error2:leg2	2.34052	1.03E-05	4.623065	3.03E-11	-0.86374	0.378
error5:leg2	2.347062	0.001608	6.182937	2.39E-10	-1.42568	0.3
error7:leg2	1.702079	0.014675	4.369657	1.75E-06	-4.1229	0.0014
error10:leg2	1.760911	0.016992	0.867213	0.368769	-6.57102	1.52E-06
error2:order2	3.413697	6.94E-10	2.491916	0.000563	-6.05571	3.29E-09
error5:order2	1.45257	0.007136	0.387148	0.583441	-4.27107	1.93E-05
error7:order2	2.20208	0.001779	1.060908	0.249558	-7.14198	4.52E-08
error10:order2	0	0	0	0	0	0
leg2:order2	-1.23987	0.00605	0.59127	0.316798	-4.60081	3.89E-08
error2:stride_num	0.001262	0.594087	0.00319	0.303309	-0.02725	5.65E-10
error5:stride_num	-0.00295	0.318725	0.004709	0.223333	-0.02326	2.14E-05
error7:stride_num	-0.00076	0.837977	0.000305	0.94983	-0.03532	2.61E-07
error10:stride_num	-0.00285	0.368172	0.000247	0.952535	-0.03441	4.68E-09
leg2:stride_num	-0.00487	0.110839	0.00472	0.23745	-0.00793	0.16
order2:stride_num	-0.00209	0.3922	0.010127	0.001512	-0.02846	3.17E-10
error2:leg2:order2	-1.5703	0.029319	-0.96551	0.305666	5.787862	1.44E-05
error5:leg2:order2	-1.6076	0.1186	-0.90435	0.502152	8.242315	1.56E-05
error7:leg2:order2	0.257232	0.790446	-1.58638	0.210454	9.366771	1.80E-07
error10:leg2:order2	0	0	0	0	0	0
error2:leg2:stride_num	-0.00178	0.585997	-0.00026	0.951881	0.008399	0.165
error5:leg2:stride_num	-0.00299	0.51754	-0.01142	0.05914	0.013386	0.118
error7:leg2:stride_num	0.002076	0.660746	0.001806	0.770516	0.029202	0.000855
error10:leg2:stride_num	0.000909	0.852295	-0.00166	0.794579	0.036837	4.62E-05
error2:order2:stride_num	-0.00706	0.01247	-0.01167	0.001611	0.034157	7.36E-11
error5:order2:stride_num	0.004264	0.258307	-0.00974	0.048611	0.024305	0.000502
error7:order2:stride_num	0.001262	0.797293	-0.01018	0.113187	0.049261	6.41E-08
error10:order2:stride_num	0	0	0	0	0	0
leg2:order2:stride_num	0.005312	0.125671	-0.0075	0.098498	0.030004	3.03E-06
error2:leg2:order2:stride_num	0.003435	0.371154	0.005662	0.259937	-0.02878	5.22E-05
error5:leg2:order2:stride_num	0.003918	0.514474	0.007796	0.321544	-0.04151	0.000192
error7:leg2:order2:stride_num	-0.00593	0.339703	0.010051	0.216441	-0.05237	5.41E-06
error10:leg2:order2:stride_num	0	0	0	0	0	0

Notes: Peak plantarflexion significantly increased and peak hip flexion decreased across 2-10% error compared to 0% error. Leg and order factors were observed to have significant main and interaction effects on joint kinematics. No estimates were available for 10% error at the second exposure, as the trial data was unavailable due to file corruption during data collection.

Table B.13: S018 linear mixed effects model fit to joint kinematics

	Hip Estimate	Hip P value	Knee Estimate	Knee P value	Ankle Estimate	Ankle P value
(Intercept)	-1.05914	2.67E-12	-0.35882	0.009795	-0.87806	0.1793
error2	2.591046	5.68E-14	-0.15543	0.622708	-0.56117	0.705979
error5	-1.93485	2.71E-12	0.5332	0.035653	-1.16411	0.329872
error7	0.750148	0.040074	-0.59294	0.077882	0.625508	0.692771
error10	2.318936	1.92E-09	-1.3488	0.000144	-0.22237	0.89401
leg2	-0.0056	0.979089	0.054629	0.78102	0.750458	0.417376
order2	6.012629	8.73E-156	-1.97593	1.82E-23	-1.21098	0.19032
stride_num	0.007061	7.70E-16	0.002392	0.002887	0.005854	0.121311
error2:leg2	-1.85961	9.35E-06	0.037556	0.922418	-2.15546	0.235262
error5:leg2	-3.41827	1.78E-10	0.260826	0.595746	-2.29114	0.322342
error7:leg2	0.21028	0.673807	-0.58549	0.202974	-1.56664	0.469354
error10:leg2	-0.91413	0.084817	-0.87183	0.07416	2.163966	0.346483
error2:order2	-5.61515	9.26E-36	0.896419	0.028401	1.038265	0.589673
error5:order2	-2.79887	9.56E-13	0.282305	0.432326	2.289929	0.176201
error7:order2	-3.10938	1.95E-09	-0.01929	0.967639	3.350126	0.134642
error10:order2	-5.02532	4.95E-20	1.2807	0.010664	2.719368	0.249332
leg2:order2	-1.65783	4.37E-08	1.446755	2.08E-07	-0.57122	0.662604
error2:stride_num	-0.0073	5.32E-07	-0.00204	0.127375	0.000699	0.911627
error5:stride_num	0.005027	0.004235	-0.00585	0.000302	0.00834	0.273377
error7:stride_num	0.001983	0.413009	-0.00183	0.412701	0.000335	0.97455
error10:stride_num	0.003114	0.107897	-0.00377	0.034428	0.008985	0.284425
leg2:stride_num	6.10E-05	0.960599	-0.00036	0.753349	-0.005	0.350538
order2:stride_num	0.009797	2.61E-15	-0.00708	4.82E-10	-0.01417	0.008037
error2:leg2:order2	2.731031	9.66E-07	0.387213	0.449672	4.315658	0.073618
error5:leg2:order2	5.861704	1.09E-07	2.541825	0.012196	4.159442	0.383514
error7:leg2:order2	0.492235	0.486013	2.337095	0.000331	2.110159	0.490787
error10:leg2:order2	1.457079	0.052117	0.265888	0.700134	-1.20599	0.710644
error2:leg2:stride_num	0.005939	0.000873	-0.00089	0.58919	0.004003	0.604344
error5:leg2:stride_num	0.01683	5.58E-09	-4.35E-05	0.9869	-0.00123	0.921591
error7:leg2:stride_num	0.001995	0.502735	-0.00151	0.581948	0.012616	0.328102
error10:leg2:stride_num	0.002328	0.452724	0.00719	0.011789	-0.01128	0.401378
error2:order2:stride_num	0.001486	0.423051	0.002379	0.163646	0.004562	0.570405
error5:order2:stride_num	-0.01424	1.08E-08	0.007161	0.001753	0.001022	0.924401
error7:order2:stride_num	-0.01769	2.55E-07	0.007423	0.01862	0.004248	0.774785
error10:order2:stride_num	-0.01413	2.60E-07	0.005504	0.029074	0.006208	0.600973
leg2:order2:stride_num	-0.01201	8.17E-12	0.000784	0.62643	0.007388	0.330015
error2:leg2:order2:stride_num	0.00241	0.303384	0.001684	0.434656	-0.00854	0.399997
error5:leg2:order2:stride_num	-0.0089	0.123092	-0.00837	0.114961	-0.00831	0.739759
error7:leg2:order2:stride_num	0.016923	5.96E-05	-2.31E-05	0.995248	-0.00335	0.854489
error10:leg2:order2:stride_num	0.013019	0.003009	-0.00261	0.517088	0.0175	0.35718

Notes: S018 increased hip flexion at 2, 7, and 10% error and decreased hip flexion at 5% error with no significant changes in knee or ankle kinematics. There were also interaction effects observed between error level, leg, and order for hip kinematics.

Table B.14: S021 linear mixed effects model fit to joint kinematics

	Hip Estimate	Hip P value	Knee Estimate	Knee P value	Ankle Estimate	Ankle P value
(Intercept)	-0.12464	0.25491	3.827106	7.35E-82	2.379791	2.21E-49
error2	1.62453	6.44E-13	-1.4372	0.000323	-1.51186	3.60E-06
error5	1.938684	1.42E-18	-0.16039	0.679977	-1.82341	9.83E-09
error7	0.566616	0.054694	-5.56358	5.25E-26	-3.93395	5.23E-20
error10	0.45219	0.146581	-6.44588	7.50E-31	-3.49481	1.19E-14
leg2	1.174558	4.53E-14	-1.03327	0.000175	0.631592	0.00491
order2	-1.06669	1.31E-10	0.904812	0.002076	-0.73906	0.002052
stride_num	0.003586	4.22E-13	0.003485	6.87E-05	0.000316	0.657377
error2:leg2	-1.0121	0.000487	1.420463	0.005781	0.937876	0.025488
error5:leg2	-0.09895	0.837198	-0.22408	0.793116	-0.90061	0.196429
error7:leg2	-0.8789	0.029123	3.914353	4.59E-08	1.412035	0.01547
error10:leg2	-1.94164	6.05E-06	3.686307	1.30E-06	1.309992	0.034753
error2:order2	-2.29857	1.40E-12	2.009672	0.000464	1.882415	5.87E-05
error5:order2	0.332878	0.291254	-0.03646	0.948044	1.087199	0.017301
error7:order2	0.901118	0.031958	3.563539	1.80E-06	3.367631	3.27E-08
error10:order2	1.17615	0.008151	6.053161	2.09E-14	3.612948	2.10E-08
leg2:order2	-0.42209	0.071688	-0.41343	0.319996	1.287484	0.00015
error2:stride_num	-0.00748	7.52E-21	-0.00051	0.715352	0.003025	0.008509
error5:stride_num	-0.01521	5.22E-29	-0.01352	1.70E-08	0.005056	0.009627
error7:stride_num	-0.00074	0.701837	0.017143	5.38E-07	0.010578	0.000148
error10:stride_num	-0.00577	0.000131	0.00742	0.005514	0.004494	0.039321
leg2:stride_num	-0.00149	0.033488	8.25E-05	0.946984	-0.00164	0.106334
order2:stride_num	-0.00551	2.80E-10	-0.00399	0.009752	0.00402	0.001429
error2:leg2:order2	0.891998	0.032891	-2.06331	0.005425	-1.06153	0.07943
error5:leg2:order2	0.637141	0.328469	1.885587	0.103156	-0.48768	0.60536
error7:leg2:order2	-0.06522	0.909645	-3.60862	0.000407	-1.11595	0.179843
error10:leg2:order2	1.498666	0.01431	-4.05256	0.000191	-1.3582	0.125072
error2:leg2:stride_num	0.004346	1.54E-05	-0.00462	0.009469	-0.00035	0.810914
error5:leg2:stride_num	0.000401	0.882782	0.002945	0.541402	0.007139	0.069723
error7:leg2:stride_num	-0.00245	0.294437	-0.02405	7.05E-09	-0.00513	0.129277
error10:leg2:stride_num	0.006225	0.010838	-0.0141	0.001146	-0.00323	0.360608
error2:order2:stride_num	0.011841	2.04E-21	-0.0021	0.3384	-0.00451	0.011884
error5:order2:stride_num	0.00631	0.001423	0.004682	0.181938	-0.00168	0.557332
error7:order2:stride_num	-0.00104	0.706359	-0.01186	0.015849	-0.00799	0.046533
error10:order2:stride_num	0.001685	0.442087	-0.00884	0.02307	-0.00343	0.279464
leg2:order2:stride_num	0.001116	0.365821	4.58E-06	0.99833	-0.00174	0.32949
error2:leg2:order2:stride_num	-0.00497	0.001912	0.006721	0.017942	0.002772	0.23138
error5:leg2:order2:stride_num	-0.00341	0.344385	-0.00521	0.415693	0.001589	0.760803
error7:leg2:order2:stride_num	0.007814	0.021001	0.019619	0.001096	-0.00021	0.966064
error10:leg2:order2:stride_num	-0.00439	0.213505	0.014503	0.020686	0.001234	0.809259

Notes: Participant S021 significantly decreased ankle plantarflexion and increased peak swing hip flexion across 2-10% error compared to 0% error. The participant also decreased minimum knee flexion at 2, 7, and 10% error. There were significant main effects of leg and exposure order, as well as interaction effects between error, leg, and order for hip, knee, and ankle kinematics.

Table B.15: S022 linear mixed effects model fit to joint kinematics

	Hip Estimate	Hip P value	Knee Estimate	Knee P value	Ankle Estimate	Ankle P value
(Intercept)	-0.1587	0.112248	0.033578	0.827934	-0.3621	0.091765
error2	0.432814	0.040297	-0.27574	0.398043	2.050583	6.32E-06
error5	-0.31806	0.08155	-0.41892	0.137892	1.326075	0.000733
error7	0.842605	0.000502	0.105991	0.77694	1.734342	0.00086
error10	-0.64286	0.011764	-0.44308	0.261313	2.096297	0.000133
leg2	0.314889	0.026016	-0.08515	0.696959	-0.68416	0.024418
order2	-0.06073	0.667307	-0.62666	0.004152	2.043595	1.99E-11
stride_num	0.001058	0.06692	-0.00022	0.801994	0.002414	0.051746
error2:leg2	-0.39937	0.126726	0.396156	0.327213	2.259163	5.93E-05
error5:leg2	-0.50863	0.151799	0.867881	0.113784	4.796791	3.59E-10
error7:leg2	-2.73616	1.95E-16	-0.79909	0.118412	3.730541	1.65E-07
error10:leg2	-1.15782	0.001079	0.206761	0.705544	1.677181	0.027481
error2:order2	-0.99367	0.000432	0.531802	0.222753	-1.60228	0.008238
error5:order2	0.05719	0.824695	0.699387	0.079881	-0.85409	0.123791
error7:order2	-1.71071	6.04E-07	0.558181	0.291465	-2.13655	0.003686
error10:order2	-0.27533	0.443897	0.430436	0.438908	-3.46676	7.50E-06
leg2:order2	-0.41276	0.038999	-0.44486	0.150167	-2.522	4.77E-09
error2:stride_num	-0.0021	0.009437	-0.00032	0.79687	-0.00316	0.068519
error5:stride_num	-0.00223	0.054804	0.001263	0.482774	-0.0018	0.472811
error7:stride_num	-0.00716	8.41E-06	-0.00189	0.446392	-0.00661	0.055134
error10:stride_num	-0.00149	0.244628	-0.00045	0.821087	-0.00549	0.046327
leg2:stride_num	-0.0021	0.010235	0.000569	0.653105	0.004584	0.009187
order2:stride_num	-0.00336	3.93E-05	0.001101	0.383305	-0.0002	0.909284
error2:leg2:order2	-0.24936	0.484575	-0.4566	0.407867	2.25752	0.003254
error5:leg2:order2	-1.36531	0.006541	-1.42281	0.066769	-3.56676	0.00095
error7:leg2:order2	1.874044	6.33E-05	-0.1163	0.872302	0.992151	0.323825
error10:leg2:order2	0.907283	0.068414	1.035093	0.178753	3.164376	0.003115
error2:leg2:stride_num	0.001013	0.3282	-0.00025	0.874575	-0.00476	0.032743
error5:leg2:stride_num	-0.00038	0.843154	-0.00319	0.279883	-0.00429	0.295618
error7:leg2:stride_num	0.009247	2.83E-06	0.003124	0.305495	-0.00316	0.455552
error10:leg2:stride_num	0.001719	0.412903	-0.00198	0.541716	0.0091	0.043753
error2:order2:stride_num	0.005124	4.23E-06	-0.00095	0.579992	0.00092	0.700289
error5:order2:stride_num	0.001737	0.291237	-0.00293	0.250161	-0.00014	0.968954
error7:order2:stride_num	0.012895	1.44E-08	-0.00291	0.40703	0.011182	0.021882
error10:order2:stride_num	0.006006	0.000895	-0.00086	0.757198	0.016917	1.36E-05
leg2:order2:stride_num	0.001083	0.349065	-0.00415	0.020398	0.001228	0.621013
error2:leg2:order2:stride_num	0.000419	0.771095	0.002472	0.267249	-0.00925	0.00283
error5:leg2:order2:stride_num	0.00859	0.001458	0.007471	0.073245	0.015456	0.007681
error7:leg2:order2:stride_num	-0.0108	0.000109	0.005355	0.214177	-0.00176	0.768836
error10:leg2:order2:stride_num	-0.0046	0.116335	-0.00122	0.788411	-0.01639	0.009317

Notes: S022 significantly increased peak plantarflexion across 2-10% error compared to 0% error, which varied across legs and exposure order. Peak hip flexion at swing was significantly different at 7-10% error and had significant interaction effects between error, leg, and order.

Table B.16: S023 linear mixed effects model fit to joint kinematics

	Hip Estimate	Hip P value	Knee Estimate	Knee P value	Ankle Estimate	Ankle P value
(Intercept)	-2.54987	4.35E-43	-0.29033	0.105996	2.983852	1.02E-40
error2	-0.37403	0.274207	-0.56914	0.090745	0.384584	0.351307
error5	1.538199	4.17E-06	0.315935	0.335681	0.222751	0.579949
error7	0.469555	0.285865	-0.07837	0.856276	0.397534	0.453818
error10	3.8099	4.23E-16	1.17891	0.010164	-2.12075	0.000165
leg2	-0.92928	0.000324	-0.07101	0.779785	-1.12743	0.000299
order2	5.23E-06	0.999984	-0.45112	0.075741	0.019556	0.949936
stride_num	-0.00098	0.350892	-0.00218	0.035508	0.000182	0.886133
error2:leg2	-0.01814	0.967369	-5.3458	8.14E-34	-0.39884	0.455791
error5:leg2	-1.25361	0.053248	0.078483	0.902049	-1.72458	0.027512
error7:leg2	0.039818	0.94735	-2.4253	4.42E-05	0.790297	0.277295
error10:leg2	2.389422	0.0002	-3.39721	7.88E-08	2.904725	0.000178
error2:order2	0.219837	0.649142	0.233534	0.623148	-0.23261	0.689841
error5:order2	-1.7929	0.000147	-0.3403	0.463391	-0.67236	0.23753
error7:order2	-0.56946	0.364669	-0.46712	0.449609	-0.43818	0.563086
error10:order2	-4.16132	2.88E-10	-2.33922	0.000305	3.165824	6.78E-05
leg2:order2	-2.05824	1.88E-08	1.088913	0.002447	-1.39863	0.00151
error2:stride_num	0.003684	0.008382	0.002609	0.05763	-0.00223	0.184716
error5:stride_num	-0.00396	0.062405	-0.00094	0.651445	0.00033	0.897675
error7:stride_num	0.005598	0.056315	-0.00068	0.814394	-0.00168	0.635591
error10:stride_num	-0.01036	1.03E-05	-0.00452	0.050235	0.008924	0.001612
leg2:stride_num	0.00402	0.00709	-0.00163	0.265881	-0.00561	0.001828
order2:stride_num	0.001623	0.276696	-0.00015	0.918355	-0.00315	0.079791
error2:leg2:order2	0.491791	0.43252	6.197421	1.87E-23	-3.458	4.92E-06
error5:leg2:order2	2.733833	0.002846	-1.45823	0.105433	-4.45523	5.60E-05
error7:leg2:order2	0.101643	0.902095	3.130889	0.000119	-0.80052	0.421897
error10:leg2:order2	-0.95318	0.293217	3.744554	2.75E-05	-3.75545	0.000603
error2:leg2:stride_num	-0.0084	4.56E-06	0.003094	0.085617	0.001162	0.59853
error5:leg2:stride_num	0.004291	0.218086	0.002432	0.477871	0.005843	0.164439
error7:leg2:stride_num	-0.01141	0.001543	0.000838	0.813044	0.00203	0.640265
error10:leg2:stride_num	-0.0121	0.001272	0.02033	3.84E-08	0.00313	0.489089
error2:order2:stride_num	-0.00466	0.018378	-0.00066	0.732205	0.002474	0.299221
error5:order2:stride_num	0.002285	0.447263	-0.00033	0.910101	0.000945	0.794394
error7:order2:stride_num	-0.0088	0.021398	0.004805	0.201477	0.002546	0.580973
error10:order2:stride_num	0.00744	0.024872	0.00782	0.016512	-0.01022	0.010642
leg2:order2:stride_num	0.000327	0.876675	0.003538	0.088296	0.007008	0.00593
error2:leg2:order2:stride_num	0.002144	0.407325	-0.0092	0.000305	0.005127	0.100527
error5:leg2:order2:stride_num	-0.00743	0.131772	0.000239	0.960707	0.01615	0.00661
error7:leg2:order2:stride_num	0.004835	0.311703	-0.01521	0.001223	-0.00054	0.924961
error10:leg2:order2:stride_num	-0.00373	0.482005	-0.03075	4.15E-09	-0.0019	0.766089

Notes: Peak hip flexion increased at select error rates (5 and 10% error) and significant interaction effects were observed between error, leg, and exposure order. Minimal changes were observed in knee and ankle behavior other than increased knee flexion and decreased plantarflexion at 10% error.

Table B.17: S025 linear mixed effects model fit to joint kinematics

	Hip Estimate	Hip P value	Knee Estimate	Knee P value	Ankle Estimate	Ankle P value
(Intercept)	-2.16406	9.13E-22	0.431648	0.00358	2.94917	3.24E-13
error2	1.19589	0.000473	-0.60816	0.007149	0.156485	0.799156
error5	2.467518	2.30E-13	-0.57136	0.009949	1.368222	0.023327
error7	1.730492	4.16E-05	-0.16552	0.55269	-0.23274	0.759046
error10	2.285636	2.72E-07	0.191475	0.513761	-0.98055	0.219277
leg2	-1.19064	0.000182	-0.98309	3.00E-06	2.837622	7.34E-07
order2	-0.21343	0.440981	0.566266	0.002003	0.396281	0.426604
stride_num	-0.00148	0.543033	0.002103	0.190235	0.014397	0.000997
error2:leg2	0.142061	0.753362	-0.24523	0.412015	0.247215	0.761244
error5:leg2	1.837995	0.002916	0.29141	0.475041	-1.0479	0.345342
error7:leg2	1.74589	0.002674	0.367092	0.33924	-0.59471	0.569462
error10:leg2	1.11768	0.068424	0.236906	0.558988	1.447294	0.189725
error2:order2	-1.12114	0.014382	0.708937	0.01923	0.692325	0.400752
error5:order2	-1.15786	0.009839	0.321457	0.278141	0.544239	0.499917
error7:order2	-0.42154	0.464412	-0.11804	0.756656	2.110381	0.041883
error10:order2	-1.32561	0.029327	-0.43853	0.275422	2.955009	0.006961
leg2:order2	0.015426	0.968651	-0.72961	0.004962	0.413726	0.558081
error2:stride_num	0.002438	0.341388	-0.00113	0.506537	-0.01322	0.004156
error5:stride_num	-0.00048	0.870133	0.000618	0.750076	-0.02723	2.67E-07
error7:stride_num	0.004317	0.21008	-0.00336	0.1397	-0.00724	0.24286
error10:stride_num	-0.00132	0.665589	-0.00529	0.009065	-0.00788	0.152859
leg2:stride_num	0.009698	0.005185	-0.007	0.002283	-0.01187	0.057173
order2:stride_num	0.001378	0.596827	-0.00043	0.803219	-0.01341	0.004251
error2:leg2:order2	-0.07065	0.906341	0.542859	0.171572	-3.8765	0.000339
error5:leg2:order2	-2.0984	0.013038	0.586754	0.293496	-2.11382	0.164442
error7:leg2:order2	-2.47106	0.001823	-0.63359	0.226294	0.150801	0.915728
error10:leg2:order2	-2.52228	0.002669	-0.23616	0.670349	-1.30353	0.388045
error2:leg2:stride_num	-0.01009	0.005006	0.00619	0.009215	0.008129	0.208792
error5:leg2:stride_num	-0.01861	3.13E-05	0.001903	0.519016	0.018781	0.019412
error7:leg2:stride_num	-0.01484	0.001078	0.002059	0.492476	0.008489	0.298428
error10:leg2:stride_num	-0.00933	0.04401	0.01174	0.000129	-0.03569	1.91E-05
error2:order2:stride_num	-0.00098	0.731106	-0.00325	0.084911	0.013385	0.009081
error5:order2:stride_num	-0.00258	0.4603	-0.00212	0.359193	0.022217	0.000417
error7:order2:stride_num	-0.00885	0.040855	-0.00073	0.797157	0.007853	0.31303
error10:order2:stride_num	-0.00017	0.963499	0.001111	0.65049	0.006921	0.299913
leg2:order2:stride_num	-0.00958	0.009945	0.006717	0.006261	0.002915	0.662729
error2:leg2:order2:stride_num	0.008797	0.025898	-0.00494	0.058396	0.002101	0.767423
error5:leg2:order2:stride_num	0.018521	0.00067	-0.00766	0.033204	-0.00157	0.872502
error7:leg2:order2:stride_num	0.018093	0.001148	-0.00046	0.899518	-0.01156	0.247862
error10:leg2:order2:stride_num	0.017834	0.001822	-0.01243	0.001012	0.032128	0.001802

Notes: Participant S025 significantly increased hip flexion at error levels of 2-10% error in comparison to 0% error, with small decreases in minimum knee flexion at 2-5% error. The leg factor had a significant main effect on hip, knee, and ankle kinematics and had interaction effects with error and order for hip flexion metrics.

Table B.18: S026 linear mixed effects model fit to joint kinematics

	Hip Estimate	Hip P value	Knee Estimate	Knee P value	Ankle Estimate	Ankle P value
(Intercept)	-0.9712	0.008128	0.729921	0.000811	-0.89711	0.023388
error2	1.546301	0.024464	-1.95479	1.72E-06	-0.17564	0.812638
error5	0.014326	0.982946	0.315295	0.42817	-0.0774	0.914722
error7	1.289449	0.144588	0.005308	0.991929	1.709061	0.073026
error10	7.719182	1.85E-16	-2.1676	9.27E-05	11.04665	1.47E-27
leg2	0.578487	0.265146	-0.31435	0.3078	0.605101	0.279841
order2	1.957555	0.000163	-1.20654	9.11E-05	0.40429	0.469874
stride_num	0.006475	0.002265	-0.00487	0.000112	0.005981	0.008917
error2:leg2	-0.64262	0.470655	2.267694	1.86E-05	-0.56366	0.557413
error5:leg2	0.17422	0.893599	-0.64303	0.405751	0.060548	0.965624
error7:leg2	17.56413	5.20E-46	3.713737	2.72E-07	11.00379	6.35E-17
error10:leg2	-34.7608	6.78E-145	-0.10444	0.891272	-30.3483	7.09E-99
error2:order2	-2.33937	0.016102	2.131309	0.000224	1.432165	0.17181
error5:order2	0.241062	0.799229	-1.12172	0.046294	1.093098	0.284968
error7:order2	-0.98561	0.430335	0.086312	0.9074	0.541594	0.687834
error10:order2	-3.03282	0.021806	0.772734	0.324808	-2.63876	0.064227
leg2:order2	-0.44036	0.548442	0.968553	0.026272	0.70779	0.371195
error2:stride_num	-0.007	0.012698	0.004924	0.003136	-0.00279	0.356696
error5:stride_num	-0.00354	0.40717	0.001662	0.512307	0.003838	0.404724
error7:stride_num	-0.00901	0.125969	-0.00097	0.781001	-0.00885	0.163592
error10:stride_num	-0.09205	1.76E-80	0.027098	6.41E-22	-0.11366	3.47E-103
leg2:stride_num	-0.00385	0.200364	0.002086	0.242225	-0.00403	0.213985
order2:stride_num	-0.00701	0.019355	0.000363	0.83819	-0.00685	0.03402
error2:leg2:order2	1.127599	0.370674	-2.88707	0.000115	0.722232	0.594975
error5:leg2:order2	0.235273	0.898212	-2.69377	0.013679	14.03632	1.81E-12
error7:leg2:order2	-17.5859	2.64E-24	-4.01919	8.06E-05	-13.9823	5.22E-14
error10:leg2:order2	-6.05053	0.000904	-5.16779	1.85E-06	-3.49893	0.074997
error2:leg2:stride_num	0.006544	0.075502	-0.00444	0.042148	0.001458	0.713512
error5:leg2:stride_num	0.001938	0.78196	0.000308	0.941002	-0.00985	0.192082
error7:leg2:stride_num	-0.15491	2.03E-94	-0.02916	1.62E-11	-0.10546	3.35E-40
error10:leg2:stride_num	0.247962	1.31E-204	-0.00912	0.041531	0.221472	4.22E-147
error2:order2:stride_num	0.008628	0.02973	-0.00186	0.429799	0.001063	0.80387
error5:order2:stride_num	0.001005	0.86783	0.004995	0.163702	-0.00667	0.30559
error7:order2:stride_num	0.007823	0.347632	0.005457	0.269854	0.006101	0.497049
error10:order2:stride_num	-0.02454	0.000232	0.015396	0.0001	-0.02835	8.05E-05
leg2:order2:stride_num	0.003449	0.416414	-0.00058	0.817431	0.011555	0.011629
error2:leg2:order2:stride_num	-0.00607	0.243013	0.005894	0.056395	-0.02112	0.00017
error5:leg2:order2:stride_num	-0.00167	0.865804	0.024937	2.27E-05	-0.09206	1.01E-17
error7:leg2:order2:stride_num	0.154529	1.19E-49	0.029047	1.90E-06	0.104266	7.64E-21
error10:leg2:order2:stride_num	-0.13044	1.07E-33	-0.03037	1.66E-06	-0.08611	8.75E-14

Notes: S026 increased peak hip flexion and plantarflexion while decreasing minimum knee flexion at 10% error. There was a significant slope (estimated using stride_num factor), which may indicate that the participant modified joint kinematics within trials. There were observed interaction effects between error, leg, and order for hip, knee, and ankle kinematics.

Table B.19: S027 linear mixed effects model fit to joint kinematics

	Hip Estimate	Hip P value	Knee Estimate	Knee P value	Ankle Estimate	Ankle P value
(Intercept)	-0.15514	0.601475	-0.41153	0.056148	1.875266	7.13E-10
error2	-1.65169	0.002954	-0.35244	0.381483	0.350364	0.536715
error5	-0.73338	0.176717	0.72736	0.064706	2.643191	1.94E-06
error7	-0.38749	0.590107	0.011792	0.981965	1.591363	0.03036
error10	1.463747	0.052765	0.502472	0.359136	1.107317	0.151335
leg2	-0.26753	0.524582	1.217742	6.64E-05	5.117093	4.54E-32
order2	0.174555	0.677756	-0.38718	0.203809	1.501594	0.000471
stride_num	-0.00365	0.033705	0.000455	0.714798	0.005799	0.000948
error2:leg2	2.046808	0.004527	-0.2402	0.645745	-5.40908	2.49E-13
error5:leg2	-1.02342	0.332042	-0.29357	0.7012	-8.44704	6.08E-15
error7:leg2	-0.06489	0.947513	-4.12098	8.95E-09	-8.62105	1.68E-17
error10:leg2	-0.72969	0.48388	-0.65039	0.389557	-6.64307	4.92E-10
error2:order2	1.360073	0.083682	0.278267	0.625482	-0.68399	0.39428
error5:order2	-0.78833	0.304477	-0.99458	0.074075	-3.43396	1.22E-05
error7:order2	0.296846	0.769879	-0.7267	0.323432	-3.3803	0.001118
error10:order2	-3.60283	0.000754	-0.41321	0.593857	-2.47292	0.023496
leg2:order2	0.221671	0.709284	-0.50294	0.243508	-0.2992	0.622213
error2:stride_num	0.004195	0.064954	0.000379	0.81819	-0.00409	0.077899
error5:stride_num	-0.00043	0.900171	-0.00323	0.197865	-0.01083	0.002189
error7:stride_num	-0.00365	0.44427	0.002026	0.55813	-0.00821	0.092124
error10:stride_num	-0.00371	0.330905	-0.00088	0.751486	-0.00662	0.089179
leg2:stride_num	0.004769	0.050106	-0.00315	0.0743	-0.00561	0.024074
order2:stride_num	-0.00127	0.601949	0.000595	0.735314	-0.00759	0.002229
error2:leg2:order2	-1.96347	0.054213	0.378601	0.608649	6.176974	3.31E-09
error5:leg2:order2	2.45374	0.100119	1.138017	0.292943	9.939591	7.96E-11
error7:leg2:order2	0.591312	0.671048	5.133342	3.90E-07	9.089344	1.87E-10
error10:leg2:order2	1.969425	0.18157	0.569797	0.59401	7.356885	1.07E-06
error2:leg2:stride_num	-0.0097	0.001155	-0.0017	0.431198	-0.00501	0.100044
error5:leg2:stride_num	0.002895	0.609646	0.001019	0.804365	0.008584	0.138361
error7:leg2:stride_num	0.001464	0.803471	-0.00351	0.410427	0.013077	0.02962
error10:leg2:stride_num	-0.00199	0.744611	-0.00121	0.784617	0.005063	0.416791
error2:order2:stride_num	-0.00315	0.327334	-0.00164	0.482088	0.004891	0.136218
error5:order2:stride_num	0.008634	0.07765	0.001776	0.616656	0.012688	0.01114
error7:order2:stride_num	0.001834	0.785716	0.00078	0.87334	0.014165	0.039847
error10:order2:stride_num	0.014807	0.006072	-0.00203	0.603467	0.009018	0.101641
leg2:order2:stride_num	-0.00163	0.635299	-0.00228	0.360319	0.007667	0.029216
error2:leg2:order2:stride_num	0.009943	0.018412	0.0073	0.017012	0.002819	0.5127
error5:leg2:order2:stride_num	-0.0089	0.2673	0.0033	0.570408	-0.01824	0.025978
error7:leg2:order2:stride_num	-0.00081	0.92245	0.004379	0.468116	-0.0126	0.138205
error10:leg2:order2:stride_num	-0.00324	0.707097	0.00823	0.188733	-0.00653	0.459179

Notes: S027 significantly changed peak plantarflexion across all error rates, exposure order, and between legs with a significant slope across strides within a trial. There were minimal changes in hip and knee behavior in response to error levels, leg, and order.

Table B.20: S028 linear mixed effects model fit to joint kinematics

	Hip Estimate	Hip P value	Knee Estimate	Knee P value	Ankle Estimate	Ankle P value
(Intercept)	-0.81835	0.00149	0.24355	0.220603	-0.45704	0.300295
error2	0.360117	0.458961	0.234548	0.532286	-1.06182	0.202731
error5	0.838478	0.077124	1.777865	1.27E-06	0.293343	0.718196
error7	-9.03231	2.58E-45	1.173119	0.015857	1.081055	0.316353
error10	1.701059	0.010414	0.173492	0.735013	1.968302	0.083657
leg2	-0.11953	0.742853	-0.17359	0.537306	0.45134	0.469854
order2	-5.74466	1.67E-53	1.242422	1.15E-05	3.255359	2.27E-07
stride_num	0.005331	0.000248	-0.00159	0.157592	0.002977	0.232075
error2:leg2	-0.04679	0.940802	0.399861	0.41123	0.373096	0.729723
error5:leg2	-5.33771	7.30E-09	-2.88525	5.05E-05	-0.34298	0.827899
error7:leg2	3.285787	0.000141	-0.95097	0.153295	-3.52601	0.017076
error10:leg2	-0.91968	0.314273	-1.67759	0.017511	8.364356	9.93E-08
error2:order2	0.181346	0.792338	-0.19515	0.713752	2.577546	0.029084
error5:order2	9.518997	4.35E-44	-1.75038	0.000769	-2.15698	0.061639
error7:order2	17.77621	5.80E-84	-0.92351	0.17856	-4.54749	0.002854
error10:order2	6.133645	7.63E-11	-0.2887	0.690699	-4.75196	0.003187
leg2:order2	0.480509	0.353883	-1.85207	3.85E-06	-0.39909	0.653256
error2:stride_num	-0.00559	0.004223	0.00206	0.1722	0.004685	0.161825
error5:stride_num	-0.00323	0.283354	-0.00192	0.407437	-0.00317	0.53883
error7:stride_num	0.049118	1.79E-31	-0.00292	0.363708	0.00341	0.632802
error10:stride_num	-0.00185	0.577741	0.001649	0.520214	0.000693	0.903095
leg2:stride_num	0.000799	0.698318	0.001129	0.477929	-0.00294	0.405166
order2:stride_num	-0.01137	5.83E-08	0.001481	0.359383	-0.00959	0.007518
error2:leg2:order2	-2.48266	0.005452	7.511819	3.65E-27	-30.4868	2.39E-83
error5:leg2:order2	1.080183	0.40805	3.543081	0.000447	4.277831	0.055993
error7:leg2:order2	-4.3203	0.000397	6.597252	2.88E-12	-15.0634	6.80E-13
error10:leg2:order2	-6.32147	1.07E-06	0.471532	0.63696	1.881039	0.396271
error2:leg2:stride_num	-0.00075	0.767636	-0.00694	0.000439	0.012924	0.003183
error5:leg2:stride_num	-0.06974	6.07E-44	-0.00117	0.75922	-0.00311	0.713195
error7:leg2:stride_num	-0.02279	8.43E-06	0.00463	0.240645	0.019852	0.023442
error10:leg2:stride_num	0.006715	0.207241	-0.00264	0.521006	0.023066	0.01152
error2:order2:stride_num	0.006737	0.015809	-0.00444	0.039593	-0.002	0.675867
error5:order2:stride_num	-0.01634	0.000133	-0.00386	0.242283	0.020223	0.005768
error7:order2:stride_num	-0.04816	4.69E-16	0.005081	0.264958	0.000358	0.971754
error10:order2:stride_num	0.009637	0.040905	-0.00315	0.387453	0.022863	0.00467
leg2:order2:stride_num	0.005516	0.062986	0.000169	0.94123	0.015037	0.00312
error2:leg2:order2:stride_num	0.0028	0.443779	-0.008	0.004642	0.031812	4.04E-07
error5:leg2:order2:stride_num	0.087956	2.65E-35	0.006117	0.258486	-0.02932	0.014721
error7:leg2:order2:stride_num	0.025023	0.000567	-0.02753	9.30E-07	0.069763	2.17E-08
error10:leg2:order2:stride_num	-0.0005	0.946709	-0.00891	0.126344	-0.06378	8.66E-07

Notes: S028 decreased peak hip flexion at 7% error then increased hip flexion at 10% error and a significant slope in hip flexion metrics was observed within trials. Minimum knee flexion also increased when walking with 5-7% error controllers. Interaction effects were observed for hip, knee, and ankle kinematics between error levels, leg, and order.

BIBLIOGRAPHY

[1] Yadrianna Acosta-Sojo and Leia Stirling. Muscle activation differs between individuals during initial powered ankle exoskeleton adaptation. *Proceedings of the Human Factors and Ergonomics Society Annual Meeting*, 65:415–418, 9 2021.

[2] Yadrianna Acosta-Sojo and Leia Stirling. Individuals differ in muscle activation patterns during early adaptation to a powered ankle exoskeleton. *Applied Ergonomics*, 98:103593, 2022.

[3] Olatz Arbelaitz, Ibai Gurrutxaga, Javier Muguerza, JesúS M. PéRez, and IñIgo Perona. An extensive comparative study of cluster validity indices. *Pattern Recogn.*, 46(1):243–256, jan 2013.

[4] Pablo Arias and Javier Cudeiro. Effect of rhythmic auditory stimulation on gait in parkinsonian patients with and without freezing of gait. *PLOS ONE*, 5(3):1–8, 03 2010.

[5] Mina Arvin, Masood Mazaheri, Marco J M Hoozemans, Mirjam Pijnappels, Bart J Burger, Sabine M P Verschueren, and Jaap H van Dieën. Effects of narrow base gait on mediolateral balance control in young and older adults. *Journal of Biomechanics*, 49:1264–1267, 2016.

[6] Alan T. Asbeck, Stefano M.M. De Rossi, Kenneth G. Holt, and Conor J. Walsh. A biologically inspired soft exosuit for walking assistance. *The International Journal of Robotics Research*, 34(6):744–762, 2015.

[7] Sai K. Banala, Seok Hun Kim, Sunil K. Agrawal, and John P. Scholz. Robot assisted gait training with active leg exoskeleton (alex). *IEEE Transactions on Neural Systems and Rehabilitation Engineering*, 17(1):2–8, 2009.

[8] Ozgur Baser, Hasbi Kizilhan, and Ergin Kilic. Employing variable impedance (stiffness/damping) hybrid actuators on lower limb exoskeleton robots for stable and safe walking trajectory tracking. *Journal of Mechanical Science and Technology*, 34(6):2597–2607, Jun 2020.

[9] Vanessa K. Bowden, Natalie Griffiths, Luke Strickland, and Shayne Loft. Detecting a single automation failure: The impact of expected (but not experienced) automation reliability. *Human Factors*, 65(4):533–545, 2023. PMID: 34375538.

[10] Valentina Bruno, Ilaria Carpinella, Marco Rabuffetti, Lorenzo De Giuli, Corrado Sinigaglia, Francesca Garbarini, and Maurizio Ferrarin. How tool-use shapes body metric representation: Evidence from motor training with and without robotic assistance. *Frontiers in Human Neuroscience*, 13, 2019.

[11] Mary A Bucklin, Mary Wu, Geoffrey Brown, and Keith E Gordon. American society of biomechanics journal of biomechanics award 2018: Adaptive motor planning of center-of-mass trajectory during goal-directed walking in novel environments. *Journal of Biomechanics*, 2019.

[12] Iahn Cajigas, Mary T. Goldsmith, Alexander Duschau-Wicke, Robert Riener, Maurice A. Smith, Emery N. Brown, and Paolo Bonato. Assessment of lower extremity motor adaptation via an extension of the force field adaptation paradigm. volume 2010, pages 4522–4525. NIH Public Access, 2010.

[13] Jonathan Camargo, Aditya Ramanathan, Will Flanagan, and Aaron Young. A comprehensive, open-source dataset of lower limb biomechanics in multiple conditions of stairs, ramps, and level-ground ambulation and transitions. *Journal of Biomechanics*, 119:110320, 2021.

[14] Lucilla Cardinali, Francesca Frassinetti, Claudio Brozzoli, Christian Urquizar, Alice C. Roy, and Alessandro Farnè. Tool-use induces morphological updating of the body schema. *Current Biology*, 19(12):R478–R479, 2009.

[15] Alain Chavaillaz, David Wastell, and Jürgen Sauer. System reliability, performance and trust in adaptable automation. *Applied Ergonomics*, 52:333–342, 2016.

[16] Erin K. Chiou and John D. Lee. Trusting automation: Designing for responsivity and resilience. *Human Factors*, 0(0):00187208211009995, 0.

[17] Jesse C. Christensen, Christopher R. Wilson, Andrew S. Merryweather, and K. Bo Foreman. Kinematics of the pelvis, torso, and lower limb during obstacle negotiation while under temporal constraints. *The Anatomical Record*, 300(4):732–738, 2017.

[18] Paul R. Davidson and Daniel M. Wolpert. Internal models underlying grasp can be additively combined. *Experimental Brain Research*, 155(3):334–340, Apr 2004.

[19] Fred D Davis. Perceived usefulness, perceived ease of use, and user acceptance of information technology. *MIS Quarterly*, 13(3):319–340, 09 1989.

[20] Agostino De Santis, Bruno Siciliano, Alessandro De Luca, and Antonio Bicchi. An atlas of physical human–robot interaction. *Mechanism and Machine Theory*, 43(3):253–270, 2008.

[21] Christopher L. Dembia, Amy Silder, Thomas K. Uchida, Jennifer L. Hicks, and Scott L. Delp. Simulating ideal assistive devices to reduce the metabolic cost of walking with heavy loads. *PLOS ONE*, 12(7):1–25, 07 2017.

[22] Damien Duddy, Rónán Doherty, James Connolly, Stephen McNally, Johnny Loughrey, and Maria Faulkner. The effects of powered exoskeleton gait training on cardiovascular function and gait performance: A systematic review. *Sensors*, 21(9), 2021.

[23] Amandine Dufaug, Christine Barthod, Laurent Goujon, and Luc Marechal. New joint analysis of electromyography spectrum and amplitude-based methods towards real-time muscular fatigue evaluation during a simulated surgical procedure: A pilot analysis on the statistical significance. *Medical Engineering Physics*, 79:1–9, 2020.

[24] Susannah M. Engdahl, Sean K. Meehan, and Deanna H. Gates. Differential experiences of embodiment between body-powered and myoelectric prosthesis users. *Scientific Reports*, 10(1):15471, Sep 2020.

[25] Wyatt Felt, Jessica C Selinger, J Maxwell Donelan, and C David Remy. "body-in-the-loop": Optimizing device parameters using measures of instantaneous energetic cost. *PloS one*, 10(8):e0135342, 2015.

[26] Daniel P. Ferris and Cara L. Lewis. Robotic lower limb exoskeletons using proportional myoelectric control. In *2009 Annual International Conference of the IEEE Engineering in Medicine and Biology Society*, pages 2119–2124, 2009.

[27] Cyrus K. Foroughi, Shannon Devlin, Richard Pak, Noelle L. Brown, Ciara Sibley, and Joseph T. Coyne. Near-perfect automation: Investigating performance, trust, and visual attention allocation. *Human Factors*, 0(0):00187208211032889, 0.

[28] S. Galle, W. Derave, F. Bossuyt, P. Calders, P. Malcolm, and D. De Clercq. Exoskeleton plantarflexion assistance for elderly. *Gait Posture*, 52:183–188, 2017.

[29] Miriam González-Izal, Armando Malanda, Esteban Gorostiaga, and Mikel Izquierdo. Electromyographic models to assess muscle fatigue. *Journal of Electromyography and Kinesiology*, 22(4):501–512, 2012.

[30] Daniel F. N. Gordon, Christopher McGreavy, Andreas Christou, and Sethu Vijayakumar. Human-in-the-loop optimization of exoskeleton assistance via online simulation of metabolic cost. *IEEE Transactions on Robotics*, 38(3):1410–1429, 2022.

[31] Keith E. Gordon and Daniel P. Ferris. Learning to walk with a robotic ankle exoskeleton. *Journal of Biomechanics*, 40(12):2636–2644, 2007.

[32] Keith E. Gordon, Catherine R. Kinnaird, and Daniel P. Ferris. Locomotor adaptation to a soleus emg-controlled antagonistic exoskeleton. *Journal of Neurophysiology*, 109:1804–1814, 4 2013.

[33] Aditi Gupta, Ryan McKindles, and Leia Stirling. Relationships between cognitive factors and gait strategy during exoskeleton-augmented walking. *Proceedings of the Human Factors and Ergonomics Society Annual Meeting*, 65(1):211–215, 2021.

[34] Laura Hak, Han Houdijk, Frans Steenbrink, Agali Mert, Peter van der Wurff, Peter J. Beek, and Jaap H. van Dieën. Stepping strategies for regulating gait adaptability and stability. *Journal of Biomechanics*, 46(5):905–911, 2013.

[35] Matthew L Handford and Manoj Srinivasan. Robotic lower limb prosthesis design through simultaneous computer optimizations of human and prosthesis costs. *Scientific reports*, 6(1):19983, 2016.

[36] J. A. Hartigan and M. A. Wong. Algorithm as 136: A k-means clustering algorithm. *Journal of the Royal Statistical Society. Series C (Applied Statistics)*, 28(1):100–108, 1979.

[37] James B. Heald, David W. Franklin, and Daniel M. Wolpert. Increasing muscle co-contraction speeds up internal model acquisition during dynamic motor learning. *Scientific Reports*, 8(1):16355, Nov 2018.

[38] S Hirokawa, M Solomonow, Z Luo, Y Lu, and R D'ambrosia. Muscular co-contraction and control of knee stability. *Journal of Electromyography and Kinesiology*, 1(3):199–208, 1991.

[39] Guy Hoffman. Evaluating fluency in human–robot collaboration. *IEEE Transactions on Human-Machine Systems*, 49(3):209–218, 2019.

[40] Yingxin Huo, Xiang Li, Xuan Zhang, and Dong Sun. Intention-driven variable impedance control for physical human-robot interaction. In *2021 IEEE/ASME International Conference on Advanced Intelligent Mechatronics (AIM)*, pages 1220–1225, 2021.

[41] Rachel L. Hybart and Daniel P. Ferris. Embodiment for robotic lower-limb exoskeletons: A narrative review. *IEEE Transactions on Neural Systems and Rehabilitation Engineering*, 31:657–668, 2023.

[42] Shu Imaizumi, Tomohisa Asai, and Shinichi Koyama. Embodied prosthetic arm stabilizes body posture, while unembodied one perturbs it. *Consciousness and Cognition*, 45:75–88, 2016.

[43] K. A. Ingraham, C. D. Remy, and E. J. Rouse. The role of user preference in the customized control of robotic exoskeletons. *Science Robotics*, 7(64):eabj3487, 2022.

[44] Kimberly A. Ingraham, Maegan Tucker, Aaron D. Ames, Elliott J. Rouse, and Max K. Shepherd. Leveraging user preference in the design and evaluation of lower-limb exoskeletons and prostheses. *Current Opinion in Biomedical Engineering*, 28:100487, 2023.

[45] Rifky Ismail, Mochammad Ariyanto, Kharisma A. Pambudi, Joshua W. Syafei, and Gilar P. Ananto. Extra robotic thumb and exoskeleton robotic fingers for patient with hand function disability. In *2017 4th International Conference on Electrical Engineering, Computer Science and Informatics (EECSI)*, pages 1–6, 2017.

[46] Rachel W Jackson and Steven H Collins. An experimental comparison of the relative benefits of work and torque assistance in ankle exoskeletons. *Journal of applied physiology*, 119(5):541–557, 2015.

[47] Rachel W. Jackson and Steven H. Collins. Heuristic-based ankle exoskeleton control for co-adaptive assistance of human locomotion. *IEEE Transactions on Neural Systems and Rehabilitation Engineering*, 27(10):2059–2069, 2019.

[48] Inseung Kang, Pratik Kunapuli, and Aaron J. Young. Real-time neural network-based gait phase estimation using a robotic hip exoskeleton. *IEEE Transactions on Medical Robotics and Bionics*, 2:28–37, 2020.

[49] H. Kazerooni. Exoskeletons for human power augmentation. In *2005 IEEE/RSJ International Conference on Intelligent Robots and Systems*, pages 3459–3464, 2005.

[50] William R. King and Jun He. A meta-analysis of the technology acceptance model. *Information Management*, 43(6):740–755, 2006.

[51] JoAnn Kluzik, Jörn Diedrichsen, Reza Shadmehr, and Amy J. Bastian. Reach adaptation: What determines whether we learn an internal model of the tool or adapt the model of our arm? *Journal of Neurophysiology*, 100(3):1455–1464, 2008. PMID: 18596187.

[52] Jeffrey R. Koller, Deanna H. Gates, Daniel P. Ferris, and C. David Remy. 'body-in-the-loop' optimization of assistive robotic devices: A validation study. In *Robotics: Science and Systems*, 2016.

[53] Jeffrey R. Koller, Daniel A. Jacobs, Daniel P. Ferris, and C. David Remy. Learning to walk with an adaptive gain proportional myoelectric controller for a robotic ankle exoskeleton. *Journal of NeuroEngineering and Rehabilitation*, 12(1):97, Nov 2015.

[54] John D. Lee and Katrina A. See. Trust in automation: Designing for appropriate reliance. *Human Factors*, 46(1):50–80, 2004.

[55] Ung Hee Lee, Varun S. Shetty, Patrick W. Franks, Jie Tan, Georgios Evangelopoulos, Sehoon Ha, and Elliott J. Rouse. User preference optimization for control of ankle exoskeletons using sample efficient active learning. *Science Robotics*, 8(83):eadg3705, 2023.

[56] Tommaso Lenzi, Maria Chiara Carrozza, and Sunil K. Agrawal. Powered hip exoskeletons can reduce the user's hip and ankle muscle activations during walking. *IEEE Transactions on Neural Systems and Rehabilitation Engineering*, 21(6):938–948, 2013.

[57] Geng Li, Mohammad S Shourijeh, Di Ao, Carolynn Patten, and Benjamin J Fregly. How well do commonly used co-contraction indices approximate lower limb joint stiffness trends during gait for individuals post-stroke? *Front Bioeng Biotechnol*, 8:588908, January 2021.

[58] Jinfu Li, Bingquan Shen, Chee-Meng Chew, Chee Leong Teo, and Aun Neow Poo. Novel functional task-based gait assistance control of lower extremity assistive device for level walking. *IEEE Transactions on Industrial Electronics*, 63(2):1096–1106, 2016.

[59] Zhijun Li, Tao Zhang, Pengbo Huang, and Guoxin Li. Human-in-the-loop cooperative control of a walking exoskeleton for following time-variable human intention. *IEEE Transactions on Cybernetics*, pages 1–13, 2022.

[60] Zhijun Li, Kuankuan Zhao, Longbin Zhang, Xinyu Wu, Tao Zhang, Qinjian Li, Xiang Li, and Chun-Yi Su. Human-in-the-loop control of a wearable lower limb exoskeleton for stable dynamic walking. *IEEE/ASME Transactions on Mechatronics*, 26(5):2700–2711, 2021.

[61] Julio S. Lora-Millan, Andres F. Hidalgo, and Eduardo Rocon. An imus-based extended kalman filter to estimate gait lower limb sagittal kinematics for the control of wearable robotic devices. *IEEE Access*, 9:144540–144554, 2021.

[62] Tung-Wu Lu, Hao-Ling Chen, and Sheng-Chang Chen. Comparisons of the lower limb kinematics between young and older adults when crossing obstacles of different heights. *Gait Posture*, 23(4):471–479, 2006.

[63] Mooney Luke and Duval Jean-Francois. Unidirectional actuated exoskeleton device, 2020.

[64] Philippe Malcolm, Wim Derave, Samuel Galle, and Dirk De Clercq. A simple exoskeleton that assists plantarflexion can reduce the metabolic cost of human walking. *PLOS ONE*, 8(2):1–7, 02 2013.

[65] T. A. Martin, J. G. Keating, H. P. Goodkin, A. J. Bastian, and W. T. Thach. Throwing while looking through prisms ii. specificity and storage of multiple gaze-throw calibrations. *Brain*, 119:1199–1211, 1996.

[66] Stuart M McGill, Sylvain Grenier, Natasa Kavcic, and Jacek Cholewicki. Coordination of muscle activity to assure stability of the lumbar spine. *Journal of electromyography and kinesiology*, 13(4):353–359, 2003.

[67] Roberto Leo Medrano, Gray Cortright Thomas, Elliott J. Rouse, and Robert D. Gregg. Analysis of the bayesian gait-state estimation problem for lower-limb wearable robot sensor configurations. *IEEE Robotics and Automation Letters*, 7(3):7463–7470, 2022.

[68] Anat Mirelman, Talia Herman, Simone Nicolai, Agnes Zijlstra, Wiebren Zijlstra, Clemens Becker, Lorenzo Chiari, and Jeffrey M. Hausdorff. Audio-biofeedback training for posture and balance in patients with parkinson's disease. *Journal of NeuroEngineering and Rehabilitation*, 8(1):35, Jun 2011.

[69] E D Monsch, C O Franz, and J C Dean. The effects of gait strategy on metabolic rate and indicators of stability during downhill walking. *Journal of Biomechanics*, 45:1928–1933, 2012.

[70] Luke M. Mooney, Elliott J. Rouse, and Hugh M. Herr. Autonomous exoskeleton reduces metabolic cost of human walking during load carriage. *Journal of neuroengineering and rehabilitation*, 11(80), 2014.

[71] Spencer A. Murray, Kevin H. Ha, Clare Hartigan, and Michael Goldfarb. An assistive control approach for a lower-limb exoskeleton to facilitate recovery of walking following stroke. *IEEE Transactions on Neural Systems and Rehabilitation Engineering*, 23(3):441–449, 2015.

[72] Brian Oakley, Mustapha Mouloua, and Peter Hancock. Effects of automation reliability on human monitoring performance. *Proceedings of the Human Factors and Ergonomics Society Annual Meeting*, 47(1):188–190, 2003.

[73] Greg Orekhov, Ying Fang, Jason Luque, and Zachary F. Lerner. Ankle exoskeleton assistance can improve over-ground walking economy in individuals with cerebral palsy. *IEEE Transactions on Neural Systems and Rehabilitation Engineering*, 28(2):461–467, 2020.

[74] Xiangyu Peng, Yadrianna Acosta-Sojo, Man I Wu, and Leia Stirling. Actuation timing perception of a powered ankle exoskeleton and its associated ankle angle changes during walking. *IEEE Transactions on Neural Systems and Rehabilitation Engineering*, 30:869–877, 2022.

[75] Katherine L. Poggensee and Steven H. Collins. How adaptation, training, and customization contribute to benefits from exoskeleton assistance. *Science Robotics*, 6:1078, 9 2021.

[76] Anastasia Protopapadaki, Wendy I. Drechsler, Mary C. Cramp, Fiona J. Coutts, and Oona M. Scott. Hip, knee, ankle kinematics and kinetics during stair ascent and descent in healthy young individuals. *Clinical Biomechanics*, 22(2):203–210, 2007.

[77] John Roberts and Russ Tedrake. Signal-to-noise ratio analysis of policy gradient algorithms. In D. Koller, D. Schuurmans, Y. Bengio, and L. Bottou, editors, *Advances in Neural Information Processing Systems*, volume 21. Curran Associates, Inc., 2008.

[78] E. Rocon, J. M. Belda-Lois, A. F. Ruiz, M. Manto, J. C. Moreno, and J. L. Pons. Design and validation of a rehabilitation robotic exoskeleton for tremor assessment and suppression. *IEEE Transactions on Neural Systems and Rehabilitation Engineering*, 15(3):367–378, 2007.

[79] Jennifer M. Ross, James L. Szalma, Peter A. Hancock, John S. Barnett, and Grant Taylor. The effect of automation reliability on user automation trust and reliance in a search-and-rescue scenario. *Proceedings of the Human Factors and Ergonomics Society Annual Meeting*, 52(19):1340–1344, 2008.

[80] Adam Rozumalski and Michael H. Schwartz. Crouch gait patterns defined using k-means cluster analysis are related to underlying clinical pathology. *Gait Posture*, 30(2):155–160, 2009.

[81] KS Rudolph, MJ Axe, and L Snyder-Mackler. Dynamic stability after acl injury: who can hop? *Knee Surgery, Sports Traumatology, Arthroscopy*, 8:262–269, 2000.

[82] Mark S. Redfern and James DiPasquale. Biomechanics of descending ramps. *Gait Posture*, 6(2):119–125, 1997.

[83] Jessica C Selinger and J Maxwell Donelan. Estimating instantaneous energetic cost during non-steady-state gait. *Journal of Applied Physiology*, 117(11):1406–1415, 2014.

[84] Jessica C. Selinger, Jeremy D. Wong, Surabhi N. Simha, and J. Maxwell Donelan. How humans initiate energy optimization and converge on their optimal gaits. *Journal of Experimental Biology*, 222(19):jeb198234, 10 2019.

[85] R Shadmehr and F A Mussa-Ivaldi. Adaptive representation of dynamics during learning of a motor task. *The Journal of neuroscience : the official journal of the Society for Neuroscience*, 14:3208–3224, 5 1994.

[86] Max K. Shepherd, Dean D. Molinaro, Gregory S. Sawicki, and Aaron J. Young. Deep learning enables exoboot control to augment variable-speed walking. *IEEE Robotics and Automation Letters*, 7(2):3571–3577, 2022.

[87] Thomas B. Sheridan. Human–robot interaction: Status and challenges. *Human Factors*, 58(4):525–532, 2016. PMID: 27098262.

[88] Ben Sidaway, Jennifer Anderson, Garth Danielson, Lucas Martin, and Garth Smith. Effects of Long-Term Gait Training Using Visual Cues in an Individual With Parkinson Disease. *Physical Therapy*, 86(2):186–194, 02 2006.

[89] Amy Silder, Thor Besier, and Scott L. Delp. Predicting the metabolic cost of incline walking from muscle activity and walking mechanics. *Journal of Biomechanics*, 45(10):1842–1849, 2012.

[90] Jennifer Sloboda, Paul Stegall, Ryan J. McKindles, Leia Stirling, and Ho Chit Siu. Utility of inter-subject transfer learning for wearable-sensor-based joint torque prediction models. In *2021 43rd Annual International Conference of the IEEE Engineering in Medicine Biology Society (EMBC)*, pages 4901–4907, 2021.

[91] Maurice A. Smith and Reza Shadmehr. Intact ability to learn internal models of arm dynamics in huntington's disease but not cerebellar degeneration. *Journal of Neurophysiology*, 93:2809–2821, 5 2005.

[92] Nitish Thatte, Tanvi Shah, and Hartmut Geyer. Robust and adaptive lower limb prosthesis stance control via extended kalman filter-based gait phase estimation. *IEEE Robotics and Automation Letters*, 4(4):3129–3136, 2019.

[93] Kurt A. Thoroughman and Reza Shadmehr. Electromyographic correlates of learning an internal model of reaching movements. *Journal of Neuroscience*, 19:8573–8588, 10 1999.

[94] Kurt A. Thoroughman and Reza Shadmehr. Learning of action through adaptive combination of motor primitives. *Nature*, 407:742–747, 10 2000.

[95] Thomas K. Uchida, Ajay Seth, Soha Pouya, Christopher L. Dembia, Jennifer L. Hicks, and Scott L. Delp. Simulating ideal assistive devices to reduce the metabolic cost of running. *PLOS ONE*, 11(9):1–19, 09 2016.

[96] Brian R Umberger and Jonas Rubenson. Understanding muscle energetics in locomotion: new modeling and experimental approaches. *Exercise and sport sciences reviews*, 39(2):59–67, 2011.

[97] Jan F. Veneman, Rik Kruidhof, Edsko E. G. Hekman, Ralf Ekkelenkamp, Edwin H. F. Van Asseldonk, and Herman van der Kooij. Design and evaluation of the lopes exoskeleton robot for interactive gait rehabilitation. *IEEE Transactions on Neural Systems and Rehabilitation Engineering*, 15(3):379–386, 2007.

[98] Alexandra S. Voloshina, Arthur D. Kuo, Monica A. Daley, and Daniel P. Ferris. Biomechanics and energetics of walking on uneven terrain. *Journal of Experimental Biology*, 216(21):3963–3970, 11 2013.

[99] C.J. Walsh, D. Paluska, K. Pasch, W. Grand, A. Valiente, and H. Herr. Development of a lightweight, underactuated exoskeleton for load-carrying augmentation. In *Proceedings 2006 IEEE International Conference on Robotics and Automation, 2006. ICRA 2006.*, pages 3485–3491, 2006.

[100] Conor James Walsh, Ken Endo, and Hugh Herr. A quasi-passive leg exoskeleton for load-carrying augmentation. *International Journal of Humanoid Robotics*, 04(03):487–506, 2007.

[101] Aihui Wang, Ningning Hu, Jun Yu, Wudai Liao, Junfeng Zhang, Xia Wu, and Chuanghui Pei. Research on robot control system of lower limb rehabilitation robot based on human gait comfort. In *2019 International Conference on Advanced Mechatronic Systems (ICAMechS)*, pages 34–39, 2019.

[102] Wei Wang, Yige Liu, Pengqing Ren, Juanjuan Zhang, and Jingtai Liu. The characteristics of human-robot coadaptation during human-in-the-loop optimization of exoskeleton control. In *2018 IEEE International Conference on Robotics and Biomimetics (ROBIO)*, pages 1459–1464, 2018.

[103] Robert L. Waters and Sara Mulroy. The energy expenditure of normal and pathologic gait. *Gait Posture*, 9(3):207–231, 1999.

[104] Håkan Westerblad, Joseph D. Bruton, and Abram Katz. Skeletal muscle: Energy metabolism, fiber types, fatigue and adaptability. *Experimental Cell Research*, 316(18):3093–3099, 2010. Special Issue: Myogenesis.

[105] D M Wolpert, Z Ghahramani, and M I Jordan. An internal model for sensorimotor integration. *Science*, 269:1880–1882, 1995.

[106] Man I Wu, Brian S. Baum, Harvey Edwards, and Leia Stirling. Users maintain task accuracy and gait characteristics during missed exoskeleton actuations through adaptations in joint kinematics. In *2022 44th Annual International Conference of the IEEE Engineering in Medicine Biology Society (EMBC)*, pages 1809–1813, 2022.

[107] Man I Wu, Paul Stegall, Ho Chit Siu, and Leia Stirling. Impact of haptic cues and an active ankle exoskeleton on gait characteristics. *Human Factors*, 66(3):904–915, 2024. PMID: 35815866.

[108] Man I Wu and Leia Stirling. Emergent gait strategies defined by cluster analysis when using imperfect exoskeleton algorithms. *IEEE Robotics and Automation Letters*, 9(4):3171–3178, 2024.

[109] Aaron J. Young, Jessica Foss, Hannah Gannon, and Daniel P. Ferris. Influence of power delivery timing on the energetics and biomechanics of humans wearing a hip exoskeleton. *Frontiers in Bioengineering and Biotechnology*, 5, 2017.

[110] Juanjuan Zhang, Pieter Fiers, Kirby A. Witte, Rachel W. Jackson, Katherine L. Poggensee, Christopher G. Atkeson, and Steven H. Collins. Human-in-the-loop optimization of exoskeleton assistance during walking. *Science*, 356(6344):1280–1284, 2017.

[111] Ting Zhang and He Huang. A lower-back robotic exoskeleton: Industrial handling augmentation used to provide spinal support. *IEEE Robotics Automation Magazine*, 25(2):95–106, 2018.

[112] Libo Zhou, Weihai Chen, Wenjie Chen, Shaoping Bai, Jianbin Zhang, and Jianhua Wang. Design of a passive lower limb exoskeleton for walking assistance with gravity compensation. *Mechanism and Machine Theory*, 150:103840, 2020.

[113] A.B. Zoss, H. Kazerooni, and A. Chu. Biomechanical design of the berkeley lower extremity exoskeleton (bleex). *IEEE/ASME Transactions on Mechatronics*, 11(2):128–138, 2006.